UNIVERSIDADE FEDERAL DE GOIÁS
INSTITUTO DE CIÊNCIAS BIOLÓGICAS
PROGRAMA DE PÓS-GRADUAÇÃO EM CIÊNCIAS BIOLÓGICAS

MECANISMO DE MORTE CELULAR INDUZIDA POR COMPLEXOS DE RUTÊNIO II E III EM DIFERENTES LINHAGENS TUMORAIS

FLÁVIA DE CASTRO PEREIRA

Goiânia
2014

FLÁVIA DE CASTRO PEREIRA

MECANISMO DE MORTE CELULAR INDUZIDA POR COMPLEXOS DE RUTÊNIO II E III EM DIFERENTES LINHAGENS TUMORAIS

Tese apresentada ao Programa de Pós-Graduação em Ciências Biológicasdo Instituto de Ciências Biológicas da Universidade Federal de Goiás, como requisito parcial para obtenção do título de Doutor em Ciências Biológicas.

Área de Concentração: Biologia Celular e Molecular

Orientadora: Prof. Dra. Elisângela de Paula Silveira Lacerda.

Goiânia
2014

FLÁVIA DE CASTRO PEREIRA

MECANISMO DE MORTE CELULAR INDUZIDA POR COMPLEXOS DE RUTÊNIO II E III EM DIFERENTES LINHAGENS TUMORAIS

BANCA EXAMINADORA DA TESE DE DOUTORADO

Aluna: FLÁVIA DE CASTRO PEREIRA

Orientadora: Profa. Dra. ELISÂNGELA DE PAULA SILVEIRA LACERDA

Membros:

1. Profa. Dra. Elisângela de Paula Silveira Lacerda - UFG

2. Prof. Dr. Wagner dos Santos Gouvêa - UFG

3. Prof. Dr. Carlos Frederico Martins Menck - USP

4. Profa. Dra. Yandra Lobato - UFG

5. Prof. Dr. Cláudio Carlos da Silva - UCG

ou

6. Profa. Dra. Aliny Pereira de Lima - UFG

7. Prof. Dr. Carlos Henrique Castro - UFG

Aprovada em: 19/03/2014

“Dizem que a vida é para quem sabe viver, mas ninguém nasce pronto. A vida é para quem é corajoso o suficiente para se arriscar e humilde o bastante para aprender.”

Clarise Lispector

DEDICATÓRIA

Aos meus pais, Maria Francisca e Orlando, exemplo de coragem, vida e amor. Obrigada pelo incentivo, compreensão, amor, dedicação, orações em todos os momentos da minha vida. A vocês o meu eterno amor.

Ao meu amado noivo Wendell, pelo amor, amizade, dedicação, carinho, compreensão e incentivo. Pelo exemplo de alegria na busca de seus objetivos. Por todos os sentimentos que cultivamos ao longo desses anos. Obrigada por inundar meu coração com a maior felicidade de toda a minha vida, nosso filho!

Ao meu irmão, Patrick por sempre estar presente em minha vida.

AGRADECIMENTOS

Primeiramente, agradeço a Deus por mais esta etapa de aprendizagem em minha vida, mas, acima de tudo, agradeço por sempre ter me colocado no caminho certo, por nunca me deixar enfraquecer meio às adversidades.

Agradeço a todos que, direta ou indiretamente, contribuíram para a realização deste trabalho e, em especial,

A minha Orientadora Prof. Dra. Elisângela de Paula Silveira Lacerda, exemplo de pesquisadora a ser seguido, a quem dedico admiração e respeito. Alguém que me ensinou grandes lições sobre a conduta profissional e pessoal. A quem tenho profunda admiração, respeito e grande carinho. Muito do que sou, devo a você, obrigada por estar sempre presente e, o mais importante, obrigada por acreditar em mim.

Ao Prof. Dr. Alzir Bastista Azevedo e sua equipe do laboratório de Química da Universidade da Federal de São Carlos, pela síntese e fornecimento do composto de Rutênio inédito para a realização deste trabalho.

Agradeço a Aliny pela grande amizade, dedicação, ajuda e, principalmente, pelo companheirismo.

Agradeço a Wanessa pela amizade, compreensão e carinho em todos esses anos de convivêcia.

Agradeço a Lorena, pela a oportunidade de ser sua amiga e por todo o carinho a

mim dedicado.

A equipe do Laboratório de Genética Molecular e Citogenética, em especial a Francyelli , Thalita, Alessandra, Hugo, Sônia, Lucas, Raquel, Kézia e Patríca obrigada pela confiança, pela grande ajuda prestada durante todos esses anos e, acima de tudo, pela amizade.

Aos funcionários da Universidade, pelo auxílio e compreensão no decorrer da pesquisa.

Ao Instituto de Ciências Biológicas da Universidade Federal de Goiás pela estrutura didática e técnica para a realização dos estudos e trabalhos do doutorado.

A Coordenação de Aperfeiçoamento de Pessoal de Nível Superior (Capes), pela bolsa de estudos.

A toda a minha família pelo incentivo.

À banca examinadora que, gentilmente, aceitou o convite para participar da defesa desta tese.

A todas as pessoas que verdadeiramente torceram por mim, incentivaram-me e que hoje comemoram comigo esta conquista.

SUMÁRIO

LISTA DE ABREVIATURAS E SIGLAS

µM – Micromolar

µL – Microlitro

χ^2 – Teste do Qui-quadrado

a.C. – Antes de Cristo

A-20 - Linhagem de células de Linfoma de camundongo

A2780 - Câncer de ovário humano

A498 - Câncer renal

ACS - A *American Cancer Society*

AIF - Fator Indutor de Apoptose

APAF-1 - Protease Apoptótica Ativadora de Fator 1

ATCC – American Type Culture Collection

ATP – Adenosina trifosfato

BAK - Proteína pró-apoptótica

BAX - Proteína X associada ao Bcl2

BCL2 - Proteína antiapoptótica (Linfoma células B)

BCLX - Proteína antiapoptótica

BD – Bioscience Parmingen

BID - Domínio de Morte de Interação com BH3

BIM - Proteína pró-apoptótico

BSA – *Protein Bovine serum albumin* (Proteína albumina de soro bovino)

Ca^{2+} – Cálcio

CCNS – Quimioterápicos clico-celular não específico

CCS – Quimioterápicos ciclo-celular específico

CD95 - Ligante de Receptor de Morte Celular

CDK – Proteína quinase dependente de ciclina

CDK4 – Quinase dependente de ciclina 4

CDKs – Proteínas quinases dependente de ciclina

Ciclina D – Proteína membro da família das ciclinas

Citocromo C – Proteína heme associada à membrana externa da mitocôndria

CKIS – Inibidores de Quinase-Ciclina

CPCNP – Câncer de pulmão de células não-pequenas

CPCP – Câncer de pulmão de células pequenas

D. melanogaster – Drosophila melanogaster

DAPK - Proteína Quinase serina/treonina Associada à Morte

DCC - Deleção Carcinoma Coloretal

DCNTs – Comissão de Nomenclatura de Morte Celular

DIABLO - Inibidor Direto de Proteínas Inibidoras de Apoptose

DISC - Complexo de sinalização de indução de morte

DMEN – Dulbecco's Modified Eagle Medium

DMSO – Dimetilsulfóxido

DNA – Ácido desoxirribonucléico

DO – Densidade óptica

E. coli – Escherichia coli

ER – Retículo Endoplasmático

EVSA-T - câncer de mama

FADD - Domínio de Morte FAS-associada

FAS – Receptor de superfície envolvido na ativação da apoptose

FASL/CD95 – Receptor de superfície envolvido na ativação da apoptose

FDA – Food and Drug Administration

FITC – *Fluorescein thiocyanate* (Fluoresceína tiocianato)

GAP1 – Fase G1 – Ciclo celular

GAP2 – Fase G2 – Ciclo celular

H266 – Linhagem Câncer de pulmão

HCL – Ácido clorídrico

IARC- Agência Internacional para Pesquisa sobre o Câncer

IC_{50} – Concentração que inibe 50% das células

ICE – Enzimas Conversoras de Interleucinas

IGROV - Câncer de ovário

INCA – Instituto Nacional do Câncer

INK4 – Inibidores específicos de CDK4

I-OHP – Oxaliplatina

JC-1 – Iodeto de 5,5’,6,6’-tetracloro-1,1,3,3’-tetraetilbenzimidazolilcarbocianina

K562 - Linhagem de células de Leucemia Mieloide Crônica humana

KP1019 - Indazol *trans*-[tetraclorobis (1*H*-indazol)rutenato(III)

L929 – Linhagem Fibroblasto de Pulmão de Camundongo

LCM – Leucemia mieloide crônica

M19 - Melanona

MCF-7 - Câncer de mama

MOMP - Permeabilização Membrana Mitocondrial Externa

mRNA – RNA mensageiro

MTT – 3-(4,5-dimetil-tiazol-2-il)-2,5 difenil-tetrazólio

Na+/K+ – Sódio e Potássio

NAMI-A: ImH[*trans*-RuCl4(DMSO)Im]

NCCD - Comitê de Nomenclatura sobre Morte Celular

O_2 – Oxigênio

ºC – grau Celsius

Omi/HtrA2 – Proteína-2 exige alta temperatura

OMS – Organização Mundial de Saúde

TP53 – Proteína citoplasmática

PBS – Tampão fosfato-salino

pH – Potencial hidrogeniônico ou potencial hidrogênio iônico

PI – Iodeto de Propídio

pNA - Cromóforo p-nitroanilima

PP2A - Proteína Fosfatase 2A

Pt – Platina

qPCR – PCR em tempo real

RIP1 – Proteínas quinase interagindo com receptor 1

RIP3 – Proteínas quinase interagindo com receptor 3

RIPK 3 - Proteína Quinase de Interação com Receptor-3

RNA – Ácido ribonucleico

RNAse – Ribonuclease

ROS - espécies reativas de oxigênio

rpm – rotações por minuto

RPMI 1640 – Meio de cultura

RT-PCR – Reação em Cadeia da Polimerase com transcrição reversa

Ru – Rutênio

S –Síntese Fase S – Ciclo celular

S180 - Sarcoma 180 murino

SDS – Sulfato Dodecil De Sódio

Sigma – *Sigma-Aldrich Co St Louis, Mo, Eua*

SKBR-3 - Carcinoma de mama humano

SKI – heptaplatina

SMAC - Segundo Ativador de Caspase Derivado da Mitocôndria

SMases - ativação de esfingomielinases

TNF – Fator de Necrose Tumoral

TNFR – Receptor do fator de necrose tumoral

TNFR1 – Receptor de morte celular

TRAIL – Fator de Necrose Tumoral

UFG – Universidade Federal de Goiás

UFU – Universidade Federal de Uberlândia

WIDR - Câncer de colon

$\Delta\Psi$m – Potêncial de membrana mitocôndrial

LISTA DE FIGURAS - INTRODUÇÃO

LISTA DE TABELAS - INTRODUÇÃO

LISTA DE FIGURAS E TABELAS DO ARTIGO 1

LISTA DE FIGURAS E TABELAS DO ARTIGO 2

ANEXOS

RESUMO

Fármacos à base de cisplatina ainda são os anticancerígenos mais utilizados no mundo. Os compostos de rutênio têm sido objetos de grande atenção devido as suas propriedades antimetastática, baixa toxicidade e vários estados de oxidação (Ru (II), Ru (III) e Ru (IIV)) em condições fisiológicas. O presente trabalho teve como objetivo investigar *in vitro* os efeitos citotóxico e mecanismo de morte do complexo Ditionato de *cis*-Tetraamino(oxalato)rutênio(III) na linhagem tumoral de leucemia mielóide crônica (K562) e do complexo de rutênio (II) coordenado a ligante fosfina e nitrila $[RuCl(bcn)(bipy)(dppe)]PF_6$, em linhagem tumoral S180 a partir das técnicas de ensaio de viabilidade celular, ensaio de cinética das fases do ciclo celular, ensaio anexina V/Iodeto de Propídeo, ensaio de potencial de membrana mitocondrial e expressão gênica por PCR em tempo real. Os resultados mostraram que o complexo de rutênio (III) provoca uma significativa redução na proliferação de células K562. O complexo de rutênio (III) induziu uma IC_{50} =18,28 μM. A análise por citometria de fluxo indicou um efeito sub-G1 dos complexos de rutênio sobre células de K562. O composto provocou um aumento de dano significativo nas células em todas as concentrações testadas em comparação ao controle negativo, o que pode ser associado à citotoxicidade com efeito direto sobre o DNA das células de K562. A partir do ensaio de viabilidade celular pela técnica de redução do MTT, verificou-se que o complexo de rutênio (II) coordenado a fosfina e nitrila apresentou atividade citotóxica frente à linhagem tumoral S180 com IC_{50} 17,02±8,21μM e IC_{50} de 53,73 ± 5,71 para linfócito. Na análise do ciclo celular de células tumorais S180 tratadas com o complexo de rutênio (II), casou indução de G0/G1, fase S e G2/M. Na análise dos ensaios de apoptose, os resultados demonstraram que o complexo de rutênio (II) induziu morte celular via apoptose na linhagem tumoral S180, como evidenciado pelo aumento no número de células anexina V positivo, despolarização do potencial de membrana mitocondrial, ativação das caspase 3 (Casp3) e 8 (Casp8) e aumento dos níveis de expressão de caspase-3 (*Casp3*) (mRNA), *Bax* (mRNA) e *Tp53* . A partir dos resultados conclui-se que ambos os complexos de rutênio (II) e (III) induzem atividade citotóxica frente aos modelos de células testadas, sendo que a atividade está correlacionada às alterações nas fases do ciclo celular e indução de morte celular via apoptose.

Palavras-chave: Apoptose, Ciclo Celular, Citotoxicidade, Complexos de Rutênio II e III.

ABSTRACT

The resistance acquired by some tumor cell lines retricts the use of drugs made of platinum because of Ruthenium compounds have been objects of great attention for presenting antimetastatic properties and low toxicity. Ruthenium compounds form compounds with the most different chemical binders, presenting good behavior and expanding the possibilities offor biological applications. A wide variety of coordination has enabled studies on ruthenium complexes, andseveral oxidation stages (Ru (II), Ru (III), and Ru (IV)) under physiological conditions and the rate of binder substitution. This study ranges the citotoxic activity of ruthenium (III) compound *cis*-Tetraammine(oxalato)Ruthenium(III) Dithionate - {*Cis*-$[Ru(C_2O_4)(NH_3)_4]_2(S_2O_6)$} to treat human erythroleukemia (K562) tumor cell lineand the complex of ruthenium (II) coordinated a phosphine ligand and nitrile front tumor lineage S180 through the techniques of assay cell viability, assay kinetics of cell cycle phases, annexin V assay/ propidium iodide, test of mitochondrial membrane potential, test comet and gene expression through real time PCR. Both antiproliferative and cytotoxic activity revealed that K562 cells cultured with ruthenium (III) compound showed meaningful decrease in proliferation. Ruthenium(III) compound induced the IC_{50} value was of 18.28 µM set againts the cell cycle profiles cells not treated. Flow cytometric analysis indicated a sub-G1 arresting effect of ruthenium compound on K562 cells. Through the cell viability assay through MTT reduction technique, it was found that the complex of ruthenium (II) phosphine coordinated and nitrile presented cytotoxic activity when facing the tumor strain S180 with IC_{50} 17.02±8.21µM and IC_{50} de 53.73 ± 5.71 µM for lymphocyte. When analyzing the cell cycle of tumor cells S180 treated with complex of ruthenium (II) caused increase in cells in G0/G1 and in S phase decreased. We observed an increase G2 / M. In the analysis of apoptosis assays, the results pointed that the complex ruthenium (II) induced cell death via apoptosis in tumor strain S180 as proved the increase in annexin cells V positive, depolarization of the mitochondrial membrane potential, activation of caspase 3 (Casp3) and 8 (Casp8) and increased expression levels of caspase-3 (*Casp3*) (mRNA), *Bax* (mRNA) and *Tp53*. The results lead to the conclusion that both complexes of ruthenium (II) and (III) induce cytotoxic activity against cell models tested, and that

this activity correlates with alterations in cell cycle phases and induction of cell death via apoptosis.
Keywords: Apoptosis, Cell Cycle, Cytotoxicity, Ruthenium Complexes II and III.

1. INTRODUÇÃO

1.1. Câncer

O câncer é o resultado do acúmulo de alterações genéticas e epigenéticas que comprometem o controle do crescimento celular normal e a diferenciação terminal, sendo que o acúmulo de mutações no DNA é a causa subsequente ao desenvolvimento neoplásico e, consequentemente, ao surgimento da doença (HOLLSTEIN *et al*., 1991; LODISH *et al*., 2000; PARMIGIANI & CAMARGO, 2004).

A carcinogênese pode ser compreendida como um processo complexo de múltiplas etapas, podendo envolver muitos genes, particularmente os que regulam a estabilidade e o reparo do DNA (quebras e perdas cromossômicas), o crescimento celular, instabilidade genômica e mecanismos epigenéticos, a imunidade e a quimiorresistência às drogas. Os principais grupos de genes envolvidos nesse processo são: proto-oncogenes, que estimulam o crescimento celular, impedem a diferenciação e a morte celular; genes supressores de tumor, que limitam a proliferação das células, controlando negativamente a proliferação e a sobrevivência celular. O desequilíbrio desse sistema pode alterar a função de genes envolvidos, levando à proliferação descontrolada de células e ao acúmulo de sucessivas anormalidades genéticas, características do câncer (ANDERSON *et al*., 1994; NAGAI, 1999; SIGAL & ROTTER, 2000; CAVALCANTE, *et al*., 2002; GLEICH & SALAMONE, 2002; DOUCAS & BERRY 2006; DANTAS, et al., 2009).

As alterações genéticas conferem novas características fenotípicas às células neoplásicas, garantindo a malignidade tumoral, tais como: autossuficiência em sinais de crescimento, resistência aos sinais antiproliferativos, resistência à morte celular, potencial replicativo ilimitado, angiogênese sustentada, reprogramação do metabolismo energético, evasão do sistema imunológico, metástase, além de estresse metabólico, proteotóxico, mitótico, oxidativo e dano ao DNA (DIFFLEY & EVAN, 1999; HANAHAN & WEINBERG, 2011).

Em 2011, a Organização Mundial de Saúde (OMS) identificou o câncer como uma das quatro principais ameaças à saúde humana (junto às doenças cardiovasculares, doenças respiratórias crônicas e diabetes) (THE WORLD HEALTH ORGANISATION 2008-2011). Nessa pesquisa foram registrados 12,7 milhões de novos casos e 7,6 milhões de mortes por câncer no mundo.

Em pesquisa recente, a Organização Mundial de Saude (OMS), junto à Agência Internacional para Pesquisa sobre o Câncer (IARC), divulgou que em 2012, foram 14,1 milhões de novos casos de câncer e 8,2 milhões de mortes por câncer em todo o planeta. As estimativas de prevalência para 2012 mostram que houve 32,6 milhões de pessoas (com idade superior a 15 anos) que tiveram um câncer diagnosticado nos últimos cinco anos (THE WORLD HEALTH ORGANISATION 2014).

As estimativas da OMS é que haverão cerca de 22,2 milhões de novos casos de câncer diagnosticados anualmente em todo o mundo até 2030 (BRAY et al., 2012). No Brasil, de acordo com Instituto Nacional do Câncer (INCA) para o ano de 2014 aponta a ocorrência de aproximadamente 580 mil casos novos de câncer, o que representa um aumento de 11% em relação à previsão nacional para 2012 (INCA/MS, 2014).

1.2. Ciclo celular e fármacos quimioterápicos

O mecanismo de divisão celular é um evento precisamente controlado e a progressão de uma fase para outra é controlada por uma maquinaria bioquímica conservada, que não apenas coordena esse processo, mas também está ligada a sinais extracelulares de controle de crescimento e proliferação (PINTO & FELZENSZWALB, 2003; TAJARA, 2004).

De acordo com Almeida e colaboradores 2005 o ciclo celular pode ser dividido em cinco fases: G1, S, G2, M e G0. Na fase G0, as células encontram-se em repouso, ou seja, não estão replicando e a atividade nuclear é alta. Quando as células passam para a fase G1, ocorre a preparação para a divisão celular e a produção de constituintes essencias celulares que serão necessários na nova célula, além de preparar o DNA para a síntese, que irá ocorrer na fase S. Nas fases G1 e S há diversos mecanismos que regulam o processo de divisão celular. Na fase G2 haverá a síntese de componentes para a mitose e após a divisão celular, com a formação de duas células filhas e, finalizado o ciclo celular, as células tornam a entrar em G0. Entretanto, células tumorais após terminarem seu processo de replicação não retornam para G0, e assim que a fase M termina vão para a fase G1 (DE ALMEIDA *et al*., 2005).

O princípio do ciclo celular e as passagens por suas fases são controlados e regulados por proteínas como as ciclinas e quinases dependentes de ciclinas (CDK). Essas, por sua vez, checam a progressão do ciclo e mantêm as células em divisão, levando-as à apoptose, caso as condições não sejam favoráveis, no entanto, a falha de uma ciclina ou a mutação de alguma das proteínas envolvidas pode levar ao surgimento de tumores (BARBACID, 2005).

As funções de CDK são contrabalanceadas pela atividade dos inibidores de proteínas CDK (CKIS - Inibidores de Quinase-Ciclina), que incluem os inibidores universais p21 (Cdkn1a); p27 (Cdkn1b); e p57 (Cdkn1c) atuantes em vários períodos do ciclo celular, por meio de sua união a CDKS complexadas com as ciclinas. As proteínas INK4 (inibidores específicos da CDK4) têm como alvo específico as quinases dependentes de ciclinas D. Quatro diferentes proteínas INK4 foram identificadas: p15 (Cdkn2b), P16 (Cdkn2a), p18 (Cdkn2c) e p19 (Cdkn2d) (PINTO & FELZENSZWALB, 2003; TAJARA, 2004; SCHWARTZ & SHAH, 2005).

Um dos principais componentes envolvidos no ponto de checagem e no reparo de erros no DNA é o fator de transcrição TP53 (SENGUPTA & HARRIS, 2002; MEEK, 2009). O dano ao DNA induzido em células em proliferação resulta na ativação do ponto de checagem de reparo, a partir do qual ocorrem a parada do ciclo celular e o recrutamento da maquinaria de reparo, evitando assim que a informação genética incorreta seja transmitida para as células-filhas. Quando ocorrem danos à molécula de DNA, que são irreparáveis, essa proteína ativa a transcrição de vários genes envolvidos no controle celular (p21(*Cdkn1a*), *Gadd45*), bem como genes envolvidos na indução de apoptose *BAX* (Proteína X associada ao *BCL2*) (NIIDA & NAKANISHI, 2006; HOUTGRAAF & COLS, 2006).

Os *checkpoints* representam o controle do ciclo celular, um mecanismo de “prevenção”, cuja função é a de evitar o acúmulo de erros genéticos durante as divisões celulares, protegendo a integridade genômica das células. Os *checkpoints* realizam pelo menos quatro tarefas: induzem rapidamente um retardo no ciclo celular; ajudam a ativar o reparo do DNA; mantêm o ciclo celular bloqueado até que o reparo seja completado e reiniciam a progressão do ciclo. Dessa forma, as instabilidades genômicas podem resultar de defeitos nesses mecanismos de controle e assim levar à transformação de células normais em células tumorais (BARTEK & ELUKAS, 2007; MOTOYAMA & NAKA, 2004).

A perda do controle do ciclo celular é uma das principais características dos tumores. Alterações nos componentes do ciclo celular e nas vias de sinalização dos mecanismos de *checkpoint* ocorrem na maioria dos tumores humanos, sendo que essas alterações genéticas são resultantes da desregulação de oncogenes e genes supressores tumorais, os quais têm importantes implicações na otimização dos atuais regimes terapêuticos e na seleção de novos alvos do ciclo celular (STEWART *et al*., 2003).

Fármacos da quimioterapia antineoplásica atualmente utilizados exigem a compreensão da cinética do ciclo celular para o seu uso apropriado. Muitos dos mais potentes agentes citotóxicos atuam em fases específicas do ciclo celular e, portanto, têm atividade apenas em células tumorais que estão em processo de divisão (FRESHSNEY, 2007). Nos estudos *in vitro* da ação citotóxica dos fármacos antineoplásicas, verificam-se que há distúrbios do ciclo celular e, posteriormente, morte celular, embora cada fármaco apresente mecanismos de ação específicos. Isto sugere que vários estímulos citotóxicos iniciam os eventos que conduzem à morte celular (FRESHSNEY, 2000; ALMEIDA *et al*., 2005).

Considerando uma maior atividade em determinadas fases do ciclo celular, os fármacos antineoplásicos são classificados em três categorias: 1) ciclo celular específico/fase específica, 2) ciclo celular específico/fase não específica e 3) ciclo não específico, que diz respeito a fármacos que não agem necessariamente em fases de crescimento, mas em células em repouso (fase G0) (Tabela 1) (ALMEIDA *et al*., 2005). A figura 1 demonstra a atuação dos fármacos antitumorais sobre o ciclo celular.

Muitos dos agentes antineoplásicos convencionais são genotóxicos e desencadeiam respostas de ativação de *checkpoints* em ambos os tecidos normal e tumoral. As células que são deficientes no controle dos *checkpoints*, geralmente, são mais sensíveis aos danos genotóxicos ou microtubular que células com *checkpoints* ativos. No entanto, células tumorais com *checkpoint* funcionais são susceptíveis a reduzirem a eficácia desses medicamentos a partir do bloqueio da progressão do ciclo celular e facilitar o reparo do dano induzido por fármacos antineoplásicos (MEDEMA & MACUREK, 2012; GABRIELLI *et al*., 2012)

Tabela 1 – Relação entre ciclo celular e principais classes de agentes antineoplásicos (modificado de ALMEIDA *et al*., 2005).

1. Agentes ciclo-celular específicos *(CCS, "Cell Cycle-Specific")*	***2. Agentes ciclo-celular não específicos*** *(CCNS, "Cell Cycle-NonSpecific")*
1.1. Agentes Antimetabólitos	*2.1. Produtos Naturais*
1.1.a. Análogo do ácido fólico	*2.1.a. Antibióticos naturais*
1.1.b. Antagonistas das pirimidinas	*2.1.a.1. Antraciclinas*
1.1.c. Análogos das purinas e inibidores correlatos	*2.1.a.2. Mitomicina*
1.2. Agentes Hormonais	*2.1.a.3. Dactinomicina*
1.2.a. Adrenocorticosteróides	*2.1.a.4. Plicamicina*
1.2.b. Progestinas	*2.1.a.5. Bleomicina*
1.2.c. Estrogênios	*2.1.b. Alcalóides pirrolizidínicos*
1.2.d. Androgênios	*2.2. Complexos de Coordenação de Platina*
1.2.e. Antiestrogênio	*2.2.a. Cisplatina (cis-DDP)*
1.2.f. Antiandrogênio	*2.2.b. Carboplatina (CBDCA)*
1.2.g. Análogo do hormônio liberador de gonadotropina	*2.2.c Agentes Alquilantes Diversos*
1.2.h. Inibidor da aromatase	*2.3.a. Mostardas nitrogenadas*
1.2.i. Inibidor do hormônio peptídico	*2.3.b. Nitrossuréias*
1.3. Produtos Naturais	*2.3.c. Triazenos*
1.3.a. Alcalóides vegetais	*2.3.d. Alquil sulfonatos*
1.3.a.1. Alcalóides da vinca	**3) Agentes ciclo não específico**
1.3.a.2. Podofilotoxinas (Epipodofilotoxinas)	*3.1. Taxóides*
1.3.a.3. Paclitaxel (Taxol)	
1.3.b. Enzimas	

Figura 1 - Interação da ação de agentes antineoplásicos nas fases do ciclo celular.

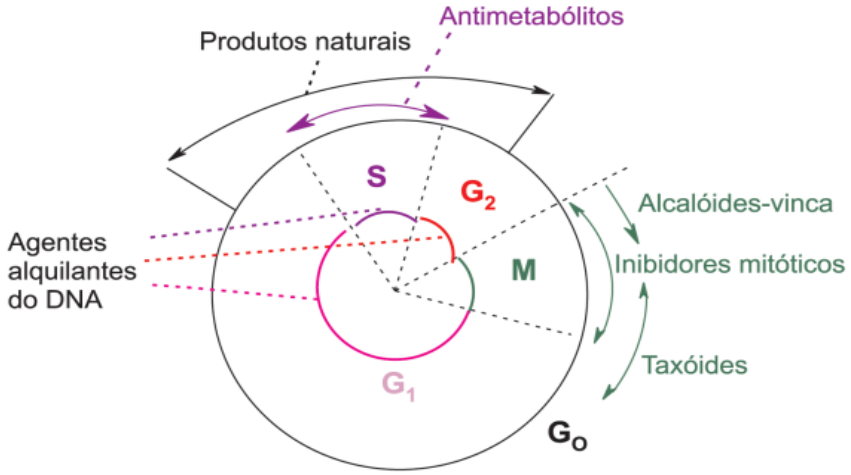

Fonte: de ALMEIDA *et al*, 2005

A radiação ionizante causa quebras de fita dupla no DNA, induzindo a ativação dos *checkpoints* nas fases G1 e G2 do ciclo celular. Os antimetabólitos,

como o hidroxiuréia, bloqueiam a replicação, parando as células na fase S do ciclo celular. Já os agentes alquilantes ou inibidores de Topoisomerase II ativam o *checkpoint* G2, enquanto drogas antimitóticas acionam o *checkpoint* mitótico (GABRIELLI *et al*., 2012).

Os agentes antineoplásicos não são ativos somente no processo de divisão celular, os mais antigos e mais usados são conhecidos como agentes alquilantes, que interagem quimicamente com o DNA. Fato é que na quimioterapia (método que utiliza compostos químicos, chamados quimioterápicos, no tratamento de doenças causadas por agentes biológicos) são descritos muitos alvos a serem estudados no intuito de que se estabeleçam novos fármacos antitumorais (ALMEIDA *et al*., 2005).

Os fármacos empregados no tratamento do câncer comprometem tanto as células normais como as neoplásicas, porém, ocasionam maior dano às células malignas que as dos tecidos normais, devido às diferenças quantitativas entre os processos metabólicos dessas duas populações celulares. Grandes avanços têm sido alcançados no desenvolvimento, seleção e aplicação de fármacos quimioterapêuticos, muitas vezes com sucessos clínicos notáveis, como no caso de tratamento para os linfomas ou de fármacos baseados em platina para o tratamento de câncer testicular. A quimioterapia antineoplásica tem como objetivo o tratamento de diversos tumores malignos, tornando-se uma das mais importantes e promissoras maneiras de combate ao câncer. Essa forma de tratamento pode ser empregada de maneira curativa ou paliativa, dependendo do tipo e extensão do tumor e da condição física do paciente (MEALEY *et al*., 1994).

Os quimioterápicos antineoplásicos podem ser classificados em: (1) agentes alquilantes, que atuam por meio da formação de ligações covalentes com o DNA, impedindo sua replicação; (2) antimetabólicos, que bloqueiam ou subvertem uma ou mais vias metabólicas envolvidas na síntese do DNA; (3) medicamentos obtidos por produção natural ou alcalóides; (4) hormônios, dos quais os mais importantes são os esteróides, isto é, glicocorticóides, estrogênios e androgênios e fármacos que suprimem a secreção de hormônios ou antagonizam sua ação; (5) imunoterápicos, embora ainda incipiente; (6) antibióticos, grupos de substâncias com estrutura química diversa, que interagem com o DNA e inibem a síntese de proteínas; (7) inibidores mitóticos, que levam à paralisação da divisão celular em metáfase ao atuarem sobre a tubulina, proteína formadora do fuso; (8) drogas alvo-dirigidos, o objetivo do tratamento com essas drogas é dirigi-las a uma

molécula anormal da célula de câncer, impedindo seu funcionamento (anticorpos e inibidores de quinases); (9) outros agentes com mecanismos de ação que não permitem a inclusão nos grupos apresentados anteriormente, como a dacarbazina, indicada no tratamento do melanoma avançado, sarcomas de partes moles e linfomas (GOODMAN & GILMAN, 2002).

1.3. Tipos de Morte celular

Desde as primeiras descrições do mecanismo de morte celular programada, que datam de meados dos anos 1960, (LOCKSHIN & WILLIAMS 1964; KERR 1965; LOCKSHIN & WILLIAMS, 1965; ELMORE, 2007), o termo apoptose foi usado pela primeira vez em um clássico artigo de Kerr, Wyllie e Currie em 1972 para descrever uma morte celular morfologicamente distinta, embora o conceito de apoptose tenha sido explicitamente descrito muitos anos antes (KERR *et al*, 1972;. PAWELETZ, 2001; KERR, 2002; ELMORE, 2007).

No entanto, é importante notar que outras formas de morte celular programada têm sido descritas e outras formas ainda podem ser descobertas (FORMIGLI *et al*., 2000; SPERANDIO *et al*., 2000; DEBNATH *et al*., 2005; GALLUZZI *et al*., 2012). Várias tentativas têm buscado classificar a morte celular com base nas características morfológicas, mas estudam mostram que somente este critério não é suficente na classificação de formas de morte celular (SCHWEICHEL & MERKER, 1973).

De acordo com o Comitê de Nomenclatura sobre Morte Celular (NCCD), a morte celular pode ser classificada de acordo com critérios morfológicos, enzimáticos (sem envolvimento de nucleases ou com o envolvimento de distintas classes de proteases como caspases, catepsinas e transglutaminase) e aspectos funcionais (morte programada ou acidental, fisiológico ou patológico) (KROEMER *et al*., 2009; GALLUZZI *et al*., 2012).

Considerando os vários critérios de classificação citados acima, os tipos de morte celular, segundo Galluzzi *et al*., (2012), são: apoptose, necrose regulada, autofagia e catástrofe mitótica. Além dessas, outras modalidades de morte celular, tais como anóiques, entose, piroptose, têm sido citadas como novas modalidades (Tabela 2).

Tabela 2 - Classificação funcional das formas de morte de células regulares (modificado de GALLUZZI et al., 2012).

	Principais características bioquímicas	**Dependência de Caspase**	**Exemplos de intervenções inibitórias**
Anoiques	Regulação baixa de EGFR. Inibição de ERK1 sinalizando falta de ß1-integrina engajada. Superexpressão de BIM. Caspase-3 (-6,-7) ativação.	++	BLC-2 superexpressão, administração de Z-VAD-fmk
Morte de célula autofágica	Lipidação de MAP1LC3 Degradação de SQSTM1	--	Inibidores VPS34. Inibição genética de AMBRA1, ATG5 , ATG7, ATG12 ou inibição genética de BCN1
Apoptose intriseca dependente de caspase	MOMP. Dissipassão irreversível de ΔΨm		Superexpressão de BLC-2. Administração de Z-VAD-fmk
Independencia de caspase intríseca apoptose	Liberaçáo de proteínas IMS. Inibição de corrente respiratória	--	Superexpressão de BLC-2
Entose	Ativação de RHO. Ativação de ROCK1		Inibição genética de metalotioneína 2A. Inibição de lisossomal
Apoptose extrínseca por morte de receptores	Dependencia de sinalização de receptor. Ativação de Caspase-8 (-10). Abertura de BID e MOMP (em células de tipo II). Ativação de Caspase-3 (-6 -7)	++	Expressão de CrmA. Inibição genética de Caspases (8 e 3)
Apoptose extrínseca por dependência de receptores	Dependência de sinalização de receptor. Ativação de PP2A. Ativação de DAPK1. Ativação de Caspase-9. Ativação de Caspase-3 (-6, -7).	++	Inibição genética de Caspases (9 e 3). Inibição genética de PP2A. Administração de Z-VAD-fmk.
Catástrofe Mitótica	Ativação de caspase-2 (em algumas instancias) Ativação de TP53 ou TP73 (em algumas instancias); araste mitótico	--	Inibição genética de TP53 (em algumas instancias) Farmacológica ou inibição genética de caspase-2 (em algumas instancias)
Necroptose	Sinalização de receptor de morte. Inibição de Caspase. RIP1 e/ou RIP3 ativação	--	Administração de necrostatin(s). Inibição genética de RIP1/RIP3

Netose	Inibição de Caspase. Ativação de oxidase NADPH	--	Inibição de autofagia. Inibição de oxidase NADPH. Inibição genética de PAD4
Piroptose	Ativação de Caspase-1. Ativação de Caspase-7. Secreção de IL-1ß e IL-18	++	Administração de Z-YVAD-fmk. Inibição genética de Caspase-1

Abreviações: ATG, autofagia; BCN1, beclin 1: ΔΨm potencial transmembranar mitocondrial; CrmA, modificador de resposta citocian A; DAPK1, proteina quinase associada a morte 1; EGFR, receptor de fator de crescimento da epiderme; ERK1, regulador extracelular de quinase 1; IL, interleucina; MAP1LC3, proteina leve 1 do microtubulo associada a cadeia 3; MOMP, permebialização da membrana externa mitocondria; NET, armadilha extracelular de neutrófilos; PAD 4, peptidilarginine deiminase 4; PAR, poli(ADP-ribose); PARP1, poli(ADP-ribose) polimerase 1; PP2A, proteina fosfatase 2A; ROCK1, RHO-associada, proteína quinase enrolada em espiral 1; SQSTM1, sequestosome 1; TG, transglutaminase; Z-VAD-fmk, N-benziloxicarbonil-Val-Ala-Asp-fluorometilquetone; Z-YVAD-fmk, N-benziloxicarbonil-Tyr-Val-Ala-DL-Asp-fluorometilquetone. Para fins de classificação, as intervenções farmacológicas e genéticas devem ser consideradas inibitórias quando realmente reduzir a incidência de morte celular, mas não quando provocar apenas uma mudança entre modalidades diferentes de células de morte ou quando alterar a morfologia da morte celular.

A necrose foi considerada por muito tempo como um mecanismo de morte celular acidental. É um processo que envolve a perda da integridade da membrana celular, com inchaço citoplasmático, formação de vacuolos, retículo endoplasmático inchado, distenção ou rompimento mitocôndrial, lise dos lisossomos e liberação do conteúdo citoplasmatico para o tecido circundante (MAJNO & JORIS 1995; TRUMP *et al*., 1997; CHAMOND *et al*., 1999) levando a inflamação (KUROSAKA *et al*., 2003) (Tabela 2).

A partir do trabalho de vários laboratórios de pesquisa, atualmente está claro que a necrose pode ocorrer de forma regulada, a partir de um mecanismo chamado “necroptose”, cujo papel é importante em processos fisiológicos e patológicos (FULDA, 2013). O termo “necroptose” tem sido recentemente utilizado como um sinônimo de necrose programada que depende da atividade da Proteína Quinase e da Interação com Receptor-1 (RIPK1) (KROEMER *et al*., 2009).

Marcadores clássicos de apoptose, como condensação de cromatina e fragmentação nucleossomal de DNA não são vistos em morte via necrose (BROWN e ATTARDI, 2005). Entretanto, semelhantes à apotose, células necróticas externalizam a fosfatidilserna antes da permeabilização da membrana plasmática, promovendo, assim, o seu reconhecimento pelos fagócitos (GALLUZZI *et al*., 2011).

Atualmente os mecanismos moleculares responsáveis pela necroptose estão em processo de identificação. A ativação da necroptose pode acontecer pelos mesmos ligantes que ativam a apoptose, como Fator de Necrose Tumoral (TNF). Nessa via, o ligante TNFα se liga ao receptor TNFR1; desse modo, essa interação

aciona o recrutamento das proteínas de Domínio de Morte Associado à TNFR (TRADD), RIP-1, (Proteínas inibidoras de Apotose) IAPs, Fator Associado a TNFR2 (TRAF-2) e Fator Associado a TNFR5 (TRAF-5), que constituem uma estrutura chamada de complexo I. As proteínas IAPs realizam a poliubiquitinação de RIP-1, acionando a ativação de NF-kB. No entanto, quando RIP-1 sofre desubiquitinação, a composição do complexo se modifica passando a se chamar complexo II (GALLUZZI *et al*., 2011).

O complexo II, também chamado de Complexo de Sinalização de Indução de Morte (DISC), é constituído por RIP-1, Proteína Quinase de Interação com Receptor-3 (RIPK-3), TRADD, Domínio de morte associada ao CD95(FADD) e CASP8 (caspase-8). Na presença de CASP8 (caspase-8) ativa, RIP-1 e RIP-3 são desativadas, acarretando em apoptose. No entanto, quando CASP8 (caspase-8) não pode ser ativada devido a condições genéticas ou farmacológicas, RIP1 e RIP3 são fosforiladas, formando assim um complexo molecular chamado de necrossoma (Figura 2). O necrosoma, por sua vez, estimula para múltiplos sinais pró-necróticos, tais como: permeabilização da membrana lisossomal e liberação citosólica de hidrolases lisossomais, ativação de esfingomielinases (SMases) e alterações metabólicas nas mitocôndrias, resultando na geração de espécies reativas de oxigênio (ROS), que danificarão diretamente macromoléculas, incluindo o DNA, proteínas, lípideos, e promoverão o decréscimo abrupto dos níveis de ATP (GALLUZZI *et al*., 2011; NIKOLETOPOULOU *et al*., 2013).

A autofagia é um processo catabólico altamente regulado que envolve a degradação de componentes próprios de uma célula a partir da maquinaria lisossomal. A autofagia desempenha um importante papel no crescimento celular, desenvolvimento e homeostase, ajudando a manter um equilibrio entre síntese, degradação e subsequente reciclagem dos produtos celulares (GALLUZZI *et al*., 2011).

Com base em características morfológicas, o termo “morte celular autofágica” tem sido amplamente empregado para indicar tipos de morte celular que são caracterizados por uma enorme vacuolização citoplasmática, frequentemente (embora nem sempre) indicando aumento do fluxo autofágico. Embora tal expressão originalmente não indique qualquer consideração funcional, os cientistas têm adotado o termo "morte celular autofágica" para indicar que autofagia seria realmente o falecimento celular (Tabela 2) (GALLUZZI *et al*., 2012).

Figura 2: Via de sinalização molecular da necroptose.

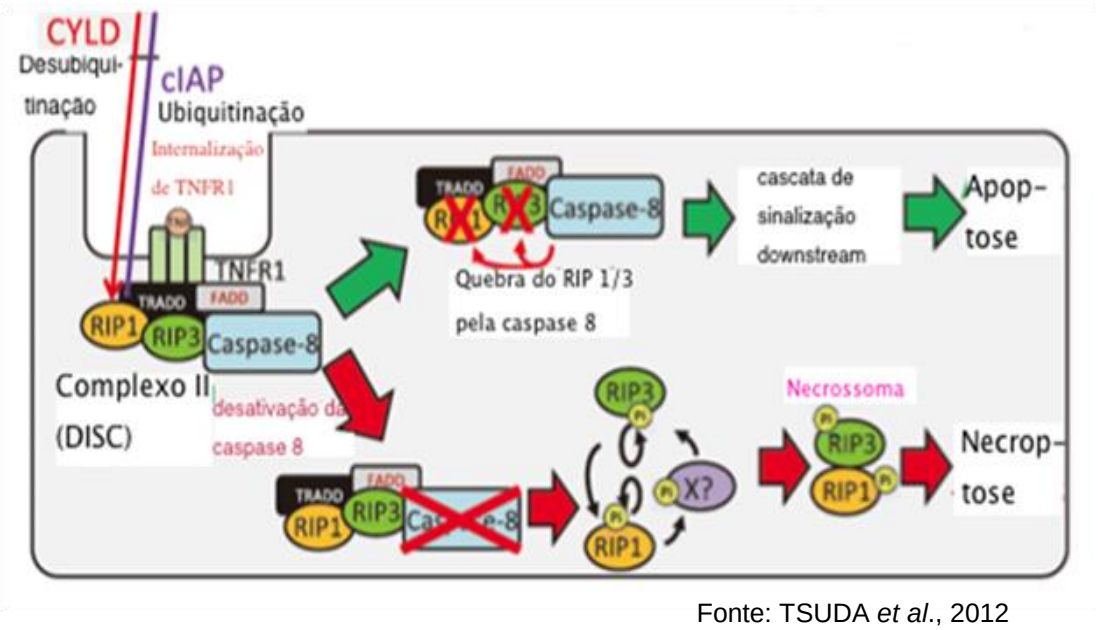

Fonte: TSUDA *et al*., 2012

O termo “morte celular autofágica” aplica-se a dois mecanismos distintos. Em primeiro lugar, processos fisiológicos de morte celular *in vivo* são mediados por autofagaia, durante o desenvolvimento da *D. melanogaster*. Em segundo lugar, autofagia parece ser responsável pela morte de algumas células cancerosas (especialmente quando moduladores essenciais de apoptose como BAX e BAK ou caspases ausentes). No entanto, na maioria dos casos conhecidos, autofagia constitui uma resposta citoprotetora ativada pelas células que morrem na tentativa de lidar com stress, o que não impede a morte celular. Ao contrário do processo de apoptose, as células que morrem por autofagia têm pouca ou nenhuma associação com o processo de fagocitose (KELEKAR, 2005; KROEMER *et al*., 2009).

"Catástrofe mitótica" é o tipo de morte celular que ocorre durante a mitose; refere-se ainda a casos de morte celular que são desencadeadas por mitose anormal e executada durante a mitose ou na interfase subsequente. É resultante de uma segregação cromossômica anormal ou de danos induzidos à molécula de DNA, acompanhados de defeitos nos *checkpoints*. Estes danos normalmente levam a alterações morfológicas, como formação de células com múltiplos micronúcleos (multinucleação) (Tabela 2) (CASTEDO *et al*., 2004; KROEMER *et al*., 2009, GALLUZZI *et al*., 2012).

A catástrofe mitótica pode ser induzida por danos de agentes hiperpolimerizadores (taxanos, epotilones), agentes despolimerizadores (como alcaloides da vinca e colchicina) e agentes que danificam o DNA. Células tumorais são, na maioria das vezes, deficientes nos *checkpoint* do ciclo celular, o que as torna mais susceptíveis à mitose catastrófica após tratamento com fármacos antineoplásicos (CASTEDO *et al*., 2004; GALLUZZI *et al*., 2012) (Tabela 2).

Anóiques, termo introduzido por Frisch e Francis em 1994, é uma modalidade de morte celular descrita para a resposta apoptótica de células aderentes devido à ausencia da matriz celular. Deve notar-se que a maioria, se não todos, dos casos de morte celular anóiques é executada pela maquinaria molecular de via intrínseca de apoptose (Tabela 2) (GALLUZZI *et al*., 2012).

Entose, termo introduzido em 2007 por Overholtzer e colaboradores, é um mecanismo de morte celular no qual há "célula-em-células". O termo entose só pode ser usado para designar morte celular quando todas as seguintes caracteristicas são observadas: em primeiro lugar, as células englobadas nunca devem sair do fagossomo e devem ser degradadas no lisossoma; em segundo lugar, o fenótipo de "célula-em-célula" deve surgir a partir de interações homotípicas e não deve envolver fagócitos; em terceiro lugar, o processo não deve ser sensível às intervenções químicas e genéticas que normalmente bloqueiam apoptose intrínseca dependente e independente de caspase (GALLUZZI *et al*., 2012) (Tabela 2).

Piroptose termo introduzido em 2000 por Brennan e Cookson para descrever a morte peculiar de macrófagos funcionalmente infectados com *Salmonella typhimurium* (GALLUZZI *et al*., 2012) (Tabela 2).

1.4. Apoptose

A apoptose é uma forma característica de morte celular programada, com importante papel durante o desenvolvimento e a homeostase celular, bem como em uma variedade de doenças, como o câncer (WYLLIE *et al*., 1980; RAMENGHI *et al*., 2000; MAURILLO *et al*., 2001).

Ao sofrer apoptose, a célula apresenta alterações morfológicas e bioquímicas típicas. A célula apoptótica é caracterizada pelo encolhimento celular e condensação, fragmentando-se e formando os corpos apoptóticos. O vazamento do Citocromo c da mitocôndria para o citosol é uma das primeiras características

bioquímicas, assim como a externalização da fosfatidilserina na membrana celular, ativação de proteasese, fragmentação do DNA internucleossomal em fragmentos de 180 a 200 pares de bases. A externalização de fosfatidilserina precede a maioria das alterações morfológicas e bioquímicas citadas (MARTIN *et al*., 1995; HENGARTNER, 2000; COOPER, 2007). No entanto, essas alterações bioquímicas não devem ser utilizadas para definir morte celular via apoptose, uma vez que esse tipo de morte celular pode ocorrer sem a fragmentação de DNA, assim como sem a ativação de caspases (GALLUZZI *et al*., 2007; LIU *et al*., 2009).

As vias de sinalização que desencadeiam o processo apoptótico são complexas, sendo subdivididas principalmente em duas: apoptose extrínsica, apoptose intrínsica (dependente de caspase e independente de caspase) (Tabela 2). O termo "apoptose extrínseca" tem sido amplamente utilizado para indicar os casos de morte celular por apoptose, que são induzidos por sinais de estresse extracelulares sendo sentidos e propagados por receptores transmembranares específicos (TNF) (Figura 3). A apoptose intrínsica pode ser desencadeada por uma infinidade de estresse intracelular, incluindo danos no DNA, estresse oxidativo, acúmulo de proteínas desordenadas no retículo endoplasmático (RE) e muitos outros. Embora a cascata de sinalização que desencadeia a apoptose intrínseca seja altamente heterogênea, tanto quanto os estímulos iniciadores, todos os mecanismos são ligados a uma mitocôndria (Figura 3) (GALLUZZI et al., 2012).

A via do processo apoptótico extrínseca é mediada por receptores de morte (TNF, TNFR1, TRAMP, TRAIL e de Fas) presentes na membrana plasmática, e a via intrínseca é mediada pela mitocôndria (HAJRA & LIU, 2004; HAIL et al., 2006). Tanto a via extrínseca quanto a intrínseca possuem um grupo independente de caspases iniciadoras (casp2, 8, 9 e 10), que convergem sinais para o mesmo grupo de caspases efetoras (casp3, 6 e 7) com finalidade de executar eventos intracelulares que resultarão na morte celular programada (HAJRA & LIU, 2004; ZHANG et al., 2004).

A via apoptótica extrínseca é desencadeada pela interação entre sinais de morte celular, como FASL/CD95 (receptor de superfície envolvido na ativação da apoptose), TNFR (receptor do fator de necrose tumoral) ou receptores TRAIL (Fator de Necrose Tumoral). O estímulo do ligante de morte resulta na oligomerização dos receptores e recrutamento da proteína adaptadora Domínio de Morte FAS-associada (FADD) e recrutamente de caspase iniciadora; casp8, formando o complexo de

sinalização de indução de morte (DISC). A auto-ativação da casp8 no DISC é seguida pela ativação de caspases efetoras, incluindo as casp3, 6, e 7, que atuam como efetoras à jusante do programa de morte celular (ASHKENAZI & DIXIT, 1998; HAJRA & LIU, 2004; HAIL *et al*., 2006; GALLUZZI *et al*., 2012).

Ainda, há ativação de outros receptores de morte na membrana plasmática, especialmente do receptor de estresse celular, bem como ação das caspases iniciadoras casp8 e 10, que integram sinais de apoptose de via extrínseca àqueles de via intrínseca. Assim, é preciso avaliar sinais na membrana plasmática capazes de agir sinergicamente com sinais mitocondriais na indução de apoptose (HAJRA & LIU, 2004; HAIL *et al*., 2006). Em células conhecidas como células de tipo 1, a ativação de casp8 é suficiente para ativar diretamente as caspases efetoras casp3 e 7, para completar a excecução da apoptose de uma maneira independente da via mitocôndrial. Já em células como hepatócitos e células pancreáticas β (células de tipo II), casp8 medeia a clivagem proteolítica de BID (Domínio de Morte de Interação com BH3), que leva à geração da permeabilização da membrana mitocondrial e, consequentemente, à ativação da via intrínseca ou mitocondrial (Figura 4) (LI & YUAN, 2008; GALLUZZI et al., 2012).

A ativação da via extrínseca pode ser desencadeada também por meio da via de receptores dependentes. Um exemplo diz respeito aos receptores UNC5A-D e Deleção Carcinoma Coloretal (DCC), os quais exercem funções de apoptose somente quando os níveis de seus ligantes (Netrina-1) estão em baixas quantidades na célula. A indução de apoptose a partir do receptor DCC é ativada quando, na ausência de seus ligantes, DCC interage com as proteínas TUCAN e DRAL para a montagem do complexo, o qual irá ativar a pró casp9. O receptor UNC5-B, na ausência do seu ligante Netrina-1, induz a apoptose a partir do recrutamento da proteína fosfatase 2A (PP2A), a qual irá realizar a desfosforilação/ativação da proteína DAPK (Proteína Quinase serina/treonina Associada à Morte). A proteína DAPK induzirá a permeabilização da membrana mitocondrial externa (MOMP) e a ativação das casp9 e casp8 (via Bid) (Figura 4). Efetores a jusante da proteína DAPK permanecem desconhecidos, mas DAPK é conhecida por induzir a morte celular por mecanismos dependentes e independentes de Tp53 (GALLUZZIet al., 2012; DELCROS e MEHLEN, 2013).

Figura 3 - Ativação da apoptose pelas vias extrínseca e intrínseca.

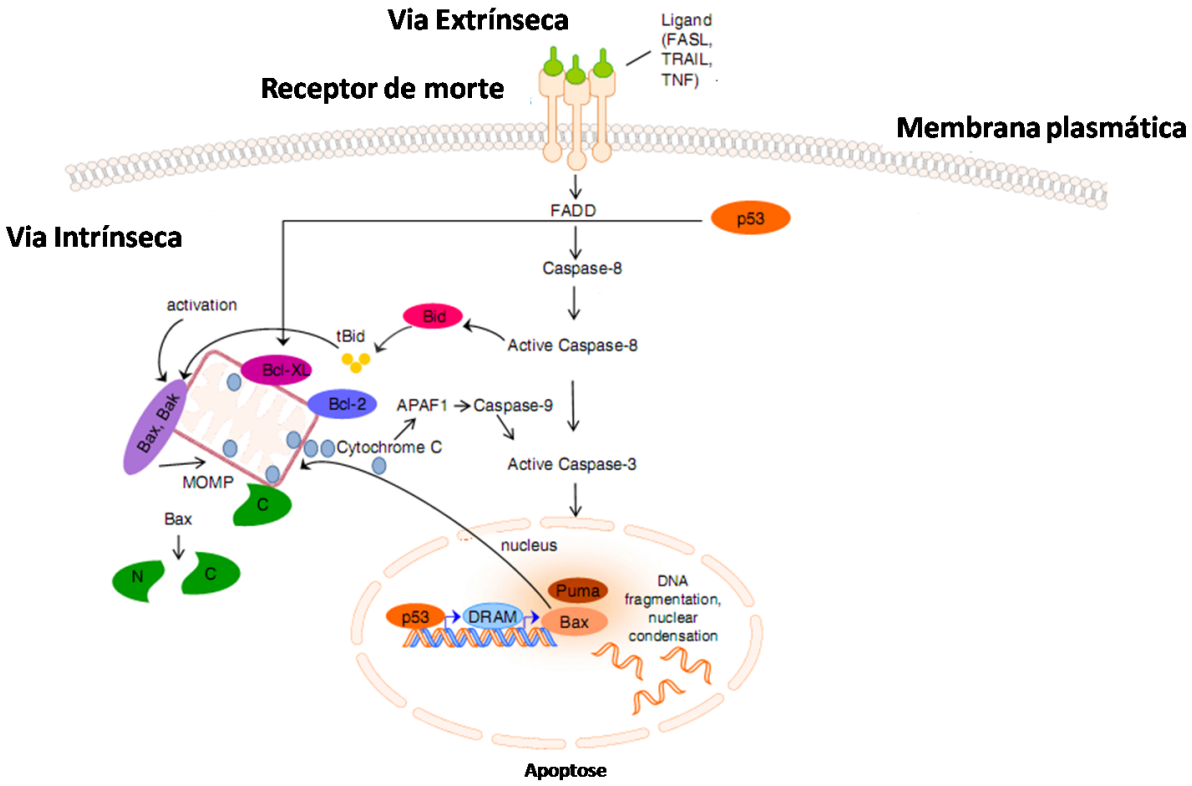

Fonte: adaptado de NIKOLETOPOULOU, 2013

A via intrínseca é desencadeada pela ação de diferentes sinais de estresse intracelular, tais como irradiação, agentes quimioterápicos, vírus, bactérias, ausência de fatores de crescimento celular e hipóxia, os quais convergem para a mitocôndria. Esta organela contém, no seu espaço intermembranar, fatores apoptogênicos, como citocromo c, AIF (*Apoptosis-Inducing Factor*) pró casp2, 3 e 9, SMAC/DIABLO (*Second Mitochodria-DerivedA activator of Caspases/direct IAP binding protein with low pI*), Omi/HtrA2 (*High temperature requirement protein-2*) e endonuclease G[53]. Além dessas proteases e as calpainas, catepsina B, gramenzima A e B, na presença de sinais apoptóticos, podem ser liberadas no citoplasma, sendo que algumas delas participam da ativação das caspases. Entretanto, dados recentes sugerem que estas podem acionar mudanças morfológicas características de apoptose de maneira independendente de caspases. Essa via apoptótica, centrada na mitocôndria, é conhecida como via intrínseca mitocondrial ou via de ativação das caspases dependente ou idependete da mitocôndria (SHARMA *et al*., 2000; MORAES *et al.,* 2007; JAATTELA E MATHIASEN, 2002; GALLUZZI *et al*., 2012).

Figura 4: Via de sinalização de receptores de morte e receptores dependentes

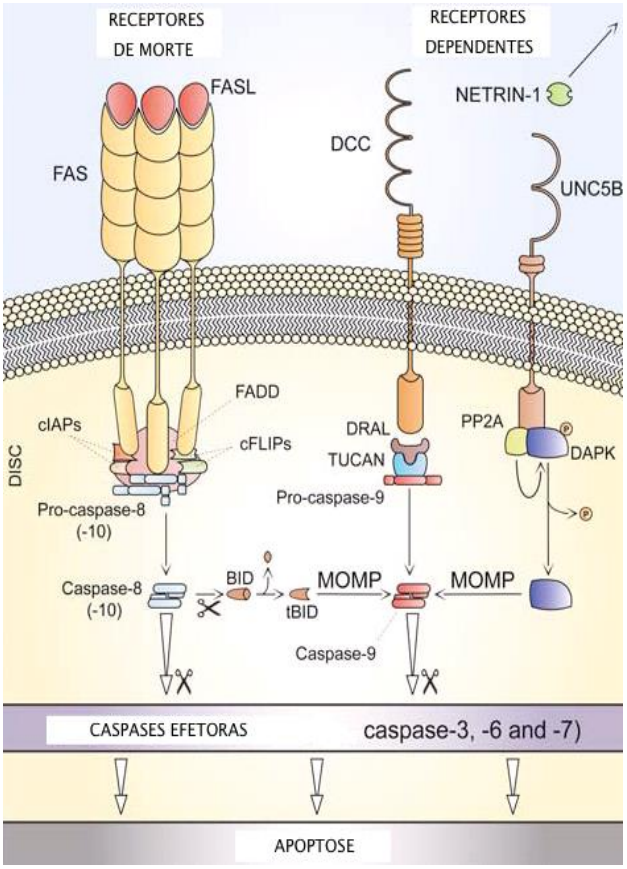

Fonte: GALLUZZI et al., 2012

A regulação da via mitocondrial é realizada pelos membros da família BCL2, proteínas citoplasmáticas capazes de integrar sinais de sobrevida ou morte celular gerados nos meio intra e extracelular (KOLLENKO et al., 2000). Essa família subdivide-se em duas classes: proteínas pró-apoptóticas (BAX, BCLXL, BCLW, McCL1, A1), as quais sensibilizam ou conduzem a célula à apoptose e anitiapoptóticas (BCL2 e BCLX) (KOLLENKO *et al*., 2000). A via mitocondrial também é susceptível à regulação negativa pelas proteínas da família dos IAPs (CIAP1 e CIAP2, XIAP e Survivina), as quais podem inibir, por exemplo, as CASP3 e 9, cuja atividade pode ser bloqueada pelo SMAC (segundo ativador mitocondrial de caspases) (Figura 5) (KOLLENKO *et al*., 2000; SHI, 2002).

Além da liberação de moléculas apoptogênicas, a alteração do potencial de membrana mitocondrial interna e a transição da permeabilidade mitocondrial levam ao colapso dessa membrana, interrompendo a síntese de ATP e aumentando, consequentemente, a produção de espécies reativas de oxigênio (GALLUZZI *et al*.,

2012).

Na via dependente de caspases, a liberação do citocromo c, a partir da mitocôndria, leva à ativação de casp 3 a partir da ligação do citocromo c à proteína adaptadora APAF1 (Protease Apoptótica Ativadora de Fator 1) e à pró casp9, levando à formação do apoptossomo e à ativação da CASP9, a qual ativará outras caspases, como as pró casp3 e 7, culminando na apoptose via mitocondrial. As proteínas Smac/Diablo e Omi/HtrA2 facilitam a ativação das caspases a partir do sequestro ou degradação de proteínas da família IAPS (STEPHEN & GREEN, 2010; GALLUZZI *et al*., 2012).

Mecanismos envolvendo a participação de proteases, como Calpainas, Catepsina B, Granenzima A e B, Omi/htra2, Endonuclease G e AIF, têm demonstrado induzir morte celular programada por mecanismos independentes de caspases. Essas proteases, na maioria das vezes, cooperam na via apoptótica dependente de caspases. Entretanto, dados recentes sugerem que elas também podem acionar mudanças morfológicas características de apoptose de maneira independente de caspases. No mecanismo de apoptose independente de caspases, as proteínas AIF e Endonuclease G relocam para o núcleo, no qual atuarão a partir da clivagem da molécula de DNA. Já a proteína Omi/htra2 atua por meio de sua atividade serina protease e realiza a clivagem de vários substratos, dentre esses as proteínas do citoesqueleto (JAATTELA & MATHIASEN, 2002; GALLUZZI *et al*., 2012). A figura 5 demonstra a via mitocondrial dependente e independente de caspase.

Pesquisas realizadas sobre o processo de apoptose demonstram que este é um processo importante na quimioterapia do câncer, uma vez que a maioria dos fármacos anticancerígenos exerce seu efeito antitumoral a partir da indução de apoptose. Trabalhos na literatura têm demonstrado que fármacos convencionais, tais como flavopiridol, cisplatina, paclitaxel, doxorrubicina, induzem apoptose em células tumorais *in vitro* (ACHENBACH *et al*., 2000; MIZUTANI *et al*., 2005; BRENES *et al*., 2007). Em muitos casos, a terapia anticancerígena eventualmente resulta na ativação de caspases, sendo que tal ativação em resposta à quimioterapia pode ser iniciada a partir da ativação da via extrínseca ou através da mitocôndria pela estimulação da via intrínseca (FULDA e DEBATIN, 2006).

Figura 5: Via de apoptose mitocondrial dependente e independente de caspases

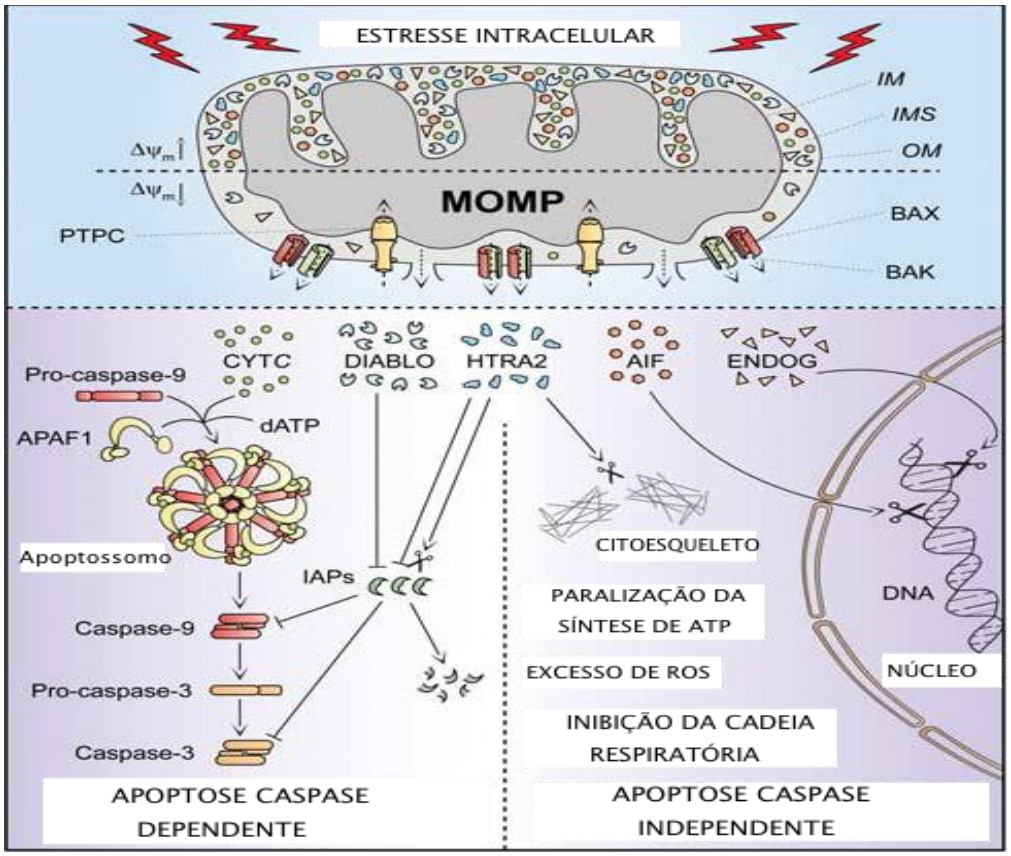

Fonte: GALLUZZI *et al*., 2012

Apesar dos avanços alcançados, alguns tipos de tumores, como os sarcomas e leucemias, monstram limitações em relação aos tratamentos quimioterápicos atuais, assim como grande resistência aos estímulos apoptóticos induzidos pelos agentes antitumorais (KIM *et al*., 2002; GHOBRIAL *et al*., 2005; VILLEDIEU *et al*., 2007; BRENES *et al.,* 2007).

1.5. Compostos baseados em metal usados na terapia antitumoral

Metais preciosos já eram usados para propostas medicinais a.C. (há mais de 3500 anos atrás). O ouro foi utilizado em várias áreas da medicina na Arábia e China. Naquela época, metais nobres eram confiáveis no benefício à saúde, pela sua raridade, contudo, pesquisas recentes têm associado as propriedades medicinais de fármacos inorgânicos as suas propriedades biológicas específicas (ALLARDICE & DYSON, 2001).

Em meados da década de 1960, Rosenberg e colaboradores, descobriram, por acaso, as propriedades anticancerígenas da cisplatina {*cis*-[$PtCl_2(NH_3)_2$]} (Figura 6), durante as investigações do efeito de campos elétricos sobre o crescimento de *Escherichia coli*. Os pesquisadores estavam usando eletrodos de platina em uma solução contendo cloreto de sódio e sais de amônio, entre outros constituintes, quando observaram um evento inesperado, as bactérias tornaram-se longos filamentos e passaram a não se replicar. A divisão celular de *E. coli* havia sido inibida. Uma análise mais extensa desta observação levou à conclusão de que o ciclo replicativo bacteriano foi inibido por complexos amino-platina formados por eletrólise (PIZARRO *et al*., 2009).

Figura 6 - Estrutura química da cisplatina.

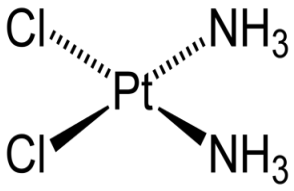

Fonte: PIZARRO et al., 2009

A pesquisa e o desenvolvimento de fármacos à base de metais foram impulsionados a partir dessa descoberta e, desde então, complexos inorgânicos têm sido alvo de inúmeras pesquisas terapêuticas, com numerosas aplicações em diversos ramos da medicina, inclusive o câncer (DYSON & SAVA, 2006; SUSS-FINK, 2010; SABALE *et al*., 2012).

Mais de 40 anos após a sua aprovação como um agente quimioterápico pela *Food and Drug Administration* norte-americana (FDA), fármacos à base de cisplatina ainda são os antineoplásicos mais utilizados do mundo. A quimioterapia à base de cisplatina é responsável pela cura de mais de 90% dos casos de câncer testicular e desempenha um papel importante em alguns tratamentos contra o câncer de cabeça e pescoço, de plumão, de ovário, câncer cervical, câncer de bexiga, melanoma e linfomas (PIZARRO *et al*., 2009).

Vários análogos de cisplatina, como a *cis*-diamina (ciclobutano-1,1-dicarboxilato)-platina(II), ou carboplatina, a oxaliplatina(l-OHP) são utilizados na terapia antineoplásica mundial; a nedaplatina, a heptaplatina (SKI), a lactato 1,2-di(aminometil)ciclobutanoplatina(II), ou lobaplatina são utilizados somente no Japão,

China e Coreia (Figura 7), além de serem aplicados nos estudos de tumores que exibem resistência à cisplatina. Estes compostos são chamados de “geração secundária” dos compostos de platina (CALAMAI *et al*., 1998; HARTINGER *et al*., 2006; PIZARRO *et al*., 2009).

Figura 7 – Estrutura química de antitumorais baseados em compostos de platina

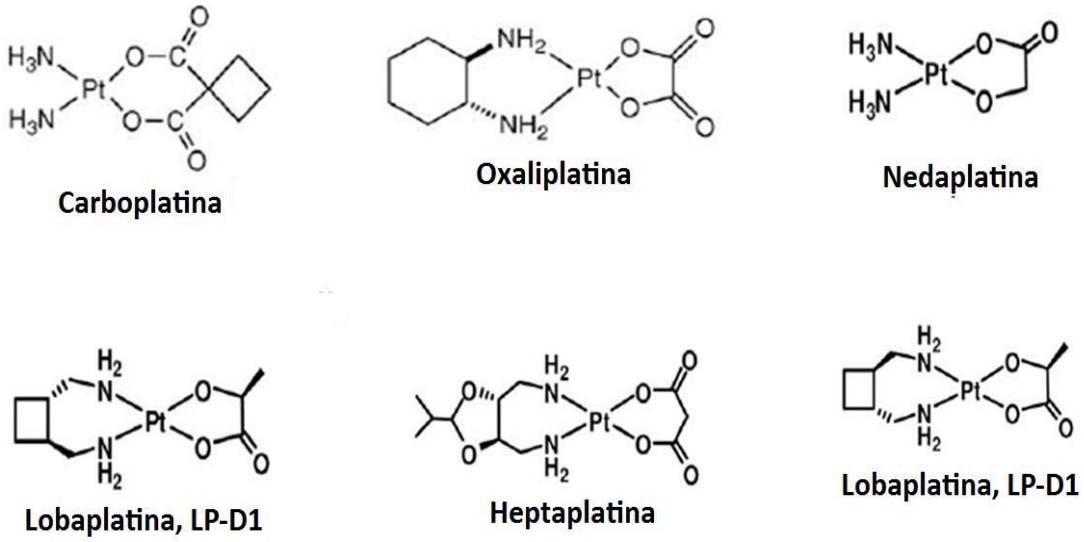

Fonte: LOOKICH & ANDERSON, 1998

O mecanismo de ação da cisplatina não está completamente elucidado. Estudos para descrever o mecanismo de ação foram realizados e eles observaram que antes de chegar ao interior celular, a cisplatina passa por reações de substituições, nas quais a principal seria a reação de hidrólise substituindo os ligantes cloretos (FONTES et al., 2005). Atualmente, é reconhecido que o alvo de ação de compostos à base de platina é a molécula de DNA, causando danos irreversíveis; evitando que a célula seja capaz de se replicar, o que leva, portanto, à morte celular (REEDIJK *et al*., 1987; PAGE 2012).

A ligação da platina ocorre preferencialmente nos átomos de nitrogênio das bases púricas do DNA, sendo que a interação mais estável é com o nitrogênio da guanina. Há vários tipos de ligação que podem ser formadas entre o DNA e a platina, visto que as principais são: monofuncionais; bifuncionais, que podem ser de três tipos – intrafita, interfita (Figura 8) e intermolecular. Devido ao fato da platina se ligar à molécula de DNA, observa-se que o processo de divisão celular é inibido, dessa forma qualquer composto que interfira nesse processo é considerado

citotóxico, podendo levar à morte celular. Compostos que apresentam esse mecanismo de ação são utilizados para o tratamento de neoplasias (FONTES *et al*., 2005).

Figura 8 – Ligação intrafita (à esquerda) e interfita (à direita) de compostos de platina e a molécula de DNA

Fonte: FONTES *et al*., 2005

Mesmo os fármacos baseados em de platina sendo utilizados mundialmente no tratamento de neoplasias, sérias limitações são enfrentadas durante a administração desses fármacos, como sintomas gastrointestinais (náuseas, vômitos, diarreia), nefro e neurotoxicidade. Outro problema enfrentado é a resistência, pois, após 4 a 6 ciclos de tratamento, os tumores, inicialmente sensíveis ao medicamento, tornam-se resistentes (KARTALOU e ESSIGMANN, 2001; JIRSOVA et al., 2006). Essas limitações têm estimulado a busca de novos complexos metálicos de transição que apresentem reduzida toxicidade e melhor efetividade, tais como complexos contendo rutênio, gálio, ferro, titânio, ouro (LOKICH & ANDERSON, 1998; KOSTOVA, 2006; ALAMA *et al*., 2009).

1.6. Complexos de Rutênio e seu Mecanismo de Ação

Em 1970, Clarke e colaboradores relataram que o rutênio (III) foi capaz de inibir a síntese de DNA e proteínas em células de carcinoma de nasofaringe *in vitro*, o que desencadeou o interesse em complexos de rutênio como potenciais fármacos anticancerígenos. Durante a década seguinte, Mestroni e colaboradores desenvolveram complexos hexacoordenados com Ru (II) dimetilsulfóxido e ligantes de cloreto, em particular os *cis*- e *trans*-$RuCl_2$ (dimetilsulfóxido)$_4$, que apresentam

atividade anticancerígenas*in vitro* e *in vivo*. Os complexos mostraram interagir tanto *in vitro* quanto *in vivo* com o DNA, seu alvo mais provável (PIZARRO *et al*., 2009).

A partir dos trabalhos de Clarke e Mestroni há mais de 30 anos, uma grande quantidade de complexos de rutênio tem sido sintetizada e testada para avaliação de possível atividade antitumoral. Os compostos de rutênio formam compostos com os mais variados ligantes e apresentam química bem “estável”, o que amplia as possibilidades de aplicações biológicas. Os estudos com complexos de rutênio têm sido possíveis pela ampla variedade de coordenação, vários estados de oxidação (Ru (II), Ru (III) e Ru (IV)) em condições fisiológicas e a taxa de substituição de ligante (LEVINA *et al*., 2009).

Os compostos de rutênio têm sido objetos de grande atenção por terem propriedades antimetastática e baixa toxicidade. A exploração de complexos de rutênio para o uso como agente antineoplásico foi iniciada na tentativa de se obter uma droga menos tóxica e mais específica. Ultimamente, complexos de rutênio como organometálicos têm demostrado interessantes propriedades antineoplásicas (HUXHAM *et al*., 2003; HARTINGER *et al*., 2006).

Complexos de rutênio e de platina apresentam diferenças em sua estrutura. Os complexos de rutênio apresentam estrutura octaédrica, em contraste ao quadrado-planar do complexo de Pt (II), o que indica que o mecanismo de ação destes compostos deve diferir da cisplatina (SAVA *et al*., 1994; ALESSIO *et al*., 1997). Para esses complexos, estas características químicas proporcionam a formação de ligações fortes com o DNA, bem como para o NAMI-A (em triagem clínica fase II), estudos funcionais demonstram que a atividade biológica está relacionada à liberação progressiva dos íons cloretos (FRAUSIN *et al*., 2005; BERGAMO et al., 2012). O NAMI-A não mostra elevada citotoxicidade *in vitro* em linhagens de células tumorais, mas apresenta-se eficaz contra processos de metástases de câncer de pulmão e, atualmente, está sendo estudado para o uso como uma terapia de segunda linha contra NSCLC em combinação com o fármaco Gemcitabina (SAVA *et al*., 1995; HARTINGER *et al*., 2006).

Estudos mostram ainda que o modo de ação destes agentes pode ser um dos motivos pelos quais complexos de rutênio, como KP1019 (em triagem clínica fase I), apresentam atividade anitumoral em neoplásias resistentes à cisplatina, apresentando atividade antitumoral contra carcinoma coloretal, induzindo aumento de ROS e morte celular via apoptose (PACOR *et al*., 2004; KAPITZA *et al*., 2005a;

HARTINGER *et al*., 2006; BERGAMO *&* SAVA, 2011). Apesar da estrutura e similaridades químicas, estes dois complexos de rutênio (III) (NAMI-A e KP1019) (Figura 9) apresentam distintas atividades antitumorais (PACOR et al., 2004; KAPITZA *et al*., 2005; ANTONARAKIS & EMADI, 2010).

Figura 9 – Estrutura química dos compostos conhecidos como NAMI-A - (H_2im)[*trans*-$RuCl_4$(Him)(DMSO)] (A), e KP1019 - Indazolium *trans*-[tetrachlorobis(H_1 indazole)ruthenate(III) (B).

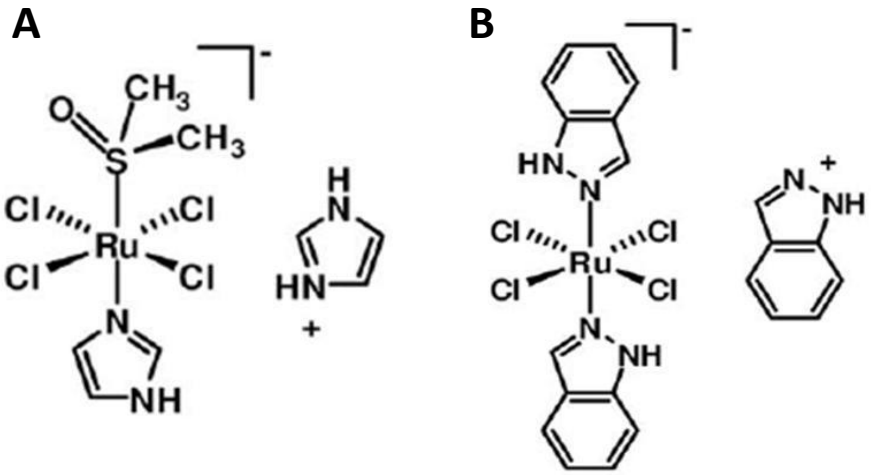

Fonte: VACCA *et al*., 2002

Os complexos de Ru (III) (NAMI-A e KP1019) têm sido extensivamente avaliados como potenciais agentes antitumorais (CLARKE et al., 2003; GIOVAGNINI et al., 2009). Outros complexos de Ru III como RM175, KP418, RAPTA-T, RDC-11 e DW1/2 (Figura 10) estão em estágio de testes pré-clínicos, assim como uma grande variedade de complexos de rutênio (II e III) com ligantes aminas, imina, polipiridil, DMSO e arenos. Alguns deles apresentam propriedades farmacológicas que instigam seus estudos (GIOVAGNINI *et al*., 2009; CHEN *et al*.,2010; LI *et al*., 2012). Uma dessas propriedades foi descrita por Clarke e Srivastava que descrevem os compostos de rutênio como fármacos que discriminam as células saudáveis das células cancerosas pelas suas caracteristicas, tais como: a hipóxia e o alto metabolismo celular requeridos pelo transporte de nutrientes a partir da maquinaria de transferrina apresentada pelas células cancerígenas (BERGAMO & SAVA 2011). Além dessas propriedades, outras caracteristicas são apresentadas pelos compostos de rutênio como o KP1019, que provavelmente não segue os atributos de ação da cisplatina, pois parece não agir sobre a maquinaria celular. Seguindo tal

raciocínio, a ação do RDC11 também segue outros fármacos à base de metal, apresentando várias reações de substiuição, assim como a quebra na regra de troca de ligantes. No entanto, sem dúvida o NAMI-A é o composto mais intrigante, por sua capacidade de agir sobre metástases (BERGAMO & SAVA 2011).

Figura 10 - Estrutura química dos complexos de rutênio III

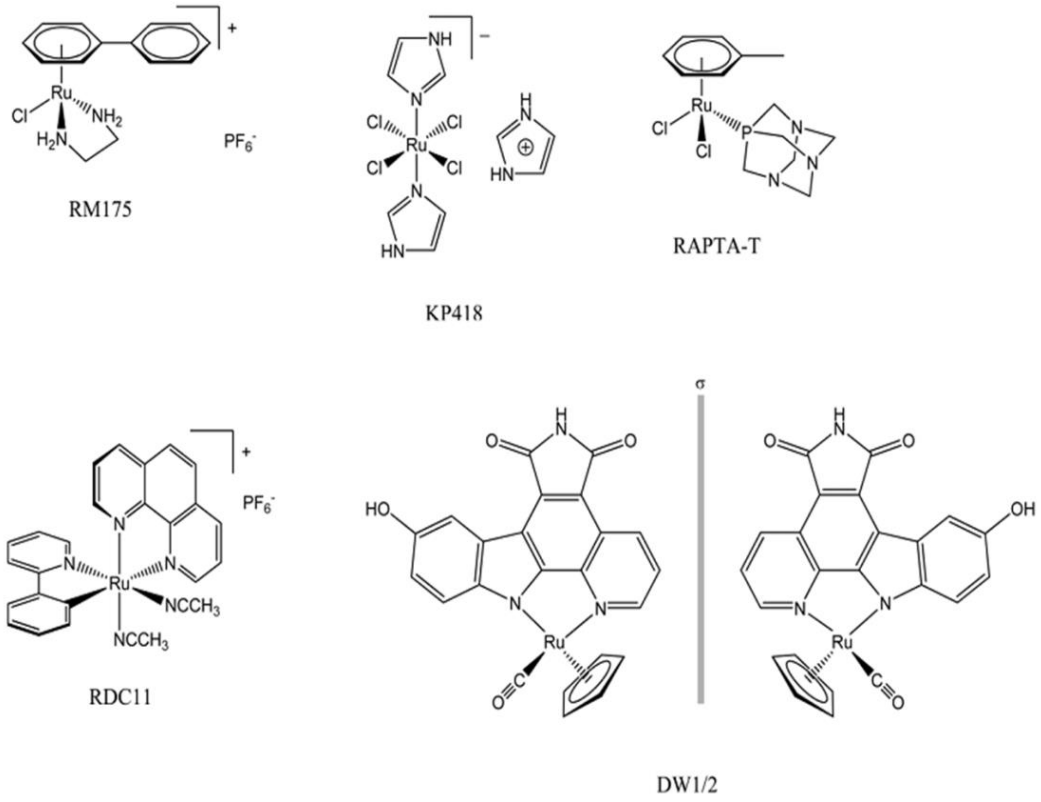

Fonte: BERGAMO & SAVA, 2011

Complexos de rutênio (II) são foco de alguns estudos e apresentam resultados promissores como potenciais agentes tumorais. O composto α-$[RuCl_2(azpy)_2]$, no qualazpy = 2-fenilazo-piridina, apresenta elevada atividade contra as linhagens de células: MCF-7 (câncer de mama), EVSA-T (câncer de mama), WIDR (câncer de colo), IGROV (câncer de ovário), M19 (melanona), A498 (câncer renal) e H266 (câncer de pulmão) (HOTZE *et al*., 2000; VELDERS *et al*., 2000). Os complexos derivados do cis-$[RuCl_2(azpy)_2]$ foram testados contra as linhagens de células A2780 (câncer de ovário humano) e A2780cisR (correspondente linhagem de célula resistente à cisplatina) e mostraram-se citotóxicos (HOTZE *et al*., 2000; VELDERS *et al*., 2000).

Diversos areno-complexos têm sido desenvolvidos como agentes anticancerígenos (ANG & DYSON, 2006), incluindo RAPTA-C ([$RuCl_2(\eta^6$-p-cimeno)(pta)], no qualpta = 1,3,5-triaza-7-phosphaadamantano) (ALLARDYCE *et al*., 2001). Estudos indicaram que estes compostos, apesar de apenas moderadamente citotóxicos *in vitro*, apresentam alta seletividade; os compostos RAPTA-C101 e [$RuCl_2(\eta^6$-oluene)(pta)] (RAPTA-T)102 apresentam significante ação sobre o crescimento de metástase no pulmão. Os ligantes do tipo areno estabilizam Ru (II) conferindo um caráter hidrofóbico, o que pode aumentar o reconhecimento e transporte a partir da membrana celular (CLARKE, 2003).

"*Piano-stool*" complexos organometálicos apresentaram citotoxicidade, contra a linhagem A2780 de câncer ovariano humano (MORRIS et al., 2001). Alguns complexos organometálicos, como [Ru(II)X(η_6-areno)(YZ)], exibem atividade anticancerígena *in vivo* e *in vitro* (MORRIS *et al*., 2001; AIRD *et al*., 2002). A explicação aceitável para a atividade destes compostos é a ocorrência da hidrólise dos haletos, favorecida pelas condições imposta pelo meio biológico, e interação do aqua complexo formado com o DNA (HAYWARD *et al*., 2005). A citotoxicidade do composto mer-[$RuCl_3$(terpy)] foi avaliada contra a linhagem de células L1210, apresentando ação significante menor que a da cisplatina, porém maior que a da carboplatina (VAN *et al*., 1995).

Existem três propriedades principais do rutênio que fazem com que seus derivados sejam bem apropriados para aplicações biológicas: mudança de ligante – os complexos de rutênio Ru (II) e Ru (III) apresentam cinética de mudança de ligante similar aos complexos de platina (II), sendo importante para as fármacos atingirem o alvo biológico sem serem modificadas; estados de oxidação – o rutênio é um elemento entre o grupo de metais em que os estados de oxidação são acessíveis em condições fisiológicas, permitindo a administração de complexos de Ru (III) que poderão ser ativados por redução formando complexo de Ru (II) nos tecidos alvos.

No sistema biológico, a redução de Ru (IV) e Ru (III) é favorecida pela glutationa, ascorbato e proteínas transportadoras de um único elétron, enquanto que o oxigênio e citocromo oxidase promovem a oxidação do Ru (II); mimetizando o ferro – a baixa toxicidade dos compostos de rutênio é explicada pela habilidade que este elemento tem de imitar o ferro na ligação a varias biomoléculas, incluindo a transferrina e a albumina. Em mamíferos, estas duas proteínas são responsáveis pela solubilização e transporte de ferro, reduzindo a toxicidade do metal (ALAMA *et*

al., 2009; PEREIRA *et al*., 2008; KOSTOVA, 2006; SILVEIRA-LACERDA *et al*., 2009b; ALLARDYCE & DYSON, 2001).

Complexos de rutênio (II e III) em relação aos mecanismos de ação podem se ligar à molécula de DNA diferentemente do complexo de platina. As pesquisas sugerem que os complexos de rutênio promovem *crosslinks* entre as duas fitas de DNA, possivelmente favorecidos pelas restrições impostas pela geometria octaédrica destes compostos. Este mecanismo difere da formação de *crosslinks* intrafita induzida pela cisplatina e, conseqüentemente, as linhagens de células tumorais que têm desenvolvido resistência à cisplatina, pela aceleração da taxa de reparo de *crosslinks* intrafita, são ainda susceptíveis aos complexos de rutênio (ALLARDYCE & DYSON, 2001).

Uma das hipóteses sugere que os compostos de rutênio (III) servem de pró-fármacos que reduzidas, *in vivo*, pelas condições citoplasmáticas das células tumorais: baixas concentrações de O_2 em decorrência do consumo atípico de nutrientes; pH baixo, devido à produção de ácido láctico na glicólise anaeróbia, compensatória da falta de oxigênio e à presença de glutationa em níveis tipicamente altos. Essas alterações no ambiente citoplasmático das células tumorais podem favorecer a conversão de Rutênio (II) a partir do Rutênio (III), intensificando ligações ao DNA, com toxicidade seletiva às células tumorais (Figura 11) (CLARKE, 2003; SILVEIRA-LACERDA, *et al*., 2009b).

Estudos de interação *in vitro* com nucleotídeos resultaram na ligação entre rutênio e DNA, o que ocorre principalmente no N7 da guanina entre "*clusters*" na dupla hélice (KÜNG *et al*., 2001) sendo, neste caso,semelhante às fármacoss à base de platina, nas quais a ligação com o DNA ocorrem preferencialmente a partir do N7 da guanina (GALLORI *et al*., 2000; CHEN *et al*., 2003).

De maneira geral, complexos de rutênio podem se ligar ao DNA por meio de ligações eletrostáticas, intercalações, ligações covalentes e não-covalentes (ZHANG *et al*., 2010; LIU *et al*., 2010; MORENO *et al*., 2011). Além de interagirem diretamente com a molécula de DNA, pesquisas atuais apontam que complexos de rutênio (II) podem também inibir a atividade de topoisomerases, por meio de ligações diretas a topoisomerases I e II e interferências na religação do DNA. Esta interferência de complexos de rutênio a topoisomerases pode levar a interrupção na maquinaria celular envolvida na replicação e transcrição (GAO *et al*., 2007; DU *et al*., 2011) (Figura 12).

Figura 11 –Mecanismo de ação do rutênio no ambiente da célula tumoral

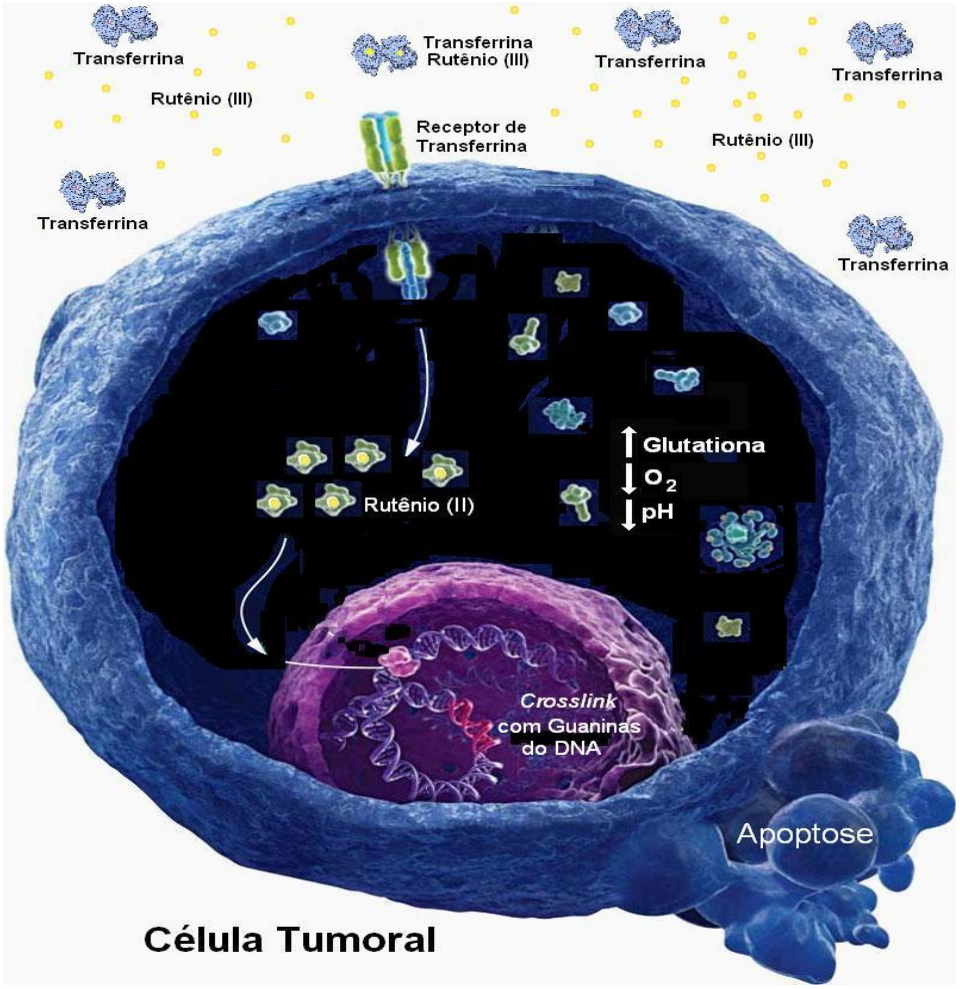

Fonte: adaptado de CLARKE, 2003

A partir do desenvolvimento de vários estudos, observou-se que o principal alvo de alguns complexos de rutênio não é o DNA. Estudos têm demonstrado que existem mecanismos induzidos pelos complexos de rutênio (III) (por exemplo, o NAMI-A) independentes do DNA. Como inibição de metaloproteases, a interferência com processos de adesão e metabolismo do óxido nítrico são responsáveis pelos efeitos antitumorais de alguns complexos de rutênio. Nestes estudos, tem se observado que apesar de NAMI-A poder interagir com o DNA *in vitro*, a ligação ao DNA não parece contribuir para o seu efeito antimetastático (PLUIM *et al*., 2004). Estes estudos demonstram, ainda, que o NAMI-A, apresenta mecanismo de ação independente do DNA, demonstrando exercer seu efeito antimetastático possivelmente pela atuação sobre moléculas de adesão e metabolismo do óxido nítrico (MORBIDELLI *et al*., 2003; SAVA *et al*., 2003; PACCOR *et al.*, 2004).

Figura 12 – Provável Mecanismo de ação de compostos de rutênio (II) no ambiente da célula tumoral

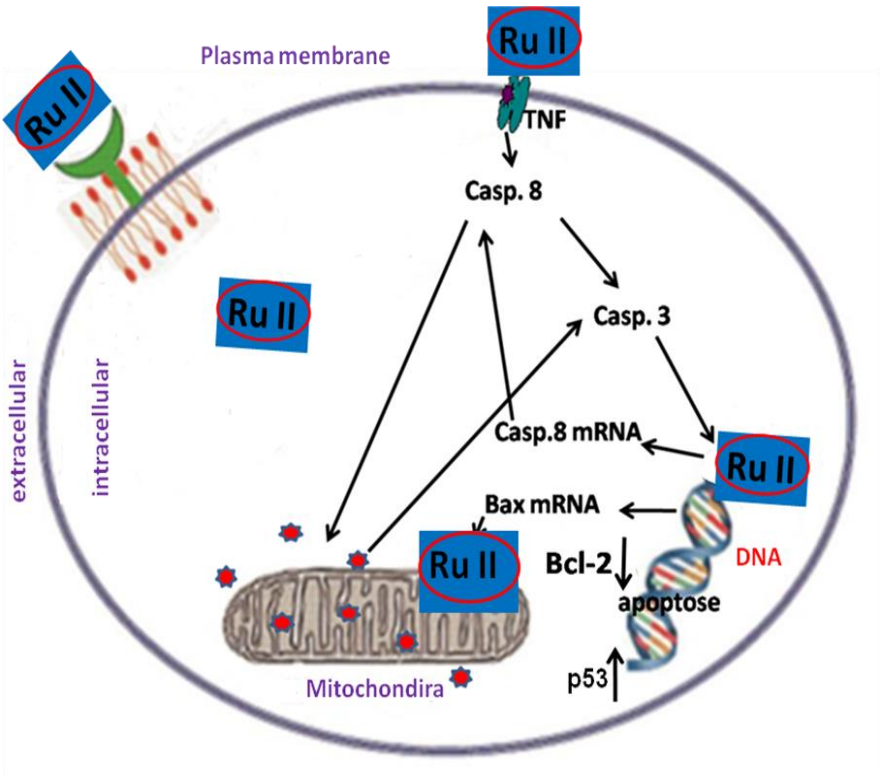

Fonte: adaptado de BERGAMO & SAVA 2010

O composto de rutênio (II) areno RAPTA-T é outro exemplo de complexo de rutênio II que apresenta atividade antimetastática e sua atividade não está relacionada à interação com o DNA. A atividade deste composto está relacionada a interações com proteínas da superfície e matriz extracelular similar ao NAMI-A (BERGAMO *et al*., 2008).

1.7. Complexos de rutênio (II)

Nos últimos anos, o desenvolvimento de complexos de rutênio (II) como agentes anticancerígenos tem aumentado nas pesquisas, exibindo atividade promissora, tanto em estudos *in vivo* como *in vitro*. Estes complexos mostram evidências de baixa citotoxicidade e toxicidade, mecanismos de ação alternativos e um espectro variável de atividade contra diversos tipos de câncer (AIRD *et al.*, 2002; YAN *et al.*, 2005; CHELOPO *et al.*, 2013).

Promissores resultados são observados nos complexos de rutênio (II) coordenados a aminoácidos, coordenados com N-Heterocíclicos, destacando-se também os ligantes piridínicos e bipiridínicos, bem como os N-doadores como

fenantrolina, piridina e imidazole. Sendo que os resultados frente à célula cancerígena dependem do tipo de ligante acoplado ao complexo (AIRD *et al.*, 2002; YAN *et al.*, 2005; CHELOPO *et al.*, 2013).

Ligantes como o N-heterocíclicos tem ganhado destaque. Uma das características destes compostos é a possibilidade de mimetizar moléculas biológicas que possuam propriedades particulares no metabolismo: ácidos nucléicos, proteínas, enzimas, alcalóides, etc. Um aumento nos estudos deste ligante se deu a partir de seu envolvimento com catálise redox e reações de transferência eletrônica. Dentre os ligantes N-Heterocíclicos, podem-se destacar os ligantes piridínicos e bipiridínicos, em especial, o ligante 2,2'-bipiridina e seus derivados. (JURIS *et al.*, 1988; KAIM e SCHWEDERSKI, 1995).

A bipiridina é derivada do acoplamento de dois anéis piridínicos e pode existir na forma de seis isômeros, um dos quais a 2,2´-bipiridina, que destaca-se por ser um ligante quelante formador de compostos de coordenação relativamente estáveis com a maioria dos íons de metais de transição. Eles estabilizam espécies de alto e baixo estado de oxidação. Por esta razão, estão entre os ligantes mais estudados na química de coordenação resultando em complexos estáveis. Ligantes bipiridínicos são excelentes na construção de complexos metálicos, de fórmula geral $[M(bpy)_3]$ e $[M(bpy)_2]$, que vai depender da geometria de coordenação preferencial do centro metálico (LE BOZEC & RENOUARD, 2000; MORENO *et al.*, 2003).

Rutênios com ligantes aromáticos N-doadores também exibem propriedades anticâncerígenas promissoras. Tais ligantes incluem derivados de fenantrolina, piridina e imidazole. Ligantes apresentando pelo menos uma porção NH em complexos de rutênio (II) facilitam uma interação efetiva com o DNA a partir de ligações de hidrogênio. Estes complexos apresentam diferentes modos de ligação à molécula de DNA e exibem uma excelente atividade anticancerígena em cânceres resistentes à cisplatina, em sistemas *in vitro* e *in vivo* (CHEN *et al.*, 2003; ZHAO e LIN, 2005)

A presença de um ligante quelante nos complexos de rutênio (II) oferece estabilidade estrutural, além da oportunidade de "afinar" a eletrônica no centro do rutênio. Diferentes elementos doadores tais como o fósforo, azoto e oxigênio, também estão sendo estudados quanto a sua atividade anticancerígena quando coordenados ao rutênio. Fernandez e colaboradores (2004) demonstraram que uma mudança de um ligante doador tem um efeito profundo sobre as propriedades

eletrônicas do complexo Ru (II). Como exemplo, podemos citar a taxa de hidrólise da ligação Ru-Cl como maior com um ligante quelante-O,O aniónico que com um ligante-N,N neutro. Esta “afinação” do ligante também resulta em uma mudança de preferência das nucleobases alvos. Estudos subsequentes estabelecem que os complexos de rutênio (II) com vários sítios de doadores quelantes foram realizados em ligantes tais como a N,N-(diaminas e bipiridina), N,O- (amino acidates) e O,O-(acetilacetonato), em que os complexos de estudo com ligantes-N,N possuíam atividade superior a dos quelantes O,O; os complexos-N,O foram inativos. Os ligantes N,N têm sido extensivamente estudados na literatura, sendo os doadores quelantes preferidos na combinação com o heteroátomo doador. (Habtemariam et al, 2005; DOUGAN *et al.*, 2008)

2. JUSTIFICATIVA

Nos últimos anos, o interesse por novos fármacos antitumorais baseados em metais vem crescendo devido aos bons resultados obtidos por grupos de pesquisa. Estudos revelam que os complexos de rutênio apresentam uma incrível capacidade de inibir a mitose, o que pode estar relacionado à inibição da síntese de DNA, ao bloqueio do ciclo celular ou até mesmo aos processos de expressão gênica.

A habilidade de modular o recebimento e a liberação de mensageiros celulares e outras moléculas intercelulares, como o Ca^{2+}, revela que as ações realizadas pelos complexos de Ru II e Ru III na célula podem ser mais complexos e amplos do que se espera, abrindo um importante caminho para o entendimento dos mecanismos pelos quais os complexos de coordenação desempenham suas atividades no ambiente celular, conhecimento este que é crucial para o sucesso da aplicação clínica destes complexos.

As pesquisas realizadas com complexos de rutênio (II e III) vêm apresentando bons resultados de acordo com a literatura. Estes complexos são interessantes por apresentarem, principalmente, atividade antitumoral, o que leva à necessidade de uma avaliação mais profunda e detalhada, a fim de compreender as diferentes propriedades químicas e biológicas desses novos compostos. Os resultados promissores divulgados e a possibilidade de trabalhar com novos ligantes exigem a realização de estudos a fim de entender a ação biológica desses compostos, como o mecanismo da cinética do ciclo celular, a via de morte celular e sua estabilidade genômica, com o objetivo de desenvolver fármacos com atividade mais acentuada e toxicidade diminuída.

O grupo de pesquisa do Laboratório de Genética Molecular e Citogenética, em parceria com laboratórios de química de outras Universidades, vem desenvolvendo trabalhos com complexos de rutênio (II e III). Os complexos de rutênio (III) já vêm sendo trabalhado pelo grupo desde 2008 e vêm apresentando resultados muito promissores com complexo de rutênio (III) com ligante amina, nos quais verificou-se sua atividade citotóxica *in vitro* frente a diferentes linhagens celulares, tais como K562 (Leucemia Mielóide Crônica), SKBR-3 (Carcinoma de mama), A-20 (Linfoma murino) e S180 (Sarcoma 180 murino). Além de apresentar atividade *in vitro*, estudos prévios demonstraram que este mesmo composto

apresentou atividade antitumoral *in vivo* sobre tumor Sarcoma 180 murino (S180) e, também, aumentou o tempo de vida dos animais tratados com este composto.

Os complexos de rutênio (II) vêm sendo trabalhados pelo grupo de pesquisa há menos tempo, desde o ano de 2010. Vários complexos de rutênio (II) estão sendo testados em diferentes modelos de células tumorais humanas e murinas. Complexos de rutênio (II) coordenados a benzonitrila, bipiridina, ácido picolínico e pirimidina foram testados. Em estudos de triagem, apresentaram promissores resultados frente a vários carcinomas, com atividade superior ou semelhante ao agente antitumoral cisplatina.

Diante destas perspectivas, são necessárias maiores investigações do mecanismo de ação destes compostos de rutênio. Estes testes tornam-se importantes para adefinição do potencial clínico destes complexos, contribuindo assim para o desenvolvimento de novos fármacos antitumorais, com propriedades complementares àquelas exibidas pelos já utilizados na clínica atual.

3. OBJETIVOS

3.1. OBJETIVO GERAL

O objetivo geral do presente estudo é avaliar o mecanismo de morte utilizando novos compostos de coordenação à base de Rutênio (II) e (III), em diferentes linhagens celulares *in vitro*.

3.2. OBJETIVOS ESPECÍFICOS

- Realizar a triagem do complexo de rutênio (III) frente à linhagem celular K562 (leucemia mielóide crônica); realizar a triagem em uma série de complexos de rutênio (II) coordenados a benzonitrila, bipiridina, ácido picolínico e pirimidina frente à linhagem tumoral S180 (sarcoma murino S180), DU145 (câncer de prostata), K562 (leucemia mieloide crônica) and A549 (câncer de plumão) e linhagem normal de PBMC (células mononucleares do sangue periférico), e selecionar um dos complexos para os ensaios seguintes pelo Indice de Seletividade;
- Avaliar o efeito genotóxico do complexo de rutênio (III) sobre o DNA;
- Avaliar se o complexo de rutênio (III) causa apoptose observando se houve quebra de DNA;
- Avaliar o efeito do complexo de rutênio (II e III) sobre a cinética do ciclo celular;
- Avaliar o efeito do complexo de rutênio (II) sobre a indução de morte celular apoptótica ou necrótica;
- Avaliar o efeito do complexo de rutênio (II) sobre a atividade de casp3, casp8 e casp9;
- Avaliar o efeito do complexo de rutênio (II) sobre o potencial de membrana mitocondrial;
- Avaliar o efeito do complexo de rutênio (II) sobre a expressão dos genes pró-apoptóticos *Casp3*, *Casp8*, *Casp9*, *Tp53* e *Bax*, por real time q-PCR.

4. METODOLOGIA

A metodologia do trabalho foi desenvolvida de acordo com o fluxograma abaixo:

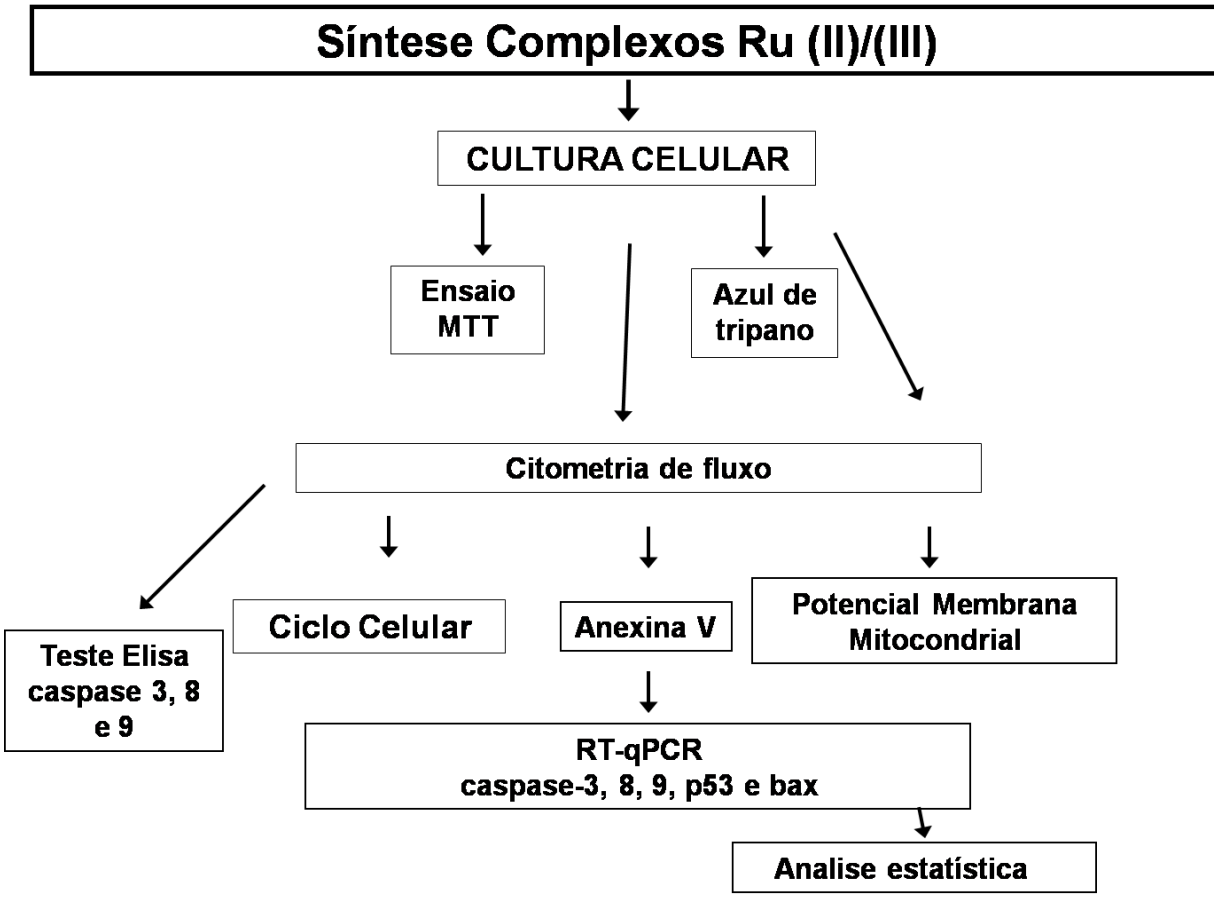

4.1. Síntese dos Compostos de Rutênio

O composto Ditionato de *cis*-Tetraamino(oxalato)rutênio(III) foi sintetizado no Laboratório de Química do Instituto de Química da Universidade Federal de Uberlândia. Já os complexos de rutênio (II) coordenados a benzonitrila, bipiridina, ácido picolínico e pirimidina foram sintetizados no Laboratório de Química do Instituto de Química da Universidade Federal de São Carlos pelo professor Alzir Azevedo Batista e encaminhados ao Laboratório de Genética Molecular e Citogenética da Universidade Federal de Goias(UFG) para realização dos ensaios de atividade biológica.

Tabela 3 – Complexos de Rutênio II e III utilizados no desenvolvimento do trabalho.

Complexos de Rutênio(II)	Complexos de Rutênio (III)
[Ru(prm)(bipy)(dppf)]PF_6	
[Ru(prm)(bipy)(dppm)]PF_6	
[Ru(prm)(bipy)(dppp)]PF_6	
[Ru(prm)(bipy)(dppe)]PF_6	
[Ru(prm)(bipy)(dppb)]PF_6	
[Ru(dmpm)(bipy)(dppf)]PF_6	
[Ru(dmpm)(bipy)(dppm)]PF_6	*cis*-[Ru(C_2O_4)(NH_3)$_4$]$_2$(S_2O_6)
[Ru(dmpm)(bipy)(dppp)]PF_6	
[Ru(dmpm)(bipy)(dppe)]PF_6	
[Ru(dmpm)(bipy)(dppb)]PF_6	
[Ru(pic)(bipy)(dppe)]PF_6	
[Ru(pys)(bipy)(dppp)]PF_6	
[RuCl(bcn)(bipy)(dppe)]PF_6	
[Ru(bcn)(bipy)(dppf)]PF_6	

4.2. Droga antitumoral controle

Como controle positivo, utilizou-se o fármaco Cisplatina (5 a 50 µM), carboplatina (50 µM) e placlitaxel (25 µM) todos liofilizados, obtida comercialmente da Sigma (Sigma-Aldrich Co St Louis, MO, EUA).

4.3. Preparação dos compostos de Rutênio para ensaios biológicos *in vitro*

O composto Ditionato de *cis*-Tetraamino(oxalato)rutênio(III) liofilizado foi pesado e dissolvido em meio de cultura RPMI 1640 ou DMEN suplementado com 10% de soro bovino fetal na concentração de 2mg.mL^{-1} (Solução estoque, solução uso 0,1 à 200 µM). Os complexos de rutênio (II) coordenados a benzonitrila,

bipiridina, ácido picolínico e pirimidina foram dissolvidos em DMSO 100% para a solução mãe. Posteriormente foi submetido a um ultra-som para dissolução completa e então o composto foi esterilizado por filtração em membranas de 0,22 µm. Como controle positivo foram utilizados os fármacos Cisplatina (50 µM), Carboplatina (50 µM) e Paclitaxel (25 µM) para os testes de MTT e Azul de Tripano.

4.4. Meio de cultura celular

Para a manutenção das linhagens de células tumorais, a dissolução dos compostos testados e a realização dos ensaios biológicos seguiram o protolocolo indicado pelo *American Type Culture Collection* (ATCC ROCKVILLE, MARYLAND, EUA) utilizando-se meio RPMI-1640 ou DMEM (SIGMA, ST. LOUIS, MO, EUA) suplementado com 10% de soro bovino fetal (GIBCO®, INVITROGEN, CARLSBAD, CA, EUA) e 1% de glutamina, eritromicina e estreptomicina (Sigma) em estufa com 5% de CO_2 a uma temperatura constante de 37ºC.

4.5. Linhagens celulares tumorais e normais

Foram utilizadas às seguintes linhagens tumorais: S180 (sarcoma murino 180) (ATCC® TIB-66), A549 (câncer de pulmão humano) (ATCC® CCL-185), DU145 (câncer de prostata) (ATCC® 64963), K562 (leucemia mieloide crônica) (ATCC® CCL-243) provenientes do *American Type Culture Collection* (ATCC ROCKVILLE, MARYLAND, EUA). As células mononucleares do sangue periférico (PBMC) foram coletadas de voluntários saudáveis com idades entre 20-30 anos, sem histórico de fumar, beber, ou o uso crônico de fármacos. O protocolo (043/2007) para estes experimentos foi aprovado pelo Comitê de Ética da Universidade Federal de Goiás e, antes de entrar para o estudo, todos os doadores de sangue assinaram um termo de consentimento informado.

4.6. Cultura de células tumorais

As células tumorais foram cultivadas em frascos para cultivo celular estéreis com 75 e 175 cm^2, contendo meio RPMI 1640 ou DMEN (de acordo com a característaca de cada linhagem), acrescentado de glutamina 2 µmol L^{-1},

bicarbonato de sódio 10 mmol L^{-1} e soro fetal bovino 10% (v/v), seguindo o protocolo da ATCC (*American Type Culture Collection).* Para fins experimentais, as células foram cultivadas em microplacas de 96 poços, fundo chato com tampa, na presença ou ausência da cisplatina, de Ditionato de *cis*-Tetraamino(oxalato)rutênio(III) e complexos de rutênio (II) coordenados a benzonitrila, bipiridina, ácido picolínico e pirimidina conforme as concentrações descritas anteriormente. As células foram incubadas em estufa a 37ºC com atmosfera contendo 5% de CO_2.

Para a realização dos ensaios, previamente as linhagens tumorais aderentes em fase de crescimento logarítmico foram removidas dos frascos de cultura celular pela adição de 1 mL de tripsina 0,5% em solução tampão Fosfato 0,01 mol.L^{-1}, pH 7,2 em solução salina 0,9% (PBS). Os frascos com solução de tripsina foram então mantidos sob agitação manual por aproximadamente 60 segundos. Em seguida, foram adicionados 10 mL de meio completo para neutralizar a tripsina e transferidos para tubos plásticos.

Para células em suspensão, as mesmas foram retiradas diretamente das garrafas e transferidas para tubo Falcon para procedimento de lavagem. As células foram lavadas três vezes por meio da centrifugação a 1000 rpm por 10 minutos em meio completo. Ao final da última lavagem, as células foram ressuspendidas em 5 mL de meio RPMI completo. Uma alíquota de 10µL da suspensão celular foi colocada em 90 µL de Azul de Tripano 1% (m:v) (SIGMA-ALDRICH CO ST LOUIS, MO, EUA) e contadas em hemocitômetro (Câmara de Neubauer).

4.7. Método de redução do tetrazólio (Teste MTT)

Para avaliar a atividade citotóxica e antitumoral dos compostos de coordenação de Rutênio (II) e (III), assim como determinar suas respectivas IC_{50} foi utilizado o método colorimétrico do MTT. O princípio deste método descrito por Mosman (1983) consiste em medir indiretamente a viabilidade celular pela atividade enzimática mitocondrial das células vivas. Para o teste do MTT, 2×10^3 de células foram semeadas em microplacas de 96 poços na presença dos compostos de Rutênio (II) e (III) por 48 e 72 h em estufa a 37ºC com atmosfera contendo 5% de CO_2. Ao final do período de incubação, foi adicionado aos poços de cultivo celular, 10 µL de MTT na concentração de 5mg.mL^{-1}, e após 3 h de incubação com o MTT,

foram acrescentados 50 µL SDS a 10% diluído em HCL/0,01N. A quantificação da densidade óptica (DO) foi medida em espectrofotômetro (AWARENESS TECHNOLOGY INE/ STAT FAX 2100). A porcentagem de viabilidade celular foi determinada a partir da seguinte fórmula: % Viabilidade = (Absorbância do Tratamento/Absorbância do controle negativo) × 100%. Após a triagem dos complexos de Ru II, o melhor composto foi designado como o que exibiu o menor valor de IC_{50} para as linhagens tumorais em relação a células saudáveis, assim pode-se dar continuidade aos outros ensaios sobre o mecanismo de morte celular. A IC_{50} foi usada para determinar o índice de selectividade (IS), para todos os complexos de ruténio (II), com a seguinte fórmula : IS = IC_{50} da célula não tumoral (PBMC) / IC_{50} da célula tumoral , e foi considerado significativo o IS ≥ 2.0 (OSTI et al. 2012).

4.8. Ensaio de citotoxicidade pela técnica de Azul de Tripano

A citotoxidade após exposição a fármacos pode ser medida pela exclusão de corantes supravitais como o azul de tripano. O princípio deste teste consiste em medir indiretamente a viabilidade celular através da integridade de membrana, onde as células mortas que apresentam a membrana danificada absorvem este corante e consequentemente coram-se em azul, já as células vivas permanecem intactas sem coloração (PERES & CURI, 2005). Para o ensaio de azul de tripano, foram realizados os mesmos procedimentos de plaqueamento para o complexos de rutênio (III) sobre a linhagem K562 semelhantes ao realizados no ensaio do MTT. No entanto, ao final do período de incubação, alíquotas de 10 µL de suspensão celular foram colocadas em 40 µL de azul de tripano à 0,4%, e desta solução foi retirada uma alíquota para contagem de células em câmara de neubauer. Para determinar a porcentagem de citotoxicidade foi utilizada a seguinte fórmula **% Citotoxidade**= (100 - Absorbância do Tratamento/Absorbância do Controle Negativo*100). Ambos os ensaios MTT e Azul de tripano foram utilizados para calcular o valor da IC_{50}. Para os ensaios foram realizados três experimentos independentes feitos em triplicata.

4.9. Eletroforese em gel de agarose

A célula da linhagem tumoral foi incubada com diferentes concentrações da droga em estudo durante 48 h, em estufa úmida, com 5% de CO_2 no ar. Uma

quantidade de 2×10^6 células foram tratadas com diferentes concentrações de *cis*-$[Ru(C_2O_4)(NH_3)_4]_2(S_2O_6)$ (de 0,15 a 150 µM) por 24 horas a 37 °C e 5% CO_2. As células foram então retiradas do tratamento e centrifugadas a 300×*g*/15 min/10°C e lavadas com PBS. As células foram então ressuspendidas a uma concetração de 1×10^6 cells mL^{-1} em um tampão de extração (Tris-HCl a 1 molar, Na_2EDTA a 2 molar, 0,5mg L^{-1} de SDS) e tratadas com 20 mg L^{-1} de RNase A a 37°C por 60 minutos. Passado o tempo, as células foram então incubadas com proteinase K (100 mg L^{-1}) a 37°C por 60 minutos. Depois da digestão por proteinase K, foi adicionada solução salina (NaCl a 6 M) e centrifugada a 13,000×*g* por 10minutos. O sobrenadante foi então coletado e um volume igual de etanol (-20°C) foi adicionado. As amostras foram então centrifugadas a 13,000×*g* por 30 minutos a 4°C. O sobredante foi então discartado e os *pellets* dissolvidos em tampão TE (1×) e guardados em ultra-freezer (-80°C) até o momento de uso.

A concentração de DNA foi detectada por UV utilizando um espectrofotômetro (Beckman DU-640, EUA). O DNA (5 µg por tubo) foi transferido para um gel de agarose a 1,5%, que foi submetido a uma eletroforese a 100V cm^{-1} por 90 minutos. O DNA nos géis foram visualizados através de transiluminação por ultravioleta, após a coloração por brometo de etídio (5 µg mL^{-1}) utilizando um sistema de imageamento Omega® (UltraLum Inc., Claremont, CA, EUA).

4.10. Ensaio cometa

O ensaio cometa é um método versátil e sensível para a detecção de quebras de fita simples e dupla no DNA. Ele tem sido amplamente utilizado como uma ferramenta para avaliações das respostas celulares aos danos no DNA, podendo ser aplicado em estudos de genotoxicidade, biomonitoramento, ecotoxicológicos e ainda em alguns estudos que envolvem saúde humana (TICE *et al*., 2008).

Umas das maiores vantagens do Ensaio Cometa é a possibilidade de sua aplicação em diferentes tipos celulares que não necessariamente estejam em proliferação, tanto *in vitro* quanto *in vivo* (COLLINS *et al*.,1997; TRZECIAK *et al*., 2008). A versão alcalina do cometa (*single-cell gel electroforesis*) foi seguida de acordo com Singh *et al*., (1988), com pequenas modificações.

A linhagem celular foi quantificada e depois foi tratada com concentrações diferentes do Ditionato de *cis*-Tetraamino(oxalato)rutênio(III), controle positivo

(Cisplatina) e negativo, por 24, 48 e 72 horas e então homogeneizados e misturados em agarose *low-melting* (baixa fusão) e imediatamente colocada em uma lâmina que já continha uma camada de gel de agarose a 1%. A lâmina com as duas camadas de agarose foi colocada a 4°C por 5 minutos. Após foram incubadas em uma solução de lise (2,5M NaCl, 10mM Tris, 100mM EDTA, 1% Triton X-100 and 10% DMSO, pH10,0) e colocada a 4°C por duas horas para remover proteínas e membranas. Posteriormente, as lâminas foram colocadas na eletroforese com tampão (300mM NaOH, 1mM EDTA, pH > 13,0). A corrida de eletroforese foi por 20 minutos, a 0,9 V/cm, 300 mA e a 4°C. Todo o procedimento foi realizado no escuro ou sob luz amarela, de forma a prevenir danos ao DNA. As lâminas foram mergulhadas em solução de neutralização (0,4M Tris, pH 7,5), lavada com água destilada e secas a temperatura ambiente.

As lâminas foram preparadas em duplicatas e 100 núcleos analisados (50 núcleos para cada duplicata) utilizando microscópio de fluorescência (Leica) equipado com filtro de excitação de 515-560nm, um filtro de barreira de 590nm, e objetiva de 40x.

Os núcleos sem danos no DNA apareceram intactos e sem cauda. Os cometas foram classificados pelo *software CometScore* 15, em classes: ausência de cauda, ou seja, sem dano (classe 0); cauda menor do que o diâmetro da cabeça (classe 1); cauda até duas vezes o diâmetro da cabeça (classe 2): cauda maior que duas vezes o diâmetro da cabeça (classe 3) e sem cabeça (classe 4). As recomendações para o ensaio cometa consideram tanto avaliações visuais quanto as avaliações usando software (BURLINSON et al., 2007). O total da contagem dos danos foi de 100 por amostra, perfazendo um total de 500 núcleos (desde a classificação 0 – sem danos – até classificação 4 – danos totais).

4.11. Análise da Cinética do Ciclo Celular por Citometria de Fluxo

As fases do ciclo celular podem ser caracterizadas por variações no seu conteúdo de DNA, que quando analisado por citometria de fluxo após marcação com iodeto de propídeo permite quantificar a percentagem de células em cada fase do ciclo celular. Para esta análise, 5 x 10^5 células tumorais foram plaqueadas em microplacas de 12 poços na presença ou ausência dos complexos de rutênio (II) e (III). Após exposição das células aos complexos de rutênio, estas foram

centrifugadas e em seguida lavadas com PBS. Ao final da lavagem o sobrenadante foi desprezado, e o “pellet” celular foi incubado com 1 mL de álcool etílico gelado (70%) por 24 h a -20°C. Ao final da incubação as células foram lavadas novamente com PBS e em seguida estas foram incubadas por 15 min em uma solução contendo ribonuclease A (RNAse A) 0,05% e iodeto de propídio (50 µg mL^{-1}). A análise da porcentagem de células em sub-G1, G0/G1, S, G2/M e foi realizada em citômetro de fluxo (FACSCalibur, BD Biosciences), através do software ModFit.

4.12. Avaliação de apoptose e necrose por coloração com Anexina V/PI

A externalizaçao de fosfatidilserina na superfície externa da membrana plasmática é um dos primeiros eventos que ocorre na superfície de uma célula em processo de apoptose ou de necrose, sendo que esta perda de assimetria do fosfolipídeo de membrana contribui para facilitar o reconhecimento por protreínas dependente de ións cálcio, como a Anexina V (BOERSMA *et al*., 2005; GALLUZI *et al*., 2012). O procedimento de detecção de apoptose e necrose por Anexina V-FITC/Iodeto de Propídio consiste na ligação da anexina V-FITC à fosfatidilserina, na membrana das células que estão iniciando o processo apoptótico ou necrótico, e na ligação do iodeto de propídeo ao DNA das células no processo final da apoptose.

Para detecção de apoptose e necrose foi utilizado o Kit de detecção de apoptose Anexina V/Iodeto de Propídio (PI) (Sigma-Aldrich, St. Louis, Mo) de acordo com as instruções do próprio fabricante. Para este ensaio 5 x 10^5 células foram semeadas em microplacas de 12 poços e incubadas na ausência ou presença dos complexos rutênio (II) e (III). Após tratamento com os complexos de rutênio as células foram centrifugadas e posteriormente lavadas com PBS. O sobrenadante foi descartado e ao pellet celular foi adicionado 400 µL de tampão de ligação e em seguida acrescentados 5 µL de Anexina V-FITC e 1 µL de iodeto de propídio. As células foram então incubadas em temperatura ambiente por 15 min, e posteriormente foi feito à aquisição dos dados em citômetro de fluxo (FACSCallibur, BD Biosciences). Para análise dos dados foi utilizado o software *Cell Quest*.

Foram classificadas como células em apoptose inicial aquelas com marcação somente para Anexina-V (AN+)/(PI-), e como células em apoptose tardia aquelas com dupla marcação de Anexina V e PI (AN+)/(PI+), células em necrose somente marcação para PI (AN-)/(PI+) e células viáveis não apresentam nenhuma marcação.

4.13. Análise Bcl2 por citometria de fluxo

Após o tratamento das células com o complexo rutênio (II) por 24 horas nas concentrações determinadas as células foram retiradas da cultura, transferidas para um tubo de citometria de fluxo e centrifugas a 1800 rpm por 3 min. Descartado o sobrenadante as células foram lavadas com PBS 1X e novamente centrifugadas. Descartado o sobrenadante elas foram re-suspendidas em 500 µL de tampão de lise por 10 min. em temperatura ambiente (20° a 30°C). Após este período as células foram novamente centrifugadas e o sobrenadante removido. Adicionado 500 µL da solução de permeabiliazação e após 10 min, centrifugadas e o sobrenadante descartado. Foram então lavadas com tampão BSA (PBS 1X, 0,5% de SFB e 0,1% de azida de sódio), centrifugadas e o sobrenadante descartado. Adicionou-se 20 µL do reagente anti-Bcl-2. O tubo foi mixado e incubado por 30 min. a temperatura ambiente (20° a 30°C). Após o tempo de incubação as células foram centrifugadas, o sobrenadante descartado e novamente lavadas com BSA. Foram re-suspendidas em 500 µL de BSA e levadas para a análise leitura no citometro de fluxo (FACSCallibur, BD Biosciences).

4.14. Análises da ativação de caspases pelo ensaio colorimétrico

Para investigação da ativação das Casp3, 8 e 9 após o tratamento com o complexo de rutênio (II) foi utilizado o Kit de proteases colorimétrico ApoTarget™(Invitrogen) de acordo com as instruções do próprio fabricante. O ensaio de atividade das caspases é baseado na detecção por espectrofotômetro do cromóforo p-nitroanilima (pNA) depois da clivagem do substrato X-pNA, onde X é a seqüência de aminoácidos reconhecida pelas caspases. Neste ensaio, 3 x 10^6 células foram semeadas em garrafas de cultura 25 cm^2 e incubadas por período de 24 horas na ausência ou presença do complexo de rutênio(II). Após incubação as células foram inicialmente centrifugadas e o pellet de células formado foi incubado com de tampão de lise em banho de gelo por 10 min. A concentração de proteínas foi medida por meio do ensaio BSA (BioRad). 75 µg do extrato de proteína, 50 µL de tampão de reação 2X suplementado com 10 mM de DTT e os substratosDEVD-pNA (Casp3), IETD-pNA (Casp8) e LEHD-pNA (Casp9) foram incubados por 2 horas a37°C. Após incubação por 2 horas, a formação de p-nitroanilide nas amostras foi

medida em espectrofotômetro (Awareness Technology INE/ Stat Fax 2100) a 405 nM. O aumento da atividade de Casp3, Casp8 e Casp9 foram determinados por meio da comparação dos resultados com o controle.

4.15. Ensaio do potencial de membrana mitocondrial JC-1

A perda do potencial de membrana mitocondrial é uma característica de apoptose, sendo que este evento precede a externalização fostatidilserina e coincide com a ativação de caspases. JC-1 (iodeto de 5,5`,6,6`-tetracloro1,1`,3,3`-tetraetilbenzimidazolocarbocianina), é um marcador fluorescente que mensura o potencial de membrana mitocondrial das células. Este corante, penetra na organela e emite fluorescência nos comprimentos de onda de luz vermelha (pico de emissão máximo 590 nm) ou verde (emissão 520 nm), de acordo com o potencial de membrana mitocondrial interna. Penetrando em altas concentrações, o corante apresenta-se na forma de j-agregado e emite coloração vermelha e, em baixas concentrações encontra-se na forma de monômero e emite coloração verde. Desta forma, em mitocôndrias funcionais, o JC-1 penetra e acumula-se no interior desta organela e emite coloração vermelha, ao passo que, mitocôndrias com baixo a médio potencial de atividade de membrana fluorescem verde (CHAZOTTE, 2011).

O efeito dos complexos de rutênio(II) sobre o potencial de membrana mitocondrial ($\Delta\Psi$m) foi mensurado utilizando o corante catiônico JC-1 (BD Bioscience). Para o ensaio 3 x 10^5 de células foram tratados com complexo de rutênio (II) durante 24 h. Após tratamento as células foram centrifugadas por 10 min a 1500 rpm e lavadas com PBS. Após serem lavadas as células foram incubadas por 15 minuntos a 37°C com o corante JC-1. Em seguida as células foram lavadas novamente e ressuspendidas em tampão de ensaio para análise em citômetro de fluxo. Os resultados foram obtidos utilizando um citômetro de fluxo (FACSCallibur BD Bioscience) e a análise dos dados foi feita através do software *Cell Quest*, (BD Biosciences).

4.16. Avaliação da expressão gênica

4.16.1 Extração RNA

O RNA total de células tratadas com complexos de rutênio (II) na

concentração de 24µM foi isolado utilizando-se o reagent Trizol (Sigma-Aldrich) seguindo as recomendações do fabricante. Para o isolamento, 1 mL de trizol foi adicionado ao pellet cellular e homogeneizado até a dissolução completa do pellet. Foram adicionados a seguir 200 µL de clorofórmio, e os tubos foram homogeneizados por inversão e deixados a temperatura ambiente durante dois minutos seguindo-se de centrifugação durante 15 min a 12.000 g a 4°C. Este procedimento resultou em três fases: a fase aquosa onde está o RNA, à interface que contém as proteínas e por fim a fase com fenol/clorofórmio. Após a transferência da fase aquosa para um novo tubo, foram adicionados 500 µL de álcool isopropílico para a precipitação do RNA. Este foi incubado em seguida por 5 min em temperatura ambiente. A seguir os tubos foram centrífugados a 12.000 g por 10 minutos a 4 °C. O RNA foi então lavado com etanol 75% e em seguida centrifugado por 10 min a 7500 g a 4°C. Após centrifugação foi descartado o álcool e os tubos foram colocados em capela para evaporação do álcool. Após evaporação completa do álcool o RNA foi dissolvido em 50 µL de água ultrapura. A seguir o material foi tratado com DNAse I (Sigma Aldrich) seguindo protocolo sugerido pelo próprio fabricante. Após tratamento com DNAse I o material foi estocado em -80°C. A concentração e o grau de pureza do material foram estimados em espectrofotometro *NanoDrop* (*Thermo Scientific, Delaware, EUA)*. O grau de pureza foi avaliado de acordo com a relação 260/280. A qualidade (integridade) do RNA foi avaliado por meio de eletroforese em gel de agarose 1,2 %.

4.16.2 Síntese cDNA

Para a síntese de cDNA utilizou-se o *kit High-Capacity* cDNA *Reverse Transcription (Appyed Biossystems*), seguindo as instruções do fabricante. Uma mistura contendo dNTPS, inciadores randômicos (*random primers*) e transcriptase reversa foi preparada e adicionada a um mesmo volume de RNA (2µg). A reação de síntese de cDNA foi realizada a 25°C por 10 minutos seguida de 2 horas a 42°C.

4.16.3 Real time PCR (qPCR)

A avaliação da expressão do mRNA dos genes *Casp3*, *Casp8*, *Casp9*, T*p53* e *Bax* foi realizada por *real time* PCR utilizando o reagente *Sybr Green Master Mix*

(LGC Biotecnologia). Para reação foram utilizados 10 µL de *master mix*, 2 µL de cada *primer* (400 nM), 2 µL de cDNA final e 4µL de água. As amostras foram amplificadas no sistema *Line Gene* (*Bioer Techology*) com uma desnaturação inicial de 95° durante 15 min seguidos de 40 ciclos a 95°C durante 15 segundos, 55°C durante 15 segundos e por último 72°C durante 30 segundos. Em todas as reações foi realizada a curva de dissociação (*melting*) para verficar a presença de produtos inespecíficos. As sequências dos primer utilizados nesse ensaio são descritas na tabela 4 e foram dezenhadas com junção de éxon. A expressão relativa de cada gene-alvo foi normalizada utilizando a expressão dos genes de referência *β actina* para linhagem de camundongo S180. A expressão relativa foi realizada pelo método $2^{-\Delta\Delta CT}$. Para análise da eficiência dos *primers* foi realizada a curva padrão, em que foram utilizados os *primers* com valores de eficiências superiores a 90 %. A partir da curva padrão foram calculados o *slope* (-3,32) e o coeficiente de correlação (R^2).

Tabela 4 - Sequências de *primers* utilizados para o ensaio *real time* RT-PCR.

Gene	**Sequência do *primer***
β actina *Mus musculus*	F5'CACACCCGCCACCAGTTC3' R5'ATTCCCACCATCACACCCTG3' (161pb)
β globina *Homo sapiens*	F5'GTGCTCGCGCTACTCTCTCT3' R5'TCAATGTCGGATGGATGAAA3' (143pb)
Bax Mus musculus	F5'GCTACAGGGTTTCATCCAGG3' R5'GGAGACACTCGCTCAGCTTC3' (113pb)
Caspase 3 *Mus musculus*	F5'GGAGCTTGGAACGCTAAGAA3' R5'GTCCACTGACTTGCTCCCAT3' (112pb)
Caspase 3 *Homo sapiens*	F5'CCTCTTCCCCCATTCTCATT3' R5'CCAGAGTCCATTGATTCGCT3' (122pb)
Caspase 8 *Mus musculus*	F5'AGGTACTCGGCCACAGGTTA3' R5'TGGGATGTAGTCCAAGCACA3' (137pb)
Caspase 9 *Mus musculus*	F5'TAGCTGGAACACTGGGCATTGAGT3' R5'AACATACCCATCGGTGCATTTGGC3'(146pb)

Tp53 *Mus musculus*	F5'-TGGAAGACTCCAGTGGGAAC-3' R5'-TCTTCTGTACGGCGGTCTCT-3' (87pb)

4.17. Análise Estatística

Para comparação entre os grupos tratados e controle, foram utilizados Teste T Student e Análise de Variância (Anova), seguido de pós-teste Bonferrone (*software* GraphPad-Prism V4). Foram considerados como diferença significativa valores de p menores que 0,05 ($p<0.05$).

5. PRODUÇÃO CIENTÍFICA

ARTIGO 1 - Citotoxic effects of the compound cis-tetraammine(oxalato)ruthenium(III) dithionate on k562 human erythroleukemia cells

Autores – Flávia de Castro Pereira, Aliny Pereira de Lima, Cesar Augusto Sam Tiago Vilanova-Costa, Alessandra de Santana Braga Barbosa Ribeiro, Lucas Carlos Gomes Pereira, Wanessa Carvalho Pires, Luiz Alfredo Pavanin, Wagner Bastita dos Santos, Elisangela de Paula Silveira-Lacerda

Situação – Aceito pela *Springer Plus*

ARTIGO 2 – Ruthenium [RuCl(bcn)(N-N)(P-P)]PF_6 complexes: *In vitro* pre-clinical trials and a potential metallodrug against sarcoma S180 tumor cells

Autores - Flávia de Castro Pereira, Aliny Pereira de Lima, Wanessa Carvalho Pires, Thallita Monteiro, Lorena Félix Magalhães, Wanderson Costa, Benedicto Augusto V. Lima, Angelica Ellen Graminha, Alzir Azevedo Batista, Javier Ellena, Elisângela de Paula Silveira-Lacerda

Situação – Artigo a ser submetido a revista ≥ B1 PlosOne

5.1. ARTIGO 1

Cytotoxic effects of the compound cis-tetraammine(oxalato)ruthenium(III) dithionate on k562 human erythroleukemia cells

Flávia de Castro Pereira[1], Aliny Pereira de Lima[1], Wanessa Carvalho Pires[1], Alessandra de Santana Braga Barbosa Ribeiro[1], Lucas Carlos Gomes Pereira[1], Cesar Augusto Sam Tiago Vilanova-Costa[1], Luiz Alfredo Pavanin[2], Wagner Batista dos Santos[3], Elisângela de Paula Silveira-Lacerda[1]*

1-Laboratório de Genética Molecular e Citogenética, Instituto de Ciências Biológicas, Universidade Federal de Goiás - UFG, Goiânia, Goiás, Brazil;
*Corresponding Author: silveiralacerda@gmail.com
2 - Instituto de Química, Universidade Federal de Uberlândia - UFU, Uberlândia, Minas Gerais, Brazil;
3 - Instituto de Química, Universidade Federal de Mato Grosso - UFMT, Barra do Garça, Mato Grosso, Brazil;
*Autor Correspondente: Elisângela de Paula Silveira-Lacerda, e-mail: silveiralacerda@gmail.com

Laboratório de Genética Molecular e Citogenética
Instituto de Ciências Biológicas - ICB I - Sala 200
Universidade Federal de Goiás
Campus Samambaia (Campus II)
Cx. Postal: 131
Goiânia-GO, Brasil -74001-970
Telefone/Fax +55-62-3521-1481
Telefone Celular: +55-62-9293-3121

ABSTRACT:

Chemotherapy is a common treatment for leukemia. Ruthenium complexes have shown potential utility in chemotherapy and photodynamic therapy. The identification of new chemotherapeutics agents is critical for further progress in the treatment of leukemia. Ruthenium complexes generally have lower toxicities compared to cisplatin attributed to their specific accumulation in cancer tissues. Based on these evidences, in the present work we studied the citotoxic activity of the ruthenium(III) compound *cis*-Tetraammine(oxalato)Ruthenium(III) Dithionate - {*Cis*-$[Ru(C_2O_4)(NH_3)_4]_2(S_2O_6)$} against human erythroleukemia (K562) tumor cell line. The antiproliferative and cytotoxic activity revealed that K562 cells cultured with concentrations 40 to 150 µM of ruthenium(III) compound showed significant reduction of proliferation after 72h of exposition, with viabilities ranging from 88.2% to 55.6% when treated with 40 µM for 24 to 72h; and 76.2% to 26.7% when treated with 150 µM for 24 and 72h. The ruthenium(III) compound induced low [22.4% (24h) to 28.2% (48h) and 29.8% (24h) to 35.7% (48h) for concentrations 10 and 40 µM, respectively] to moderate [44% (24h) and 53% (48h) for concentration 150 µM] of cytotoxic activity against K562. After incubation for 48 h, the IC_{50} value was 18.28 µM. Compared to the cell cycle profiles of untreated cells, flow cytometric analysis indicated a sub-G1 arresting effect of ruthenium compound on K562 cells, inducing a 1.7-fold, 2.2-fold and 2.4-fold increase in the number of sub-G1 cells for 24, 48 and 72 h, respectively, when compared to control. The compound also caused a significant increase in tailed cells in any of the concentrations tested compared with negative control, that can be associated cytotoxicity with direct effect on K562 cells DNA. Additional studies are needed to determine the molecular mechanisms of the active components and to evaluate the potential *in vivo* anticancer activity of the *cis*-tetraammine(oxalato)Ruthenium(III) dithionate.

Keywords: *cis*-Tetraammine(oxalato)Ruthenium(III) Dithionate; Cytotoxic activity; K562, Ruthenium(III) compounds; immunomodulatory activity, Apoptosis.

1. Introduction

Leukemia is a major type of cancer affecting a significant segment of the population, and especially children. In fact, leukemia is the most frequent childhood cancer, with 26% of all cases, and 20% mortality [1]. The American Cancer Society (ACS) estimated that 47,150 new cases of leukemia would be diagnosed in the United States in 2012, whereas about 23,540 adults and children would die of leukemia during 2012 [2].

Although the incidence rate for this disease remains relatively unchanged, some success has fortunately been attained in its treatment. But even if the success of clinical trials in identifying new agents and treatment modalities has been significant, current treatments have many limitations related to their side effects and the development of acquired drug resistance [3] The new therapeutic agents thus needed should be more active and produce less side effects and they also should act through a mechanism different from that of cytotoxic agents already used [4,5].

Chemotherapy is a common treatment for leukemia [6]. In general the therapy uses a number of different anticancer drugs, which destroy cancer cells by preventing them from growing and dividing rapidly. Unfortunately, a number of the body's normal, non-cancerous cells (e.g., hair cells, red and white blood cells, blood-clotting platelets, and cells of the gastrointestinal mucosa) also divide rapidly and are harmed by chemotherapy [6,7]. The side effects of chemotherapy hamper many normal activities of patients undergoing treatment [7].

The preparations of metallo complexes with potential antitumor activity has been one of the main targets of transition metal chemistry since Rosenberg's discovery of cisplatin {*cis*-diamminedichloridoplatinum(II), *cis*-[$Pt(NH_3)_2Cl_2$]} cytotoxic activity in the 1960s [8]. In 1978, cisplatin was approved as the first platinum based drug for the oncology treatment, although several negative side-effects (nephrotoxicity, neurotoxicity, nausea, etc.) had been induced on treated patients [9]. Nevertheless, cisplatin was followed by carboplatin {*cis*-diammine-1,1´ -cyclobutanedicarboxylateplatinum(II), [$Pt(NH_3)_2$(cbdc)], approved in 1985} and oxaliplatin {1R,2R-diamminocyclohexaneoxalatoplatinum(II), [Pt(dach)(ox)], approved in 1996}, which met requirements of improving antitumor activity and reducing disadvantages of cisplatin, carboplatin and oxaliplatin represent the second, and third platinum-based drug generations, respectively ([9,10]. Nowadays, not only platinum-

bearing complexes are extensively studied with the aim to broaden a spectrum of transition metal-based complexes which could be used in the treatment of cancer [10].

In addition to the other metal complexes cisplatin have been developed using heavy metals. For example, gold complexes have been developed for the treatment of rheumatoid arthritis, silver complexes as anti-microbial agents, antimony complexes for the treatment of leishmaniasis, vanadium(IV) complexes as antiviral and antidiabetic agents, arsenic trioxide (Trisenox) for the treatment of acute promyelocytic leukaemia, and metal-activated bleomycin for the treatment of Hodgkin's lymphoma and testicular cancer.Transition-metal-based therapeutic agents currently under clinical trials include third generation antitumor platinum complexes such as liposomal cisplatin (Lipoplatin), satraplatin, and picoplatin, the antimalarial ferrocene–quinoline conjugate ferroquine [11].

Rhodium and Iridium has also been used for the synthesis of these metal complexes , as they allow greater selectivity and affinity molecules . The iridium (III) already shows results TNF- α in inhibiting HepG2 line through a hydrophobic binding [12,13]. These metal complexes possess many advantages that make them suitable for the development of new therapeutic agents and compounds of ruthenium has been highlighted why ruthenium complexes have shown potential utility in chemotherapy and photodynamic therapy [14,15]. Ruthenium complexes generally have lower toxicities compared to cisplatin attributed to their specific accumulation in cancer tissues [16]. *In vitro* and *in vivo* studies show high anticancer activity of ruthenium complexes and some of them are currently undergoing clinical trials [17,18].

The identification of new chemotherapeutics agents is critical for further progress in the treatment of leukemia. In comparison to the platinum(II) antitumor complexes currently used in the clinic, ruthenium compounds offer potentially reduced toxicity, a novel mechanism of action, the prospect of non-cross-resistance, and a different spectrum of activity [14]. The reduced toxicity is in part due to the ability of ruthenium complexes to mimic the binding of iron to molecules of biological significance, exploiting the mechanisms that the body has evolved for non-toxic transport of iron [19]. This reduced toxicity, together with non-cross-resistance in cisplatin-resistant cancer cells, is particularly attractive attributes of these complexes [20].

Based on these evidences, in the present work we studied the citotoxic activity of the ruthenium(III) compound *cis*-Tetraammine(oxalato)Ruthenium(III) Dithionate {*cis*-$[Ru(C_2O_4)(NH_3)_4]_2(S_2O_6)$} against human erythroleukemia (K562) tumor cell line.

2. Results

2.1. The *cis*-$[Ru(C_2O_4)(NH_3)_4]_2(S_2O_6)$ compound reduces viability of K562 cells

Results derived from Trypan blue staining essay revealed that K562 cells cultured with concentrations 40 and 150 μM of ruthenium(III) compound showed significant reduction of proliferation after 72h of exposition, with viabilities ranging from 88.2% to 55.6% when treated with 40 μM for 24 and 72h; and 76.2% to 26.7% when treated with 150 μM for 24 and 72h **Figure 2**.

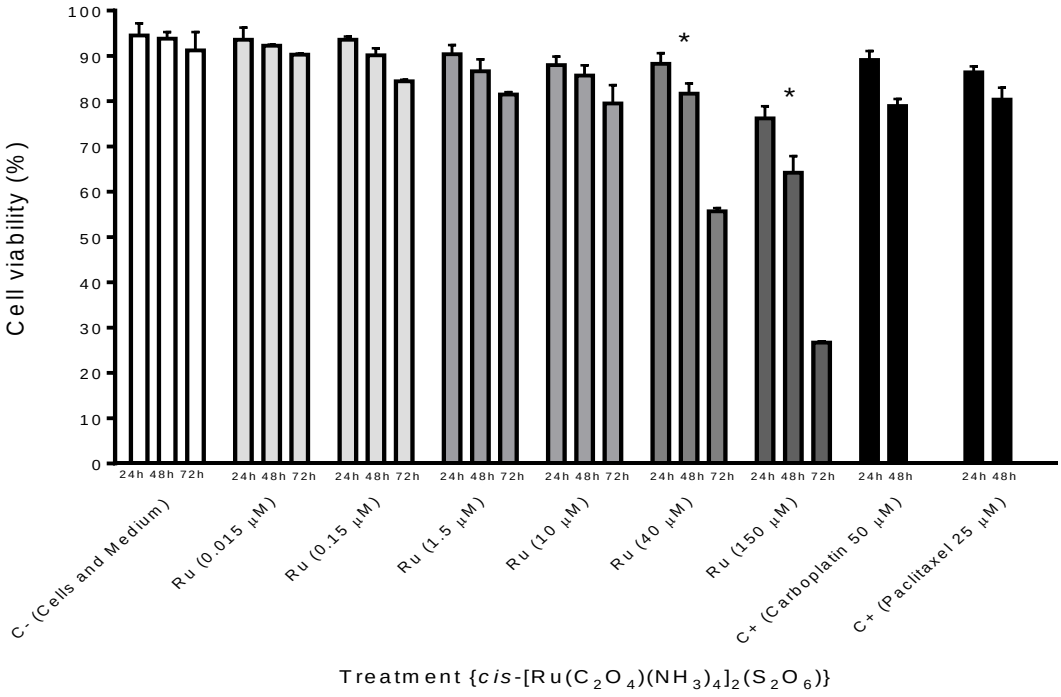

Figure 2. Anti-proliferative activity of *cis*-tetraammine(oxalato)Ruthenium(III) Dithionate compound towards K562 cell line. The tumor cells were cultured in the presence or absence of *cis*-$[Ru(C_2O_4)(NH_3)_4]_2(S_2O_6)$ (0.015 – 150 μM) for 24 h and 48 h as described in Material and Methods. The cell viability was assessed by correlation between the viable cells (that excluded trypan blue dye) and dead cells (stained cells) using a newbauer chamber. The data show the mean±S.D. (standard deviation) of three independent experiments [GraphPad Prism version 4.02 for Windows (GraphPad Software, San Diego, California, USA)]. *$p<0.05$ vs. negative control.

2.2. The *cis*-$[Ru(C_2O_4)(NH_3)_4]_2(S_2O_6)$ compound presents cytotoxic activity towards K562 tumor cell lines

To verify the cytotoxic activity of *cis*-$[Ru(C_2O_4)(NH_3)_4]_2(S_2O_6)$ on K562 cell lines, tumor cells were cultured for 24 and 48h in the presence of different concentrations of ruthenium compound. MTT reduction assay revealed that ruthenium compound produced concentration and time-dependent cytotoxicity effects on K562 cells. The results **Figure 3 b** show that the ruthenium(III) compound induced low [22.4% (24h) to 28.2% (48h) and 29.8% (24h) to 35.7% (48h) for concentrations 10 and 40 µM, respectively] to moderate [44% (24h) and 53% (48h) for concentration 150 µM] of cytotoxic activity against K562. After incubation for 48 h, the IC_{50} value was 18.28 µM (Figure 3 a).

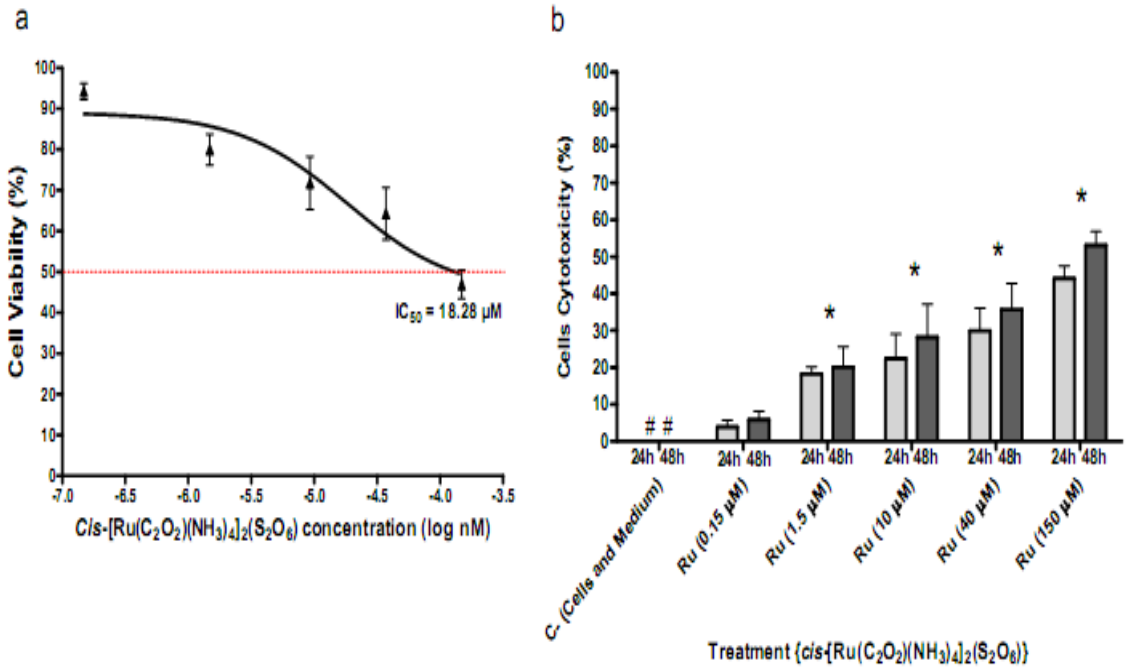

Figure 3. Cytotoxic activity of *cis*-tetraammine(oxalato)Ruthenium(III) Dithionate compound towards K562 cell line (a and b). The tumor cells were cultured in the presence or absence of *cis*-$[Ru(C_2O_4)(NH_3)_4]_2(S_2O_6)$ (0.15 – 150 µM) for 24 h and 48h as described in Material and Methods. The compound cytotoxicity was assessed by measuring the absorbance of dissolved formazan using a microplate reader. The reduction of yellow 3-(4,5-dimethylthiazol-2-yl)-2,5-diphenyl tetrazolium bromide (MTT) to dark-blue, insoluble formazan only occurs in mitochondria of the living cells. The data show the mean±S.D. (standard deviation) of three independent experiments [GraphPad Prism version 4.02 for Windows (GraphPad Software, San Diego, California, USA)]. *p<0.05 vs. negative control. # = 0%. Dotted line = IC_{50} concentration for 48h of treament**.**

2.3. The *cis*-$[Ru(C_2O_4)(NH_3)_4]_2(S_2O_6)$ induced apoptosis in K562 cells as verified by DNA ladder analysis.

The significantly reduced number of K562 cells in the presence of *cis*-tetraammine(oxalato)ruthenium(III) dithionate on previous assays suggests that this compound could be inducing cell death via apoptosis. To examine pro-apoptotic properties of the ruthenium(III) compound, K562 cells were cultured in the presence of different concentrations of ruthenium compound (from 0.15 – 150 µM) and then DNA ladder analysis was performed via agarose gel electrophoresis. K562 cells cultured in the presence of ruthenium compound but not in medium alone presented DNA fragmentation (Data not shown).

2.4 The *cis*-$[Ru(C_2O_4)(NH_3)_4]_2(S_2O_6)$ presents genotoxic effects against K562 tumor cells.

The alkaline comet assay has been used to assess the possible genotoxicity of *cis*-tetraammine(oxalato)ruthenium(III) dithionate against K562 cells. Results indicate that K562 tumor cells cultured with ruthenium(III) complex show a significant increase in DNA damage index in any of the concentrations tested compared with negative control, in a dose-dependent manner (**Figure 4**). Results show an average DNA damage index of 59 for 10 µM, 140 for 40 µM, 176 for 150 µM when K562 tumor cells were exposed to ruthenium(III) for 24 h; and 108 for 10 µM, 154 for 40 µM and 197 for 150 µM, for 48 h of exposition. Thus, the concentration of *cis*-$[Ru(C_2O_4)(NH_3)_4]_2(S_2O_6)$ might be associated cytotoxicity with direct effect on K562 cells DNA ($p<0.05$).

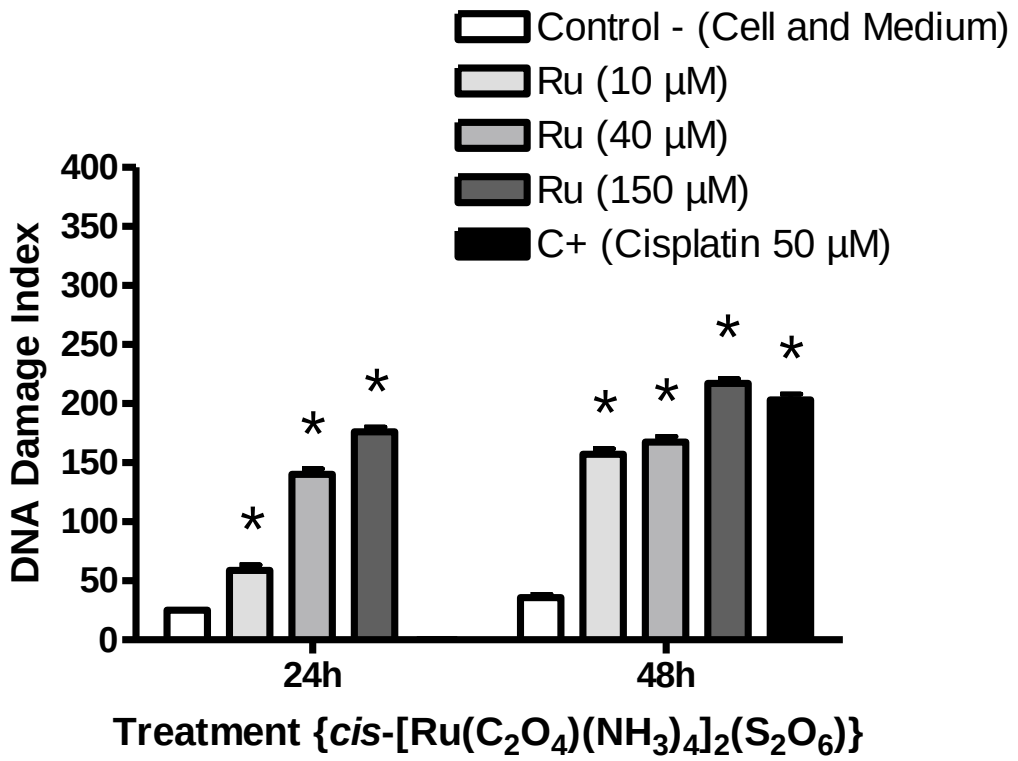

Figure 4. Induction of DNA strand breaks of K562 cells cultured in the presence of *cis*-$[Ru(C_2O_4)(NH_3)_4]_2(S_2O_6)$ compound. Cultures of K562 cells were exposed to increasing concentrations of ruthenium (III) complex for 24 and 48 h and submitted to SCGE-analysis. DNA damage index was measured as described in materials and methods section. Results in the figure represent the mean ±S.D. of 3 independent experiments using triplicate samples. *Increased above control at $p<0.05$.

2.5 The *cis*-$[Ru(C_2O_4)(NH_3)_4]_2(S_2O_6)$ increased the number of K562 tumor cells in sub-G1 phase, an indicative of apoptosis.

The cell cycle distribution of K562 cells treated with different concentrations of ruthenium compound (from 1.5 – 150 µM) for 24, 48 and 72h revealed a prominent increasing of cells on sub-G1 phase at concentration 40 and 150 µM and reduction on G0/1, S and G2/M phases. **Figure 5** shows that treatment with 40 and 150 µM of *cis*-$[Ru(C_2O_4)(NH_3)_4]_2(S_2O_6)$ for 24, 48 and 72h caused an increase in the proportion of cells in the sub-G1-peak correlating with fewer cells in G0/G1, S and G2/M. The fraction of sub-G1 cells increased from 34.5% in the control to 59% at 24h; 30.7% in the control to 68.6% at 48h; 35.5% in the control to 84.7% for 72h on cells treated with 40 µM of *cis*-tetraammine(oxalato)Ruthenium(III) dithionate. The same effect

was observed when k562 tumor cells were treated with 150 µM of ruthenium(III) compound. The ruthenium(III) compound caused a minor S phase accumulation after incubation at concentrations of 40 and 150 µM for all periods of exposition **Table 1**.

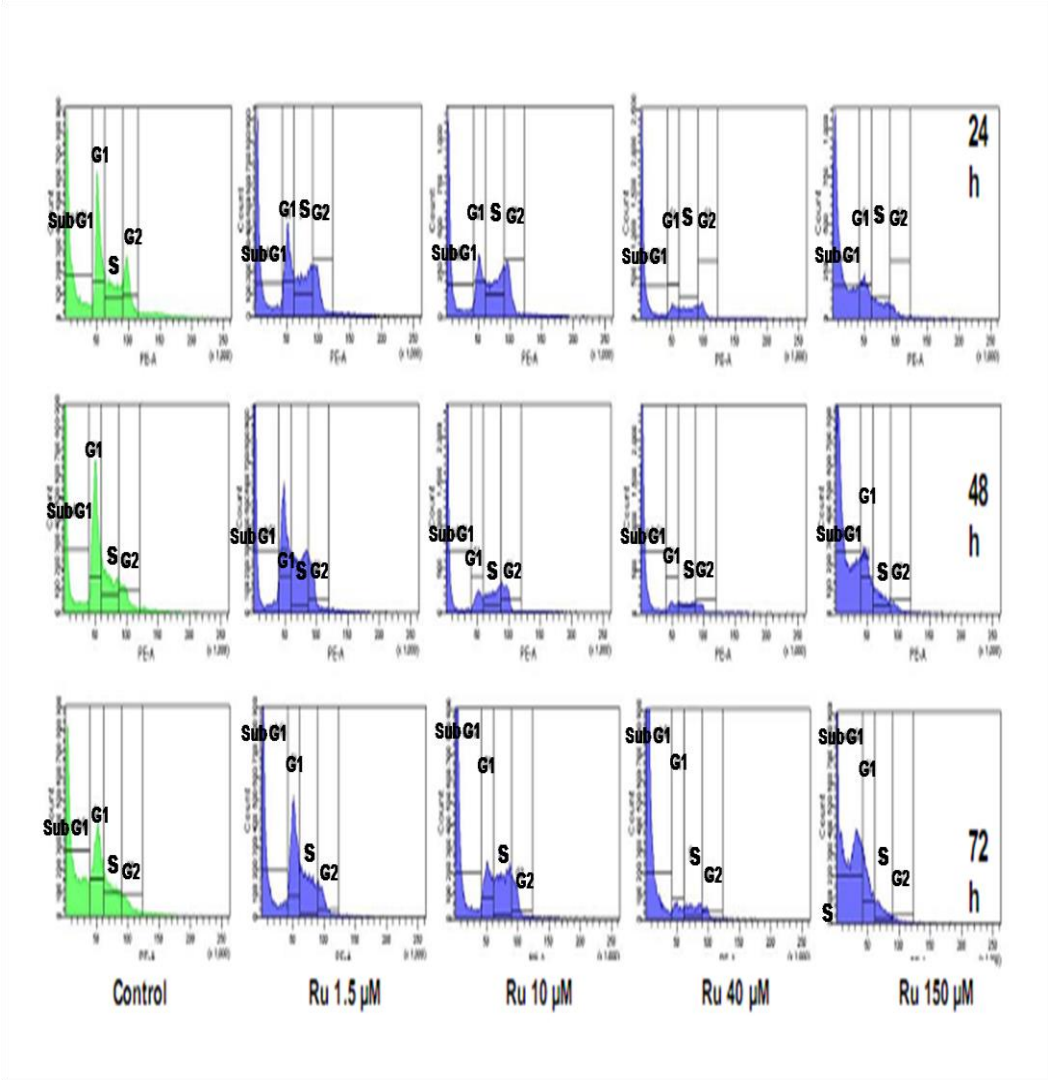

Figure 5. Cell cycle profile histogram of K562 cells treated with *cis*-tetraammine(oxalato)Ruthenium(III) Dithionate. Tumor cells were cultured with different concentrations of *cis*-$[Ru(C_2O_4)(NH_3)_4]_2(S_2O_6)$ (from 1.5 – 150 µM), maintained for 24, 48 and 72h h, and then collected, washed with PBS, and stained with propidium iodide as described in “Material and Methods” section. PI fluorescence was analyzed by flow cytometry (FACS Canto II, BD Biosciences, San José, CA, USA).

Table 1. Cell cycle analysis of K562 tumor cell lines after treatment with *cis*-tetraammine(oxalato)Ruthenium(III) Dithionate**.**

	Control		Ru 1.5 µM		Ru 10 µM		Ru 40 µM		Ru 150 µM	
24 h	**Mean**	**±S.D**	**Mean**	**±S.D**	**Mean**	**±S.D**	**Mean**	**±S.D**	**Mean**	**±S.D**
Sub-G0/G1	34.45	±0.6	30.20	±2.1	31.20	±1.4	59.00	±2.3	68.90	±1.8
G1	27.20	±0.3	25.25	±2.1	19.55	±0.9	11.50	±1.7	14.75	±0.9
S	19.05	±0.1	27.50	±1.1	29.10	±1.1	18.60	±2.1	11.40	±0.8
G2	14.10	±0.1	14.85	±0.8	18.10	±0.7	9.15	±1.6	4.00	±0.1
48 h										
Sub-G0/G1	30.70	±0.7	24.65	±1.1	40.55	±2.6	68.60	±1.1	67.60	±0.1
G1	35.65	±0.6	31.70	±1.0	14.85	±2.6	8.35	±0.4	19.30	±0.4
S	21.35	±0.4	30.05	±0.8	26.35	±2.1	14.35	±0.9	9.75	±0.2
G2	10.00	±1.4	12.50	±0.3	17.05	±2.3	7.85	±0.1	2.95	±0.1
72 h										
Sub-G0/G1	35.50	±16.0	34.50	±1.4	45.95	±1.1	84.70	±0.3	70.50	±2.8
G1	35.45	±10.1	31.75	±0.5	17.05	±0.2	4.95	±0.1	18.70	±1.0
S	20.05	±4.7	23.80	±0.6	26.05	±0.6	7.20	±0.6	9.25	±1.6
G2	7.45	±0.8	9.30	±0.4	10.50	±0.3	3.10	±0.1	1.45	±0.2

3. Discussion

Apoptosis is an active physiological process resulting in cellular self-destruction that involves specific morphological and biochemical changes in the nucleus and cytoplasm [25]. Agents that suppress the proliferation of malignant cells by inducing apoptosis may represent a useful mechanistic approach to both cancer chemoprevention and chemotherapy. While many anticancer agents have been developed, unfavourable side effects and resistance are serious problems [26]. Since the introduction of cisplatin in cancer therapy, metal complexes and organometallic compounds have been gaining importance in oncology [26, 27]. Metal-based compounds increase the possibility of developing molecules better-suited for binding to specific biological targets [27, 18].

Ruthenium complexes appear particularly promising; although they exhibit lower cytotoxicity as compared to cisplatin, they are better tolerated *in vivo* [27, 18, 4]. Research on bioactive ruthenium(II) complexes is very active [28]. These studies

have led to the development of ruthenium based anticancer agents [29,30,18]. Research groups of Sadler, Dyson, Keppler and Reedijk have synthesized a remarkably large number of Ru(II)/Ru(III) organometallic complexes that are being tested for anticancer activity. Ruthenium complexes are slitly cytotoxic but do not affect normal cells significantly. Ruthenium drugs are very promising candidates for novel cancer therapy, with two drugs already in clinical trials, NAMI-A and KP1019 [31,32,18]. Thus, there is growing interest in the use of new organometallics for the treatment of various cancers and the development of safer and more effective therapeutic agents [26,5]. In the present work, we studied the cytotoxic activity of *cis*-tetraammine(oxalato)ruthenium(III) dithionate cytotoxicity towards human erythroleukemia (K562) tumor cell line.

The antiproliferative activity of *cis*-tetraammine(oxalato)ruthenium(III) dithionate, a ruthenium-based complex, have been evaluated *in vitro* against human leukemia (K562) cells using trypan blue and MTT assay. Inhibition of cell proliferation is an important potency indicator for chemotherapeutic drugs. As shown in Figures 2 and 3 a and b, the tested compound induces cell death in a dose and time dependent manner on K562 cells. It is found that the effect was improved linearly while prolonging the incubation time. The determined IC_{50} values of this complex, 18.28 µM (Figure 3a), is considerably the same of those of the commercially used antineoplastic drugs cisplatin (IC_{50} = 11 µM) and oxaliplatin (IC_{50} = 18 µM) on the same tumor cell line [10]. These results corroborate previous observations that Ruthenium(III) complexes induces cytotoxicity towards tumor cells such as human Jurkat, HeLa and SK-BR-3, and murine S-180 and A-20 tumor cell lines [19, 5].

For ruthenium(II) complexes as methylimidazole (RMC1) we also found having cytotoxicity of 17.34 mg mL^{-1} for A549, 18.89 mg mL^{-1} for A375 and 20.25 mg mL^{-1} for Hep G2, respectively. The same compound exhibits cytotoxicity of 51.59 mg mL^{-1} for HBE (basal lineage), as well as demonstrating that the compound RMC1 ruthenium II [33]. The complex $[Ru(phen)_2(\beta\text{-MOPIP})]^{2+}$ can effectively inhibit proliferation of the A375 cell line with a low IC_{50} (5.9±1.1 mM). $[Ru(bpy)_2(dppn)]^{2+}$ exhibits high cytotoxicity against human HT-29 and MCF-7 cancer cell lines comparable to that of cisplatin induces cell death in a dose and time dependent manner [34], and $[Ru(dmp)_2(DBHIP)]^{2+}$ can effectively induce apoptosis of the BEL-7402 cell line [35].

The lower general toxicity of ruthenium compounds compared to platinum drugs has been attributed to the ability of ruthenium compounds to specifically accumulate in cancer tissues. The higher specificity of these compounds for their targets may also be linked to their selective uptake by the tumor compared with healthy tissue and to selective activation by reduction to cytotoxic species within the tumor [36,20,14].

Ruthenium-chloro complexes tend to undergo hydrolysis in aqueous media leading to the generation of cationic $Ru–OH_2$ complexes capable of reacting with DNA with greater ease than the corresponding chloro complexes [37,38,39]. The hydrolyzed complexes interact with the N7 of guanine in DNA duplexes leading to disruption of the structure of genetic material [40].

To explore the mechanisms of the cytotoxic effects produced by *cis*-tetraammine(oxalato)Ruthenium(III) dithionate, drug-induced changes in cell cycle distribution were examined. Compared to the cell cycle profiles of untreated cells, flow cytometric analysis indicated the sub-G1 arresting effect of ruthenium compound on K562 cells, as ruthenium(III) dithionate already induced a 48.2% increase in the number of sub-G0/G1 cells after a 48h incubation. The ruthenium(III) compound caused a minor S phase accumulation after incubation at concentrations of 40 and 150 µM for all periods of exposition **Figure 5**. Treatment with 40 µM of *cis*-$[Ru(C_2O_4)(NH_3)_4]_2(S_2O_6)$ induced respectively a 1.7-fold, 2.2-fold and 2.4-fold increase in the number of sub-G0/G1 cells when compared to control for 24, 48 and 72 h, respectively **Table 1.**

Furthermore, another important biochemical sign of apoptosis was studied: DNA laddering and fragmentation (data not shown), possibly representing DNA cleavage into oligonucleosomal fragments through activation of the cysteine protease caspase-3, which is involved in the proteolytic cleavage of key downstream proteins such as poly (ADP-ribose) polymerase (PARP) [41,42]. This process ultimately results in DNA fragmentation and apoptotic death [41]. Although this type of binding has been suggested to mimic, to some extent, cisplatin-induced DNA crosslinking, other types of damage may exist that dominate or contribute to the biological activity of this drug prototype.

Several studies have been using this test to corroborate the results obtained in other assays. In the present study, results derived from DNA laddering assay did not show K562 DNA fragmentation, instead the results shows DNA integrity and even

differences on DNA content. Is important note that this data does not corroborate with more sensitive techniques such as flow cytometry and comet assay, used in this work. These techniques confirmed that the ruthenium(III) compound interfere on cell cycle and induces cells to enter apoptosis. Thus, we can infer that the technique of DNA gel electrophoresis is not best assay to assess the degradation of genome DNA.

The present study also evaluated the DNA-damaging effects detected by the alkaline version of the comet assay in K562 cancer cells. This assay has been used as a test to predict the risk to develop certain diseases (renal cell carcinoma, cancers of the bladder, esophagus, and lung) due to susceptibility of the individual to DNA damage [23]. The in vitro comet assay is proposed as an alternative to cytogenetic assays in early genotoxicity/photogenotoxicity screening of drug candidates as well as for neurotoxicity [43].

The alkaline comet assay has been used to assess the genotoxicity of chemicals, environmental exposures to carcinogens, toxins, and physical agents both *in vitro* and *in vivo* [44,45]. This method was also used to measure DNA repair capacity in live cells [46] and acellular systems [47].

In our study, *cis*-$[Ru(C_2O_4)(NH_3)_4]_2(S_2O_6)$ shows a significant increase in tailed cells in any of the concentrations tested compared with negative control (**Figure 4**). Consequently, the concentration of *cis*-$[Ru(C_2O_4)(NH_3)_4]_2(S_2O_6)$ might be associated cytotoxicity with direct effect on K562 cells DNA. Thus, it can be deducted that ruthenium-based compounds present selectivity to enter both tumor and normal cells. It is known that all the body cells present transferrin receptors, particularly tumor cells, in which these receptors are found in higher numbers. Due to these features, higher quantities of ruthenium complexes penetrate tumor tissue, reduce ruthenium(III) to ruthenium(II) and binding to DNA (guanine), and promote strand breaks [42,48,49,50,51,52]. Another hypothesis is that even in small quantities this compound might enter normal cells, because ruthenium(III) complexes are activated only by its reduction when it finds an environment with high concentration of glutathione, low pH, and occurrence of hypoxia. It is very common to find tumor cells presenting these conditions since it is known that these cells have high levels of glutathione and oxygen consumption when the nutrients are quickly used due to their accelerated development promoting hypoxia [49]. Consequently, these cells need more glycolitic energy, which increases the level of lactic acid in the tissues and

causes a decrease in the media pH. It is worth emphasizing that ruthenium(III) compounds can be used as pro-drugs that are activated by in vivo reduction to ruthenium(II) [52,49].

Broadening the chemotherapeutic arsenal depends on understanding existing agents with a view toward developing new modes of attack. Indeed, few of the organometallics compounds may function in a manner analogous to cisplatin, which appears to bend DNA by cross-linking adjacent guanines, thereby causing a class of DNA binding proteins to adhere to the site. Overall, the broad class of ruthenium(III) antitumor agents appears to differ from cisplatin by favoring interstrand rather than intrastrand cross-links [53]. In agreement with this hypothesis, it was demonstrated that NAMI-A induced apoptosis in the ECV304 transformed human endothelial and KP1019 in colorectal carcinoma cell lines via activation of caspase-3 and DNA fragmentation [41,54,55].

Despite the resounding success of cisplatin and closely related platinum antitumor agents, the movement of other transition-metal antitumor agents toward the clinic has been exceptionally slow [53]. Non-Platinum chemotherapeutic metallopharmaceuticals hold much promise for the future, and needs to be actively explored in a large variety of tumor types in combination therapies. Besides the already well established NAMI-A and KP-1019 activities on gastrointestinal, breast, prostate, and ovarian cancers [56,57,58] the present results indicate that *cis*-$[Ru(C_2O_4)(NH_3)_4]_2(S_2O_6)$ is worthy of further development as a potential anti-tumor drug that could be used in the treatment of leukemia. Thus, additional studies are needed to determine the molecular mechanisms of the active components and to evaluate the potential *in vivo* anticancer activity of the *cis*-tetraammine(oxalato)Ruthenium(III) dithionate.

4. Material and methods

4.1. Synthesis of *cis*-$[Ru(C_2O_4)(NH_3)_4]_2(S_2O_6)$

The *cis*-$[Ru(C_2O_4)(NH_3)_4]_2(S_2O_6)$ complex (**Figure 1**), was synthesized at the Universidade Federal de Uberlândia (UFU, Minas Gerais, Brazil) following a standard protocol described by Pereira et al [21]. The compound was characterized by electronic spectra at room temperature with the HP 8453 spectrophotometer with diodes arrangement, interfacing a compatible PC HP Vectra XM, using quartz cells.

Carbon and hydrogen microanalyses were performed by the staff of the Analitical Centre of the Chemistry Institute of Universidade de São Paulo (USP, São Paulo, Brazil).

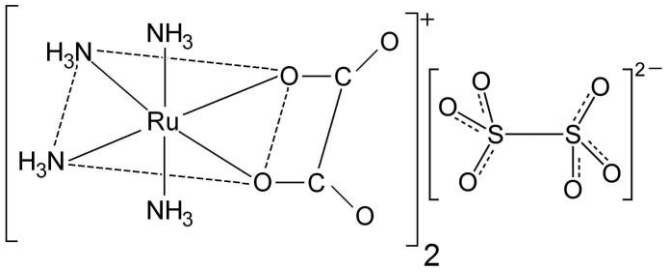

Figure 1. Chemical structure of *cis*-tetraammine(oxalato)Ruthenium(III) Dithionate.

4.2. Cell culture.

The human erythroleukemia (K562) cell line (ATCC number CCL-243^{TM}) was obtained from the American Type Culture Collection (ATCC, Rockville, MD, USA). The cells were cultured in RPMI 1640 medium (pH 7.2-7.4) supplemented with 100U mL^{-1} penicillin G, 100μg mL^{-1} streptomycin, 2 mM L-glutamine, 1.5 g L^{-1} sodium bicarbonate, 4.5 g L^{-1} glucose, 10 m*M* HEPES, 1.0 m*M* sodium pyruvate and 10% fetal calf serum (FCS) (all reagents were obtained from Gibco, Grand Island, NY, USA) at 37°C, 5% CO_2 and humidified atmosphere.

The cells were disposed into 96 well plates (1×10^5 cells/well) and cultured in RPMI 1640 medium. Cells were harvested at specified intervals and the number of cells per well was determined by cell counting with a hemocytometer (Neubauer chamber). Briefly, tumor cells were aspirated, washed in sterile PBS and an aliquot of the cell suspension was put in Trypan Blue 1% (m/v) (Sigma-Aldrich, St. Louis, MO, USA) and counted. Only cell dilutions with > 95% of viable cells were included in the posteriors analysis.

4.3. Cell Citotoxicity (Trypan blue staining)

The citotoxicity of the K562 cells was evaluated by the trypan blue exclusion assay. The tumor cells were incubated for 24 h, 48 h and 72 h with different concentrations of the tested ruthenium compound *cis*-$[Ru(C_2O_4)(NH_3)_4]_2(S_2O_6)$ (from

0.015 – 32 μM) at 37 °C. Additionally, Carboplatin (50 μM) and Paclitaxel (25 μM) were applied as positive control. After incubation, the cells were washed in PBS (pH 7.4) and suspended in a complete RPMI 1640 medium. Then 40 μL of the trypan blue solution (0.4%, Sigma) and 10 μL of the cell suspension were mixed and after 5 min the percentage of viable K562 cells was evaluated under brightfield optical microscope using a newbauer chamber. The correlation between the viable cells (that excluded trypan blue dye) and dead cells (stained cells) were assessed. The results are presented as mean±S.D. (standard deviation) from three independent experiments.

4.4. Viability assay.

Cytotoxic activity of *cis*-$[Ru(C_2O_4)(NH_3)_4]_2(S_2O_6)$ on K562 was measured by modified MTT assay [22], which is based on the reduction of yellow 3-(4,5-dimethylthiazol-2-yl)-2,5-diphenyl tetrazolium bromide (MTT) to dark-blue, insoluble formazan in mitochondria of the living cells. The MTT assay was performed in 96-well tissue culture plates (Nalge-Nunc, Rochester, NY, USA) as follows: the cells (1×10^5/well) were seeded in tissue culture plates and incubated with the different concentrations of ruthenium compound (from 0.15 – 150 μM) dissolved in a total volume of 100 μL/well for 24 h and 48 h at 37 °C and 5% CO_2. The cells incubated with medium only served as a control. Following the exposure to the tested substances, the cells were incubated with 10 μL of MTT solution (5 mg mL^{-1}) (Sigma-Aldrich, St. Louis, MO, USA) for 3 h. The microplates were then centrifuged (300× *g*/15 min/10°C) and the culture media were discarded. Afterwards 200 μl of PBS/20% of SDS (lauryl sulfate) solution (Sigma-Aldrich, USA) was added to each well to stop the reaction and plates were kept in the dark overnight. After the next 12 h the absorbance of dissolved formazan was measured by a Stat Fax 2100 microplate reader (Awareness Technology, Palm City, FL, USA) at 565 nm. The cell viability was expressed in % related to control (100% of viability). The cytotoxic rate was calculated as follows: cytotoxicity (%) = [1 - (absorbance of the treated wells)/(absorbance of the control wells)]×100%. The cytotoxic effect of the tested substances was determined in at least three independent experiments, where each one of the culture plates contained the wells with tested concentration in triplicate, the wells with control (cells in medium) and the blank (culture medium alone). The

50% inhibitory concentration (IC_{50}) value was determined using GraphPad Prism 4.02 for Windows (GraphPad Software, San Diego, CA, USA).

4.5. DNA laddering assay.

Briefly, 2×10^6 cells (K562) were treated with different concentrations of *cis*-$[Ru(C_2O_4)(NH_3)_4]_2(S_2O_6)$ (from 0.15 – 150 µM) for 24 h at 37 °C and 5% CO^2. Cells were harvested and centrifuged at 300×*g*/15 min/10°C and washed with PBS. The cells were then ressuspended at a concentration of 1×10^6 cells mL^{-1} in an extraction buffer (1 mol Tris-HCl, 2 mol Na_2EDTA, 0,5g m L^{-1} SDS) and treated with 20 mg L^{-1} RNase A at 37°C for 60 min, followed by incubation with proteinase K (100 mg L^{-1}) at 37°C for 60 min. An equal volume of saline solution (NaCl 6 M) was added to the cells and centrifuged at 13,000×*g* for 10min. The supernatant was collected and 2 volume ethanol (-20°C) were added. The samples were centrifuged at 13,000×*g* for 30 min at 4°C. The supernatant was then discarded and the pellets dissolved in TE buffer (1×). The concentration of DNA was detected using a UV spectrophotometer (Beckman DU-640, USA). The DNA (5 µg/tube) was transferred to a 1.5% agarose horizontal gel, and electrophoresis was performed at 100V cm^{-1} for 90 min. The DNA in the gels was visualized by ultraviolet transillumination after staining with ethidium bromide (5 µg mL^{-1}) using an Omega® molecular imaging system (UltraLum Inc., Claremont, CA, USA).

4.6. Comet Assay

An aliquot of from each K562 culture was taken after 24 and 48 h incubation for the alkaline version of the comet assay [23]. The compound *cis*-$[Ru(C_2O_4)(NH_3)_4]_2(S_2O_6)$ was studied at different concentrations (from 10 – 150 µM). Briefly, 300 µL of the cell suspension was centrifuged for 5 min (500 rpm) in a refrigerated microcentrifuge (Sorvall Legend Mach 1.6 R, Thermo Fisher Scientific, Waltham, MA, USA). The resulting pellet was homogenized with 80 µL of a low melting point agarose (0.5%), spread onto microscope slides pre-coated with a normal melting point agarose (1.5%), and covered with a cover slip. After 5 min at 4°C, the cover slip was removed, and the slides were immersed in cold lysis solution

[2.4 *M* NaCl, 100 mM ethylenediamine tetraacetic acid (EDTA), 10 mM Tris, 10% DMSO, and 1% Triton-X, pH 10] for 24 h.

After lysis, the slides were placed in an electrophoresis chamber and covered with electrophoresis buffer (300 mM NaOH per 1 mM EDTA, pH>13) for a remaining 20 min to allow DNA unwinding. The electrophoresis proceeded for 20 min (25 V and 300 mA). Afterwards, the slides were submerged for 15 min in a neutralization buffer (0.4 M Tris– HCl, pH 7.5), dried at room temperature, and fixed in 100% ethanol for 5 min. All the steps were conducted in the dark to prevent additional DNA damage. Slide staining was performed immediately before analysis using ethidium bromide (20 μg mL^{-1}). Slides were prepared in duplicate, and 100 cells were screened per sample (50 cells from each slide) in a fluorescent microscope (Leica Microsystems GmbH, Wetzlar, Germany) equipped with an excitation filter of 515–560 nm and a barrier filter of 590 nm using a ×40 objective. The nucleus was classified according to the migration of the fragments using the software CometScore 15 according to [20].

For damage index calculation, cells were sorted into four classes, according to tail size. The damage index (DI) is the sum of classes of the 100 cells analyzed per fish, and may vary from 0 (all cells undamaged – 0×100) to 400 (all cells highly damaged – 4×100). The damage index is based on the length of migration and on the amount of DNA in the tail, and it is considered a sensitive measurement of detectable DNA damage [21]. To quantify the damage to the DNA, the following formula was used:

$$DI\ (au) = \frac{N1 + N2 + N3 + N4}{S/100}$$

where DI = DNA damage index, au = arbitrary unit, N1 - N4 = nucleoids in levels 1, 2, 3 and 4, S = number of nucleoids analyzed, including level 0.

4.7. Cell Cycle Analysis by flow cytometry

In order to investigate the possible effect of the ruthenium compound on cell cycle progression, K562 cells were treated with different concentrations of *cis*-$[Ru(C_2O_4)(NH_3)_4]_2(S_2O_6)$ (from 1.5 – 150 μM) for 24, 28 and 72 h. Briefly, 5×10^5 cells were harvested by centrifugation, washed with PBS, fixed with 70% (v/v) cold aqueous ethanol and stored overnight at -20 ◦C. The fixed cells were washed with PBS and incubated with propidium iodide (PI; Sigma-Aldrich, St. Louis, MO, USA)

containing 0.05% RNase. Samples were incubated at 4 ◦C in the dark and analyzed by flow cytometry (FACS CantoII, BD Biosciences, San José, CA, USA). The percentage of cells in G1, S, G2 and sub-G1 was analyzed using ModFit LT software (Verity Software House, Topsham, ME, USA).

4.8. Statistical analysis.

Three independent in vitro experiments were carried out. Statistical results were expressed as the mean ± standard deviation of the means obtained from triplicates of each independent experiment. Correlation tests were performed to determine the effects of concentration of ruthenium complex on tumor cell lines. Statistical significance of differences *($p<0.05$) as compared to untreated cells (control) was evaluated by applying analysis of variance (ANOVA) and Tukey or Dunnet's post tests, when applicable. The IC_{50} (concentration that produces a 50% inhibitory effect on the evaluated parameter) was graphically obtained from the dose-response curves.

ACKNOWLEDGMENTS

The authors gratefully acknowledge the financial support of Research and Projects Financing (FINEP) (Grant No.01.06.0941.00/CT-Saúde to Elisângela de Paula Silveira-Lacerda), Brazilian National Counsel of Technological and Scientific Development (CNPq) through fellowship to Flávia de Castro Pereira (Grant No. 131960/2008-3) and Coordination for the Advancement of Higher Education Staff (CAPES) through fellowship to Aliny Pereira de Lima and Cesar Augusto Sam Tiago Vilanova-Costa.

REFERENCES

[1] Canadian Cancer Society/National Cancer Institute of Canada: Canadian Cancer Statistics (2005), Toronto, Canada. ISSN: 0835-2976.

[2] American Cancer Society: Cancer Facts & Figures (2009). http://www.cancer.org/acs/groups/content@epidemiologysurveilance/documents/documents/acspc-031941.pdf.

[3] Robert, J. and Jarry, C. (2003). Multidrug resistance reversal agents. *Journal of Medicinal Chemistry,* **46**, 4805–4817.

[4] Menezes, C.S.R., Costa, L.C.G.P., Ávila, V.M.R., Ferreira, M.J., Vieira, C.U., Pavanin, L.A., Homsi-Brandeburgo, M.I., Hamaguchi, A. and Silveira-Lacerda, E.P. (2007). Analysis in vivo of antitumor activity, cytotoxicity and interaction between plasmid DNA and the *cis*-dichlorotetraammineruthenium(III) chloride. Chemical–*Biological Interactions,* **167**,116–124.

[5] Silveira-Lacerda, E.P., Vilanova-Costa, C.A.S.T., Hamaguchi, A., Pavanin, L.A., Goulart, L.R., Homsi-Brandenburgo, M.I., dos Santos, W.B., Soares, A.M. and Nomizo, A. (2009b). The Ruthenium Complex *cis*-(Dichloro) tetraammineruthenium(III) Chloride Presents Selective Cytotoxicity Against Murine B Cell Lymphoma (A-20), Murine Ascitic Sarcoma 180 (S-180), Human Breast Adenocarcinoma (SK-BR-3), and Human T Cell Leukemia (Jurkat) Tumor Cell Lines. *Biological Trace Element Research.* doi: 10.1007/s12011-009-8498-3.

[6] Ge, H., Kong, X., Shi, L., Hou, L., Liu, Z. and Li, P. (2009). Gamma-linolenic acid induces apoptosis and lipid peroxidation in human chronic myelogenous leukemia K562 cells. *Cell Biology International,* **33**, 402-410.

[7] Kim, R., Tanabe, K., Uchida, Y., Emi, M., Inoue, H. and Toge, T. (2002). Current status of the molecular mechanisms of anticancer drug-induced apoptosis e the contribution of molecular-level analysis to cancer chemotherapy. *Cancer Chemotherapy and Pharmacology,* **50**, 343-52.

[8] Rosenberg, B., Van Camp, L. and Krigas, T. (1965). Inhibition of cell division in *Escherichia coli* by electrolysis products from a platinum electrode. *Nature,* **205**, 698–699.

[9] Kelland, L.R. and Farrell, N.P. (2000) Platinum-Based Drugs in Cancer Therapy. *Totowa: Humana Press NJ*, 89, 251-275.

[10] Štarha, P., Trávnícek, Z. and Popa. I. (2009). Synthesis, characterization and in vitro cytotoxicity of the first palladium(II) oxalato complexes involving adenine-based ligands. *Journal of Inorganic Biochemistry,* **103**, 978–988.

[11] Dik-Lung M., Hong-Zhang He, Ka-Ho Leung, Daniel Shiu-Hin Chan, and Chung-Hang Leung (2013). Bioactive Luminescent Transition-Metal Complexes for Biomedical Applications. Medicinal Inorganic Chemistry, 52, 7666 – 7682.

[12] Eric Meggers (2009). Targeting proteins with metal complexes. Chem. Commun., 1001–1010.

[13] Chung-Hang Leung, Hai-Jing Zhong, Hui Yang, Zhen Cheng, Daniel Shiu-Hin Chan, et al, (2012). A Metal-Based Inhibitor of Tumor Necrosis Factor-a**. Angew. Chem., 51, 9010 –9014.

[14] Clarke, M.J. (2003). Ruthenium metallopharmaceuticals. *Coordination Chemistry Review*, **236**, 209-233.

[15] Ronconi, L. and Sadler, P.J. (2007). Using coordination chemistry to design new medicines. *Coordination Chemistry Reviews,* **251**, 1633-1648.

[16] Sava, G., Capozzi, I., Clerici, V., Gagliardi, G., Alessio, E. and Mestroni, G. (1998). Pharmacological control of lung metastases of solid tumours by a novel ruthenium complex, *Clinical & Experimental Metastasis,* **16**, 371-379.

[17] Jakupec, M.A., Arion, V.B., Kapitza, S., Reisner, E., Eichinger, A., Pongratz, M., Graf von Keyserlingk, N. and Keppler B.K. (2005). KP1019 (FFC14A) from bench to

bedside: preclinical and early clinical development. *Int. J. Clin. Pharmacol Ther.,* **43**: 595-596.

[18] Hartinger, C.G., Zorbas-Seifried, S., Jakupec, M.A., Kynast, B., Zorbas, H. and Keppler, B,K. (2006). From bench to bedside - preclinical and early clinical development of the anticancer agent indazolium *trans*-[tetrachloro bis(1Hindazole)ruthenate(III)] (KP1019 or FFC144). *Journal of Inorganic Biochemistry*, **100**, 891-904.

[19] Frasca, D.R., Gehrig, L.E. and Clarke, M.J. (2001). Cellular effects of transferrin coordinated to $[Cl(NH_3)_5Ru]Cl_2$ and *cis*-$[Cl_2(NH_3)_4Ru]Cl$. *Journal of Inorganic Biochemistry*, **83**, 139-149.

[20] Allardyce, C.S., Dyson, P.J., Ellis, D.J., Salter, P.A. and Scopelliti, R. (2003). Synthesis and characterisation of some water soluble ruthenium(II)–arene complexes and an investigation of their antibiotic and antiviral properties. *Journal of Organometallic Chemistry*, **668**, 35-42.

[21] Pereira, F.C., Vilanova-Costa, C.A.S.T., Lima, A.P., Ribeiro, A.S.B.B., da Silva, H.D., Pavanin, L.A., Silveira-Lacerda, E.P. (2009). Cytotoxic and genotoxic effects of cis-tetraammine(oxalato)ruthenium(III) dithionate on the root meristem cells of Allium cepa. *Biol Trace Elem Res.,* **128**(3):258–268. doi:10.1007/s12011-008-8272-y.

[22] Mosmann, T. (1983) Rapid colorimetric assay for cellular growth and survival. *J. Immunol. Methods*, **65**, 55-63.

[23] Ribeiro, A.S.B.B., Da Silva, C.C., Pereira, F.C., Lima, A.P., Vilanova-Costa, C.A.S.T., Aguiar, S.S., Pavanin, L.A., Da Cruz, A.D., Silveira-Lacerda, E.P. (2009). Mutagenic and genotoxic effects of cis-(dichloro)tetraammineruthenium(III) chloride on human peripheral blood lymphocytes. *Biol Trace Elem Res*., **130**, 249-261. doi:10.1007s12011-009-8334-9.

[24] Grisolia, C.K., Rivero, C.L.G., Starling, F.L.R.M., Silva, I.C.R., Barbosa, A.C. and Dorea, J.G. (2009). Profile of micronucleus frequencies and DNA damage in different species of fish in a eutrophic tropical lake. *Genetics and Molecular Biology*, **32** (1). doi: 10.1590/S1415-47572009005000009.

[25] Kostova, J. (2006). Ruthenium complexes as anticancer agents. *Current Medicinal Chemistry*, **13**, 1085–1107.

[26] Panchal, R.G. (1998). Novel therapeutic strategies to selectively kill cancer cells. *Biochemical Pharmacology,* **55**, 247–252.

[27] Sanna, B., Debidda, M., Pintus, G., Tadolini, B., Posadino, A.M., Bennardini, F., Sava, G. and Ventura, C. (2002). The anti-metastatic agent imidazolium *trans*-imidazoledimethylsulfoxide-tetrachlororuthenate induces endothelial cell apoptosis by inhibiting the mitogen-activated protein kinase/extracellular signal-regulated kinase signaling pathway. *Archives of Biochemistry and Biophysics*, **403**, 209-218.

[28] Chen T., Wong Y.S. (2008). Selenocystine induces apoptosis of A375 human melanoma cells by activating ROS-mediated mitochondrial pathway and p53 phosphorylation, Cell Mol. Life Sci. 65, 2763 - 2775.

[29] Yan, Y.K., Melchart, M., Habtemariam, A., and Sadler, P.J. (2005). Organometallic chemistry, biology and medicine: ruthenium arene anticancer complexes. Chem Commun 38, 4764–4776.

[30] W.H. Ang, P.J. Dyson (2006). Eur. J. Inorg. Chem. 4003–4018.

[31] Cocchietto, M., and Sava, G. (2000). Blood concentration and toxicity of the antimetastasis agent NAMI-A following repeated intravenous treatment in mice. Pharmacol Toxicol 87, 193–197.

[32] Zorzet, S., Sorce, A., Casarsa, C., Cocchietto, M., and Sava, G. (2001). Pharmacological effects of the ruthenium complex NAMI-A given orally to CBA mice with MCa mammary carcinoma. Met Based Drugs 8, 1–7.

[33] Yang X., Chen L., Liu Y., Yongguang Y., Chen T., Zheng W., Liu J. a, Qing-Yu He (2012). Ruthenium methylimidazole complexes induced apoptosis in lung cancer A549 cells through intrinsic mitochondrial pathway. Biochimie 94, 345-353.

[34] Schatzschneider, U., Niesel, J., Ott, I., Gust, R., Alborzinia, H.,and Wo ¨ lfl, S. (2008). Cellular uptake, cytotoxicity, and metabolic profiling of human cancer cells treated with ruthenium(II) polypyridyl complexes [Ru(bpy)2(N–N)]Cl2 with N–N¼bpy, phen, dpq, dppz, and dppn. ChemMedChem 3, 1104–1109.

[35] Liu Y.J., Zeng C.H., Liang Z.H., Yao J.H., Huang H.L., Li Z.Z., Wu F.H., (2010). Synthesis of ruthenium(II) complexes and characterization of their cytotoxicity in vitro, apoptosis, DNA-binding and antioxidant activity, Eur. J. Med. Chem. 45, 3087-3095.

[36] Bergamo, A., Gagliardi, R., Scarcia, V., Furlani, A., Alessio, E., Mestroni, G., Sava, G. 1999. In vitro cell cycle arrest, in vivo action on solid metastasizing tumors and host toxicity of the antimetastatic drug NAMI-A and cisplatin. J Pharmacol Exp Ther 289, 559–564.

[37] M. Melchart, A. Habtemarlam, O. Novakova, S.A. Moggach, F.P.A. Fabbiani, S. Parsons, V. Brabec, P.J. Sadler, (2007). Inorg. Chem. 46, 8950–8962.

[38] M. Bacac, A.C.G. Hotze, K.V.D. Schilden, J.G. Haasnoot, S. Pacor, E. Alessio, G. Sava, J. Reedijk, (2004). J. Inorg. Biochem. 98 402–412.

[39] A.C.G. Hotze, E.P.L. Geer, S.E. Caspers, H. Kooijman, J.G. Haasnoot, J. Reedijk, (2004) Inorg. Chem. 43 4935–4943.

[40] H. Chen, J.A. Parkinson, R.E. Morris, P.J. Sadler, J. Am. Chem. Soc. 125 (2003)179–186.

[41] Bortner, C.D., Oldenburg, N.B. and Cidlowski, J.A. (1995). The role of DNA fragmentation in apoptosis. *Trends in Cell Biology,* **5**, 21-26.

[42] Clarke, M.J. and Stubbs, M. (1996). Interactions of metallopharmaceuticals with DNA. *Metal Ions in Biological Systems,* **32**, 727-780.

[43] Witte, I., Plappert, U., de Wall, H. and Hartmann, A. (2007). Genetic toxicity assessment: employing the best science for human safety evaluation part III: the comet assay as an alternative to in vitro clastogenicity tests for early drug candidate selection. *Toxicological Sciences*, **97**, 21-26.

[44] Trzeciak, A.R., Kowalik, J., Małecka-Panas, E., Drzewoski, J., Wojewodzka, M., Iwanenko, T. and Błasiak, J. (2000). Genotoxicity of chromium in human gastric mucosa cells and peripheral blood lymphocytes evaluated by the single cell gel electrophoresis (comet assay). *Medical Science Monitor*, **6**, 24-29.

[45] Sekihashi, K., Yamamoto, A., Matsumura, Y., Ueno, S., Watanabe-Akanuma, M., Kassie, F., Knasmüller, S., Tsuda, S. and Sasaki, Y.F. (2002). Comparative investigation of multiple organs of mice and rats in the comet assay. *Mutatation Research,* **517**, 53-75.

[46] Banath, J.P., Fushiki, M. and Olive, P.L. (1998). Rejoining of DNA single- and double-strand breaks in human white blood cells exposed to ionizing radiation. *Journal of Radiation Biology,* **7**, 649-660.

[47] Dusinská, M., Collins, A., Kazimírová, A., Barancoková, M., Harrington, V., Volkovová, K., Staruchová, M., Horská, A., Wsólová, L., Kocan, A., Petrík, J., Machata, M., Ratcliffe, B. and Kyrtopoulos, S. (2004). Genotoxic effects of asbestos in humans. *Mutatation Research,* **553**, 91-102.

[48] Lebwohl, D. and Canetta, R. (1998). Clinical development of platinum complexes in cancer therapy: an historical perspective and an update. *European Journal of Cancer,* **34**, 1522-1534.

[49] Sava, G. and Bergamo. A. (2000). Ruthenium-based compounds and tumour growth control (review). *International Journal of Oncology,* **17**, 353-365.

[50] Katsaros, N. and Anagnostopoulou, A, (2002). Rhodium and its compounds as potential agents in cancer treatment (critical reviews). *Oncology/Hematology* **42**, 297-308.

[51] Galanski, M., Arion, V.B., Jakupec, M.A. and Keppler, B.K. (2003). Recent developments in the field of tumorinhibiting metal complexes. *Current Pharmaceutical Design* **9**, 2078-2089.

[52] Desoize, B. (2004). Metals and metal compounds in cancer treatment. *Anticancer Research,* **24**, 1529–1544.

[53] Clarke, M.J., Zhu, F. and Frasca, D.R. (1999). Non-Platinum Chemotherapeutic Metallopharmaceuticals. *Chemical Reviews,* **99**, 2511-2534.

[54] Nunez, G., Benedict, M.A., Hu, Y. and Inohara, N. (1998). Caspases: the proteases of the apoptotic pathway. *Oncogene*, **17**, 3237-3245.

[55] Kapitza, S., Pongratz, M., Jakupec, M.A., Heffeter, P., Berger, W., Lackinger, L., Keppler, B.K. and Marian, B. (2005). Heterocyclic complexes of ruthenium(III) induce apoptosis in colorectal carcinoma cells. *Journal of Cancer Research and Clinical Oncology,* **131**, 101-110.

[56] Pluim, D., Van Waardenburg, R.C., Beijnen, J.H. and Schellens, J.H. (2004). Cytotoxicity of the organic ruthenium anticancer drug Nami-A is correlated with DNA binding in four different human tumor cell lines. *Cancer Chemotherapy and Pharmacology*, **54**, 71-78.

[57] Bergamo, A. and Sava, G. (2007). Ruthenium complexes can target determinants of tumour malignancy. *Dalton Transactions*, **13**, 1267-1272.

5.2. ARTIGO 2

Ruthenium [RuCl(bcn)(N-N)(P-P)]PF6 complexes: *In vitro* pre-clinical trials and a potential metallodrug against sarcoma S180 tumor cells

(bcn = benzonitrile; N-N = 2,2´-bipyridine, 1,10-phenanthroline; P-P = 1,4-bis(diphenylphosphino)butane, 1,2-bis (diphenylphosphino)ethane, or 1,1´-(diphenylphosphino)ferrocene

FLÁVIA DE CASTRO PEREIRA[1], ALINY PEREIRA DE LIMA[1], WANESSA CARVALHO PIRES[1], THALLITA MONTEIRO[1], LORENA FÉLIX MAGALHÃES[1], WANDERSON COSTA[1], BENEDICTO AUGUSTO V. LIMA[2], ANGELICA ELLEN GRAMINHA[2], ALZIR AZEVEDO BATISTA[2], JAVIER ELLENA[3], ELISÂNGELA DE PAULA SILVEIRA-LACERDA[1]

[1]Laboratory of Molecular Genetics and Cytogenetics, Institute of Biological Sciences, Federal University of *Goiás* - UFG, Goiânia, GO, Brazil

[2]Chemistry Department, Federal University of São Carlos – São Carlos, São Paulo, Brazil

[3]São Carlos Physics Institute, University of São Paulo, São Carlos, SP, Brazil

**Corresponding authors: Email, silveiralacerda@gmail.com; daab@ufscar.br*

Running title: Apoptotic activity of *Ruthenium II* in S180 cells

ABSTRACT

Ruthenium complexes are considered to be a very promising approach to treating cancer, primarily because of their relatively low toxicity and high antitumor activity. Ruthenium exhibits the ability to mimic iron in its binding and transferring properties, and these are most likely the primary reasons for its low toxicity. This low toxicity could allow for the administration of a higher dose of a drug for a longer period to a patient, leading to a more efficient antineoplastic chemotherapy. Therefore, the motivation to use ruthenium complexes in cancer treatment has led our research group to synthesize new complexes with this metal and test them against different types of tumor cells, yielding promising results. In this paper, we will describe results involving biological studies that employed the $[RuCl(bcn)(bipy)(dppb)]PF_6$, $[RuCl(bcn)(phen)(dppb)]PF_6$, $[RuCl(bnc)(bipy)(dppf)]PF_6$ and $[RuCl(bcn)(bipy)(dppe)]PF_6$ complexes. The present work studied the cytotoxic activity, apoptosis, changes in cell cycle and gene expression of a $[RuCl(bcn)(bipy)(dppe)]PF_6$ treated sarcoma 180 (S180) tumor cell line. Ruthenium II complexes were tested in cell culture, cell viability testing with MTT, apoptotic cell analysis by flow cytometry, cell cycle analysis by flow cytometry, mitochondrial membrane potential ($\Delta\Psi m$), Bcl-2 flow cytometry testing, caspase activity measurement, and real time quantitative PCR. The cytotoxicity of the complex was evaluated by MTT assay, and the mechanism of cell deaths induced by the complex was investigated. The results demonstrated that the $[RuCl(bcn)(bipy)(dppe)]PF_6$ complex inhibits S180 cell growth with an IC_{50} value of 17.02 μM ± 8.21. The complex also exhibits higher cytotoxicity (53.73 μM ± 5.71) towards lymphocytes than normal cells. The flow cytometric analysis revealed that the complex inhibits the growth of tumor cells by inducing apoptosis, as evidenced by the increase in cells with positive annexin V and G0/G1 phase cell cycle arrest. Further investigation showed that the [RuCl(bcn)(bipy)(dppe) complex induces a loss in the mitochondrial membrane potential, and the complex provokes decreased Bcl-2 protein expression and increased caspase 3 activation, but the increased activation of caspase 8 caused a decrease in caspase 3, 8, 9, Bax and p53 gene expression. In conclusion, the ruthenium $[RuCl(bcn)(bipy)(dppe)]PF_6$ complex was promising against S180 tumor cells, and it may be a candidate for further investigation as a chemotherapeutic agent against sarcomas.

Keywords: Ruthenium complexes, Sarcoma 180 (S180), apoptosis induction, expression of pro-apoptotic genes

Introduction

Chemotherapy based on transition metal compounds became promising after the discovery of cisplatin by Barnett Rosenberg [1 - 3]. Cisplatin is a chemotherapeutic that is used to treat carcinomas of the ovary, testis, bladder tumors, head and neck [3 - 5]. However, because of the high toxicity, tumor resistance and side effects of cisplatin and its derivatives, the search for a more effective and less toxic antitumor drug became necessary [1 - 3]. In this context, ruthenium complexes are considered a very promising approach, primarily because of their relatively low toxicity and high antitumor activity [4 - 7]. Ruthenium exhibits the ability to mimic iron in terms of its binding and transferring properties, and this is the most likely reason for its low toxicity. This low toxicity could allow for the administration of a higher dose of the drug for a longer period to the patient, leading to more efficient antineoplastic chemotherapy [8 – 12].

NAMI (ImH[trans-RuCl4(DMSO)(Im)]) and KP1019 (InH[trans-RuCl4In2]) [13, 14] have successfully completed phase II clinical trials for the treatment of metastatic tumors and colon cancers, respectively, but both have limitations as antitumor drugs [15]. Few studies have been performed on the anticancer activity of ruthenium (II) polypyridyl complexes [16, 18]. Therefore, the use of ruthenium complexes for cancer treatment has motivated our research group to synthesize new complexes with this metal and to test them against different types of tumor cells, yielding promising results. In this paper, we will describe a few results of biological studies that employed $[RuCl(bcn)(bipy)(dppb)]PF_6$, $[RuCl(bcn)(phen)(dppb)]PF_6$, $[RuCl(bnc)(bipy)(dppf)]PF_6$ and $[RuCl(bCN)(bipy)(dppe)]PF_6$ complexes. The diphosphines were chosen for their ability to stabilize Ru(II) complexes, and the diimines can assist in complex intercalation with DNA. A benzonitrile ligand was introduced into the complexes to make them anionic and more soluble in the cell culture medium.

Material and Methods

Chemicals

All manipulations were performed under purified argon by standard Schlenk technique. Reagent grade solvents were appropriately distilled and dried before use.

All chemicals used in this work were purchased from Sigma-Aldrich, St. Louis, USA. The cis-[$RuCl_2$(dppb)(bipy)], cis-[$RuCl_2$(dppf)(bipy)], and cis-[$RuCl_2$(dppb)(phen)] starting complexes, in which dppb = 1,4-bis(diphenylphosphine)butane, dppf =1,10-bis(diphenylphosphine)ferrocene, bipy = 2,20-bipyridine, and phen = 1,10-phenanthroline, were prepared according to methods from the literature [19]. The synthesis of the [RuCl(bcn)(bipy)(dppb)]PF_6, [RuCl(bcn)(phen)(dppb)]PF_6 and [RuCl(bnc)(bipy)(dppf)]PF_6 complexes were published elsewhere [19].

Synthesis

The synthesis of *cis*-[RuCl(bzCN)(P–P)(N–N)](PF_6) complexes [N–N = 2,2`-bipyridine (bipy) or 1,10-phenantroline (phen), P–P = 1,4-bis-(diphenylphosphino)butane (dppb) or 1,10-bis(diphenylphosphino)-ferrocene (dppf), and bzCN = benzonitrile] was performed as described in reference [19] by reacting with the corresponding *cis*-[$RuCl_2$(P–P)(N–N)] precursor, which was dissolved in CH_2Cl_2 with three times the excess bzCN, but by using KPF_6, instead of NH_4PF_6, in methanol under an argon atmosphere. The synthesis methodology for the [RuCl(bCN)(bipy)(dppe)]PF_6 complex was similar, and cis-[$RuCl_2$(dppe)(bipy)] was used as the precursor. In this case, the *cis*-[$RuCl_2$(dppe)(bipy)] (72.66 mg; 0.100 mmol) was dissolved in CH_2Cl_2 (40 mL) with an excess of benzonitrile (21 µL, 0.200 mmol). The KPF_6 (27.70 mg, 0.15 mmol) was dissolved in methanol (ca. 5 mL) and added to the ruthenium solution under an argon atmosphere for 24 h. The reaction volume was reduced to approximately 2 mL and ether (~15 mL) was added to precipitate the product, which was filtered off and washed with water (2 x 10 mL) and ether (2 x 5 mL). The yield was 90%. Crystals of the [RuCl(bcn)(bipy)(dppe)]PF_6.0.75($C_4H_{10}O$) species from the CH_2Cl_2/Et_2O solution yielded suitable crystals for determining the X-ray structure, which is illustrated in Figure 1.

Microanalysis for [RuCl(bCN)(bipy)(dppe)]PF_6.2H_2O: C% (calc) 52.98/52.96; H%, 4.53/4,23; N%, 4.19/4.30

Hydrogen NMR data for the [RuCl(bCN)(bipy)(dppe)]PF_6 complex: ^{1}H (400 MHz,

$(CD_3)_2CO$): δ 9.40 ppm (1H, m; bipy); 8.63 ppm (1H, d, *J* = 8.4 Hz; bipy); 8.49 ppm (2 H, t, *J* = 9.2 Hz; Ph); 8.36 – 8.28 ppm (2 H, m; bipy); 8.25 – 8.18 ppm (2 H, m; Ph); 7.86 ppm (1 H, t, J = 6.4 Hz; bipy); 7.81 – 7.71 ppm (1 H, bipy; 3 H, Ph, m); 7.65 ppm (1H, t, *J* = 8.0 Hz; bCN); 7.50 – 7.37 ppm (8 H, m, Ph); 7.31 ppm (2 H, dt, *J* = 8.0 e 2.4 Hz, bCN); 7.20 ppm (1 H, m, bipy); 7.12 ppm (1 H, m, bipy); 7.01 – 6.92 ppm (2 H, bCN; 2 H, Ph, m); 6.82 – 6.75 ppm (2 H, t, *J* = 8.8; Ph); 6.68 – 6.62 ppm (1 H, m; Ph); 3.70 – 3.44 ppm (2 H, m, CH_2); 3.14 – 2.98 ppm (1 H, m, CH_2); and 2.95 – 2.79 ppm (1 H, m, CH_2).

Apparatus

The 31P{1H} NMR experiments were recorded on a BRUKER 9.4 T instrument (400 MHz for hydrogen frequency) in CH_2Cl_2 by using a capillary containing D_2O. The microanalyses were performed in the Microanalytical Laboratory of the Department of Chemistry at the Universidade Federal de São Carlos, São Carlos (SP) by using a FISIONS CHNS, mod. EA 1108 microanalyses.

X-ray crystallography

The crystals of the isolated complexes were grown by the slow evaporation of dichloromethane/diethyl ether solution. These crystals were mounted on an Enraf-Nonius Kappa-CCD diffractometer with graphite monochromated Mo-Ka (k = 0.71073 Å) radiation. The final unit cell parameters were based on all the reflections. Data collections were taken by using the COLLECT program. The integration and scaling of the reflections were performed with the HKL Denzo-Scalepack system of programs. Gaussian absorption corrections were performed. The structures were solved by direct methods with SHELXS-97. All hydrogen atoms were stereochemically positioned and refined with the riding model. The ORTEPs shown in Figure 1 were prepared by using ORTEP-3 for Windows. The data collections and some experimental details are summarized in Table 2.

Table 2**:** Crystallographic data for the [RuCl(bzCN)(bipy)(dppe)]PF_6 complex.

	1.1.1. [RuCl(bCN)(bipy)(dppe)]PF_6
Empirical formula	$[RuC_{43}H_{37}N_3P_2Cl]PF_6.0.75(C_4H_{10}O)$
Formula weight	994.78
Temperature / Wavelength	293(2) K / 0.71073 Å
Crystal system	Monoclinic
Space group	$P2_1/c$
Unit cell dimensions	a = 16.4610(2) Å b = 17.5844(5) Å, β = 98.408(1)°. c = 16.5738(2) Å
Volume / Z	4664.41(10) $Å^3$ / 4
Density (calculated)	1.417 Mg/m^3
Absorption coefficient	0.557 mm^{-1}
F(000)	2030
Crystal size	0.26 x 0.38 x 0.15 mm^3
Theta range for data collection	3.02 to 25.68°.
Index ranges	$-20 \leq h \leq 20$, $-20 \leq k \leq 21$, $-19 \leq l \leq 20$
Reflections collected	32036
Independent reflections	8831 [R(int) = 0.0534]
Completeness to theta = 25.35°	99.6 %
Max. and min. transmission	0.939 and 0.819
Data / restraints / parameters	8831 / 1 / 559
Goodness-of-fit on F^2	1.038
Final R indices [I>2σ(I)]	R1 = 0.0493, wR2 = 0.1391
R indices (all data)	R1 = 0.0671, wR2 = 0.1511
Largest diff. peak and hole	0.639 and -0.563 e.$Å^{-3}$

Cell Culture

S180 (mouse sarcoma S180), DU145 (prostate cancer), K562 (chronic myeloid leukemia) and A549 (lung cancer) cells were obtained from the Rio de Janeiro Cell Bank/RJ, Brazil. The cells were cultured in RPMI1640/DMEM medium (pH 7.2-7.4) supplemented with 100 µm L^{-1} penicillin G, 100 µg mL^{-1} streptomycin, 2 mM L-glutamine, 1.5 g L^{-1} sodium bicarbonate, 10 mM HEPES and 10% fetal calf serum, 1% (w/v) (all reagents were obtained from Gibco, Grand Island, NY) at 37°C under a 5% CO_2, humidified atmosphere. The human peripheral blood mononuclear cells (PBMC) were collected from healthy volunteers aged 20-30 years with no history of smoking, drinking, or chronic drug use. The PBMCs were isolated by density centrifugation of heparinized blood on Lymphoprep (Nycomed, Oslo, Norway), washed three times with Hank's balanced salt solution (Sigma Chemical,

St. Louis, MO, USA), counted, suspended in RPMI 1640 medium (Gibco, Invitrogen, Carlsbad, CA, USA), supplemented with 10% fetal calf serum (Gibco), and incubated (37°C, 5% CO_2) for 24 h before drug treatment [52].

The protocol (043/2007) for these experiments was approved by the Ethics Committee of the Universidade Federal de Goiás and, prior to joining the study, all blood donors signed an informed consent form.

Cytotoxicity assays

The effects of [RuCl(bcn)(bipy)(dppe)](PF_6), RuCl(bnc)(phen)(dppb)(PF_6), RuCl(bnc)(bipy)(dppb)(PF_6) and [RuCl(bnc)(bipy)(dppf)]PF_6 on the viability of S180, DU145, K562, A549 and lymphocyte cells were studied by MTT assay as described previously [20]. In brief, 1×10^5 S180, D145, K562, A549 and lymphocyte cells were plated in 96-well tissue culture plates and treated with different concentrations of the ruthenium (II) complex (0.2, 2, 20, 50, 100 and 200 µM) for 48 h. After treatment, 10 µL of MTT (5 mg mL^{-1}) was added to each well, and the plates were incubated at 37°C for another 3 h. The purple formazan crystals were dissolved in 50 µL of SDS, and the absorbance was determined at 565 nm by using a Stat Fax 2100 microplate reader (Awareness Technology, Palm City, FL, USA). The cell viability was calculated as follows: Viability (%) = (Absorbance of the treated wells)/(Absorbance of the control wells)×100. Each concentration was tested in three different experiments that were run in triplicate. The IC_{50} (the compound concentration (in µM) that produces a 50 % reduction in cellular viability) was obtained from the dose-response curves by using GraphPad Prism 4.02 for Windows (GraphPad Software, San Diego, CA, USA). After screening the Ru complexes, the best compound was designated as the one that exhibited a value lower than the IC_{50} for the tumor strains in relation to the healthy cell so that the other tests on the cellular death mechanism could be studied. The IC_{50} was determined by using the selectivity index (IS) for all ruthenium complexes (II) and cisplatin with the following formula: IS= IC_{50} non-tumor cell (PBMC)/IC_{50} tumor cell (EAT), and it was considered significant at IS ≥ 2.0 [22].

Analyzing the cell cycle by flow cytometry

The possible effect of the ruthenium compound on cell cycle progression was investigated after treating the S180 cells for 24 and 48 h with 24 μM of [RuCl(bcn)(bipy)(dppe)]PF_6. In brief, 5×10^5 cells were harvested by centrifugation, washed with PBS, fixed with 70% (v/v) cold aqueous ethanol and stored overnight at -20°C. The fixed cells were washed with PBS and incubated with propidium iodide (PI; Sigma-Aldrich, St. Louis, MO, USA) containing 0.05% RNase. The samples were incubated at 4°C in the dark and analyzed by flow cytometry (FACSCalibur, BD Biosciences, San José, CA, USA). The percentage of cells in sub-G1, G0/G1, S, and G2/M was analyzed with ModFit LT software (Verity Software House, Topsham, ME, USA) [53].

Detecting apoptosis by using the annexin V binding assay

Apoptosis-mediated cell death and necrosis were distinguished by using double labeling assays. After treating with [RuCl(bcn)(bipy)(dppe)]PF_6 for 24 and 48 h, 5×10^5 S180 cells were examined by using a FITC-labeled Annexin V/Propidium Iodide (PI) Apoptosis Detection Kit (BD Biosciences) according to the manufacturer's instructions. The S180 cells were treated with [RuCl(bcn)(bipy)(dppe)]PF_6 (24 μM) for 24 and 48 h. In brief, 5 x 10^5 cells were harvested and washed with PBS. The cells were re-suspended in 400 μL binding buffer. Next, 5 μL of Annexin V-FITC and 3 μL of PI were added. Flow cytometric analysis was performed immediately after supravital staining. Data acquisition and analysis were performed in the flow cytometer (FACSCalibur, BD Biosciences, Franklin Lakes, NJ) by using Cell Quest software. The positive criteria for cells in the early stages of apoptosis were Annexin V-positive and PI-negative, whereas the cells in the late stages of apoptosis were both Annexin V and PI-positive [54].

Evaluating mitochondrial membrane potential ($\Delta\Psi_m$)

The dual emission dye, named JC-1, was used to measure the $\Delta\Psi m$ according to the methods described previously [55]. In brief, 3 x 10^5 of S180 treated with [RuCl(bcn)(bipy)(dppe)]PF_6 (24 μM) were incubated with 2.5 mg mL^{-1} JC-1 (dissolved in DMSO) for 15 min. at a room temperature of 37°C in an incubator with 5% CO_2 under darkness. After centrifugation for 5 min. at 200 × g, the cells were

washed twice with PBS at 4°C, re-suspended in 5 mL of PBS, and analyzed on a FACSCalibur flow cytometer. JC-1 is a lipophilic ionic fluorescence dye, and it is capable of selectively entering the mitochondria, which will change color from red (FL-2) to greenish (FL-1) once the $\Delta\Psi m$ declines. The data were analyzed in Cell Quest, and these values represent the mean fluorescence intensity.

Assaying caspase-3, 8 and 9 activity

A direct measurement of the caspase 3, 8, and 9 activities were performed by using an ApoTarget Caspase-3, 8, and 9 Protease Assay (Invitrogen) according to the manufacturer's recommendations. After treating with $[RuCl(bcn)(bipy)(dppe)]PF_6$ (24 μM) for 24 h, the cells were lysed with chilled cell lysis buffer. The protein concentration was then measured by using the BSA Protein Assay Kit (BioRad). An aliquot of the protein extract (75 μg) was mixed with 50 μL of 2X reaction buffer supplemented with 10 mM DTT and the substrates of DEVD-pNA (caspase-3), IETD-pNA (caspase-8), or LEHD-pNA (caspase-9). The mixtures were then incubated for 2 h at 37°C. The formation of p-nitroanilide in the samples was subsequently measured by using an ELISA microplate reader at 405 nm. The increased activities of caspase-3, caspase-8, and caspase-9 were determined by comparing the results with the control.

Analyzing Bcl-2 by flow cytometry

After treating the S180 cells with the $[RuCl(bcn)(bipy)(dppe)]PF_6$ complex for 24 h with concentrations of 24 and 48 μM, the cells were taken from the culture and transferred to a flow cytometry tube, and they were centrifuged at 1800 rpm for 3 s. The supernatant was discarded, and the cells were washed with 1X PBS and centrifuged again. After discarding the supernatant again, the cells were re-suspended in 500 μL of lyses buffer for 10' at room temperature (20° to 30°C). After this time, the cells were centrifuged one more time and the supernatant was removed. 500 μL of permeabilization solution was then added for 10', the cells were centrifuged again and the supernatant discarded. The cells were then washed with BSA buffer (1X PBS, 0.5% SFB and 0.1% sodium azide). The cells were centrifuged

after washing and the supernatant was discarded. 20 µL of the Bcl-2 reagent was added. The tube was mixed and incubated for 30´ at room temperature (20° to 30°C). The cells were centrifuged and the supernatant was discarded after the incubation, and the cells were washed again with BSA. Afterwards, the same cells were re-suspended in 500 µL of BSA and analyzed immediately.

Total RNA extraction and cDNA synthesis

The S180 cells were treated with 24 µM [RuCl(bcn)(bipy)(dppe)]PF_6 for 3, 6 and 12 h. Total RNA was extracted with Trizol reagent (Sigma-Aldrich, USA) by following the manufacturer's protocol. Total RNA (2.0 µg) was used to produce complementary DNA (cDNA) with random primers (Applied Biosystems, USA) in a 20 µL reaction mixture according to the manufacturer's protocol**.**

Real-time quantitative PCR

Real-time PCR was performed in a Line Gene K (Bioer Technology) instrument. Real-time PCR reactions were performed in a 20 µL reaction mixture, including 2 µL of cDNA, 10 µL of SYBR Green PCR Master Mix (LGC Biotechnology, UK), and 2.0 µL of 400 nM forward and reverse primers. The PCR program was initiated at 95°C for 15 min followed by 40 cycles of 95°C for 15 s, 55°C for 15 s, and 72°C for 30 s. The data were analyzed according to the comparative Ct method, and they were normalized to the β-actin reference gene expression in each sample. The primer sequences are shown in Table 3.

Table 3: Primer sequences used for the real time RT-PCR assay.

Gene	Primer sequences
β-actin	F5'CACACCCGCCACCAGTTC3' R5'ATTCCCACCATCACACCCTG3'(161 bp)
bax	F5'GCTACAGGGTTTCATCCAGG3' R5'GGAGACACTCGCTCAGCTTC3'(113 bp)
caspase 3	F5'GGAGCTTGGAACGCTAAGAA3' R5'GTCCACTGACTTGCTCCCAT3' (112 bp)
caspase 8	F5'AGGTACTCGGCCACAGGTTA3' R5'TGGGATGTAGTCCAAGCACA3'(137 bp)

caspase 9	F5’TAGCTGGAACACTGGGCATTGAGT3’ R5’AACATACCCATCGGTGCATTTGGC3’(146pb)
p53	F5'TGGAAGACTCCAGTGGGAAC-3' R5'TCTTCTGTACGGCGGTCTCT-3'(87pb)

Statistical Analysis

A statistical analysis of the results was performed by one-way ANOVA and Tukey’s or Dunnett’s post-test for multiple comparisons with a control. All statistical analyses were performed with the statistical software GraphPad Prism, version 4. A probability of 0.05 or less was deemed statistically significant. The following notation was used throughout the analysis: *p<0.05 and **p<0.01, relative to the control.

Results and discussion

The X-ray structure of [RuCl(bcn)(bipy)(dppe)]PF_6.0.75($C_4H_{10}O$) is illustrated in Figure 1.

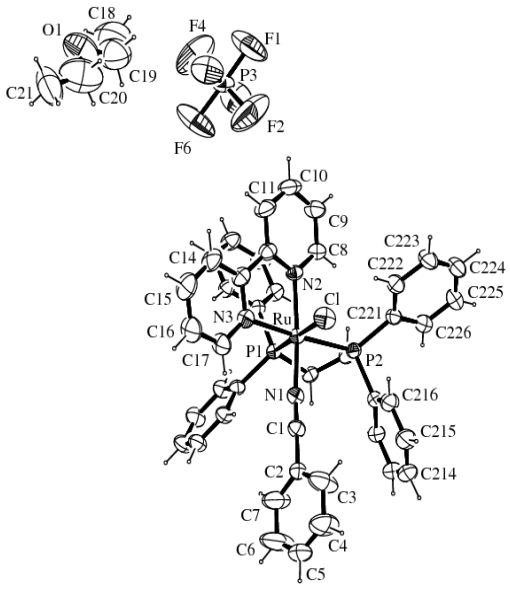

Figure 1 - ORTEP illustrates the [RuCl(bzCN)(bipy)(dppe)]PF_6.0.75$C_4H_{10}O$ complex, showing the atom labels and the 50% probability of ellipsoids. This figure also shows the selected bond lengths (Å) and angles (º) for the [RuCl(bzCN)(bipy)(dppe)]PF_6 complex, with estimated standard deviations in parentheses as follows: Ru–P1 (*trans* Cl)= 2.2775(9); Ru–P = 2.3096(10); Ru–N3 (*trans* P2)= 2.128(3); Ru–N2 = 2.079(3); Ru–Cl= 2.4336(10); Ru–N1 = 2.022(3); N1-C1 = 1.140(5); O(1)-C(19) = 1.239(17); O(1)-C(20) = 1.360(15); P–Ru–P = 84.84(3); and Cl–Ru–N≡C = 86.40(9).

The X-ray structures of the [RuCl(bzCN)(dppb)(phen)]PF_6 and [RuCl(bzCN)(dppf)(bipy)]Cl complexes were previously published [19], and their bond lengths and angles are similar to those reported here for the [RuCl(bzCN)(bipy)(dppe)]PF_6 complex. For all four complexes studied in this work, the benzonitrile ligand was *trans* to the nitrogen from the diimine [19]. The bond lengths of Ru-N for the nitrogen were *trans* to the phosphorus atoms in all four complexes, and they were also longer than the distance for the nitrogen *trans* to the cyan group as a consequence of the high *trans* effect of the phosphorus atoms.

The $^{31}P\{^{1}H\}$ RMN of the complexes presents two doublets, that is, δ 66.2 and 58.4 ppm, and $^{2}J_{P-P}$ = 17.8 (Hz) in $CH_2Cl_2(D_2O)$ solution, showing that the phosphorus atoms are magnetically different, as expected from its X-ray structure.

Cytotoxicity assay

The cytotoxicity of complexes [RuCl(bcn)(bipy)(dppe)]PF_6, RuCl(bnc)(phen)(dppb)(PF_6), RuCl(bnc)(bipy)(dppb)(PF_6) and [RuCl(bnc)(bipy)(dppf)]PF_6 to different cell lines such as S180 (mouse sarcoma S180), DU145 (prostate cancer), human peripheral blood mononuclear cells (PBMC), K562 (chronic myeloid leukemia) and A549 (cancer lung) was assayed by observing the cell survival after 48 h of exposure to the desired concentration range (0,2 - 200 μM) of MTT [20]. The resulting IC_{50} values are listed in Table 3.

These compounds show different phosphines that are coordinated with the ruthenium element, and the results indicated a significant increase in their activity [21]. The following IC_{50} values were found for the [RuCl(bcn)(bipy)(dppe)]PF_6 and RuCl(bnc)(bipy)(dppf)(PF_6) complexes: PBMC 53.73 ± 5.71 and 51.14 μM, respectively. It is interesting to note that the IC_{50} values for PBMC are considerably higher than they are for S180 and A549 with their IC_{50} values of 17.02 μM ± 8.21 and 38.26 μM ± 0.79 μM, respectively. For the K562 and DU145 IC_{50} strains, the IC_{50} values were 11.6 ± 5.74 and 16.7 ± 1:22, respectively, for the [RuCl (BCN) (bipy) (dppe)] PF6 complex. For the [RuCl (BNC) (bipy) (dppf)] PF6 complex, the IC_{50} was 10.17 ± 1.1 for K562 and 10:01 ± 8.83 for DU145. The IC_{50} of the [RuCl (BNC) (phen) (dppb)] PF6 complex for S180, DU145, K562, A549 and PBMC was 8.89 ± 3.93, 4.18 ± 0:34, 4:42 ± 0.88, 20.87 ± 12:13 and 17:24, respectively. For the [RuCl (BNC) (bipy) (dppb)] PF6, the IC_{50} values for S180, DU145, K562, A549 and PBMC

complexes were 13.85 ± 4.19, 1.83 ± 1.01, 9.79, 0.73 and 10.5 ± 20:37, respectively. These complexes were selective, and they were more cytotoxic in tumor cell lines such as S180 and showed high resistance to current treatments. Thus, the [RuCl(bcn)(bipy)(dppe)]PF_6 complex was evaluated as its possible mechanism of cell death in S180 tumor cells.

The selectivity index (SI) indicates the selectivity of the studied complexes and their potential use for *in vivo* preclinical and clinical testing. IS values ≥ 2 are considered significant according to table 1. The [RuCl (BCN) (bipy) (dppe)] PF6 complex has a good selectivity index that is equal to 3 for S180 [22].

Table 1 – The IC_{50} (μM) values of ruthenium II complexes against the selected cell lines. Data show means ± SD of three independent experiments.

	IC_{50} (μM)					**IS**			
Ruthenium Complexes	*S180*	*DU145*	*K562*	*A549*	*PBMC*	*S180*	*DU145*	*K562*	*A549*
[RuCl(bcn)(bipy)(dppe)]PF_6	17.02±8.21	7.16±1.22	11.6±5.74	20	53.73±5.71	3	8	5	3
[RuCl(bnc)(phen)(dppb)]PF_6	8.89 ± 3.93	4.18 ±0.34	4.42 ±0.88	20.87 ±0.13	17.24	2	4	4	1
[RuCl(bnc)(bipy)(dppb)]PF_6	13.85±4.19	1.83 ±1.01	9.79	20.37 ±0.73	10.5	1	6	1	1
[RuCl(bnc)(bipy)(dppf)]PF_6	14.94 ± 3.1	10.01±8.83	10.17±1.1	38.26 ± 0.79	51.14	3	5	5	1

Analyzing the cell cycle by flow cytometry

The cell cycle distribution of S180 cells that were treated with the near-IC_{50} value of [RuCl(bcn)(bipy)(dppe)]PF_6 (24 μM) was examined by flow cytometry. The effect of the ruthenium complex [RuCl(bcn)(bipy)(dppe)]PF_6 on the S180 cell cycle was evident in the cells that were investigated by flow cytometry. In Fig. 2, there are histograms indicating the DNA quantity distribution. After 24 h of exposing S180 cells to [RuCl(bcn)(bipy)(dppe)]PF_6 (24 μM), we noticed an increase in the G0/G1 phase from 22% to 50% in relation to the negative control ($p<0,001$) and there was a decrease in the S phase of 25%. The cell cycle distribution at 48 h showed a time-dependent and discrete increase in the sub-G1 (12%) peak, but it was not statistically

significant (p<0,01). There was also an increase of 35% in the G2/M phase (Figure 2).

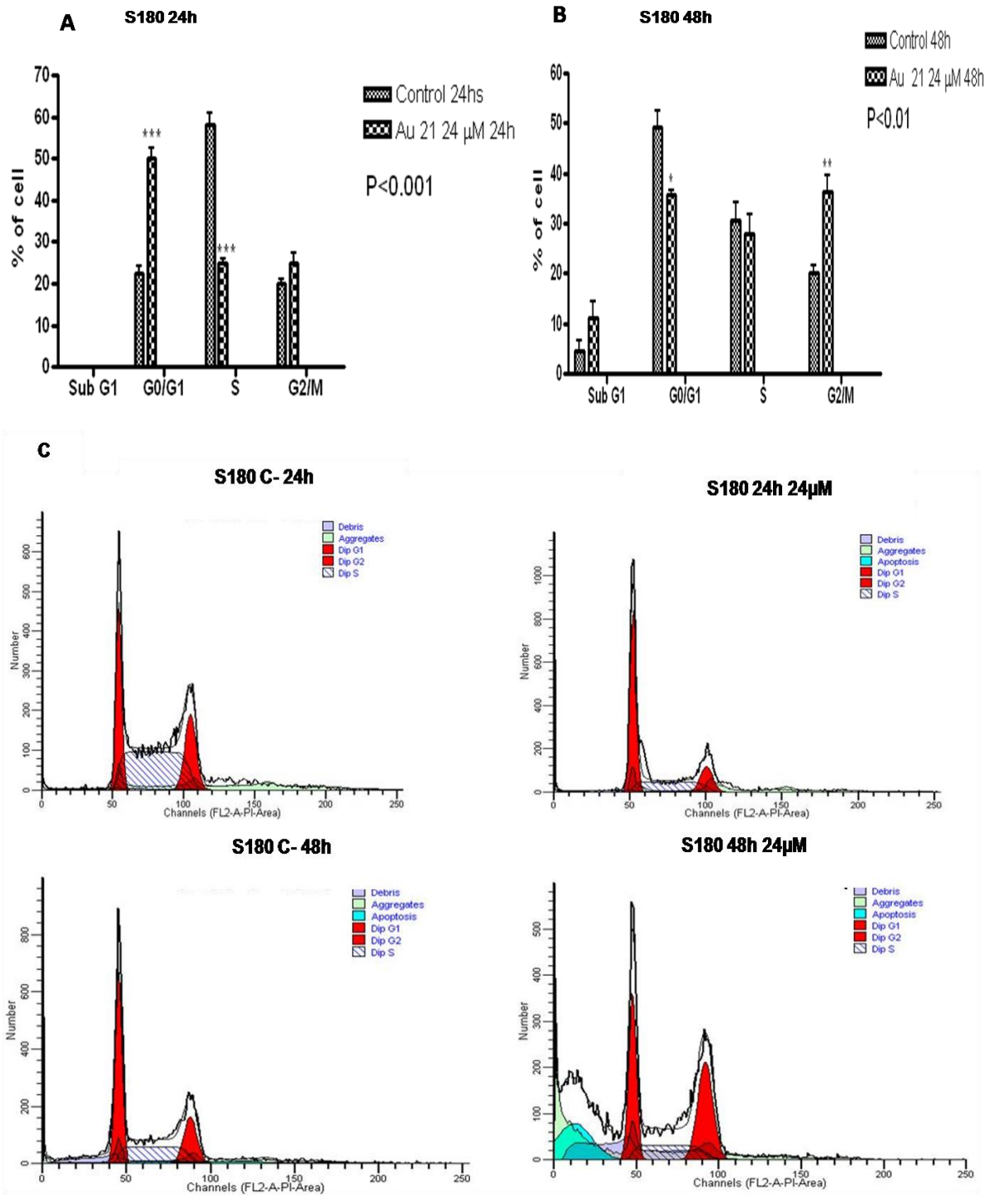

Figure 2 - The cell cycle status of the S180 cells after treating with [RuCl(bcn)(bipy)(dppe)]PF_6 (24 µM) complex for 24 and 48 h (Graphical A and B). C - A histogram of the PI fluorescence (x-axis) versus counts (y-axis) is shown (G0/G1, S, and G2/M). Data were analyzed with ModFit software (Becton Dickinson, San José, CA, USA). Data show the means±SD of three experiments. Significant differences from the untreated control are indicated by **p<0.01 and ***p<0.001.

Detecting apoptosis by using the Annexin V binding assay

Apoptosis is a tightly regulated physiological process that is characterized by a series of biochemical events and ultrastructural alterations (*e.g.*, the activation of caspases, phosphatidylserine externalization, membrane blebbing, cell shrinkage, nuclear fragmentation, chromatin condensation, and chromosomal DNA fragmentation) [23]. In apoptotic cells, phosphatidylserine is translocated from the inner to the outer leaflet of the plasma membrane, where it can be detected by its binding to intracellular protein annexin V, which is labeled with a fluorophore [24]. The annexin V assay is able to distinguish apoptotic cells from viable or necrotic cells on the basis of the resulting fluorescence of the former cells. A simultaneous dead cell stain employs the fluorochrome propidium iodide (PI), which can only penetrate dead cells that have lost or are losing membrane integrity. PI intercalates into DNA to produce a highly fluorescent adduct, which is indicative of late apoptosis or necrosis [25].

The objective of this work was to investigate if [RuCl(bcn)(bipy)(dppe)]PF_6 could induce apoptosis or necrosis in S180 cells, using annexin V-FITC/propidium iodine staining. As shown in Figure 3 A and B, after treating with 24 μM of [RuCl(bcn)(bipy)(dppe)]PF_6 for 24 and 48 h, the S180 cells in initial apoptosis (annexin V + and PI-) represented 2.89% (24 h) and 5.06% (48 h) of the total cells, and the cells in late apoptosis (annexin V + and PI-) represented 32.56% (24 h) and 30.09% (48 h) ($p<0,001$) of the total cells, respectively. There are histograms showing the dot plot distribution in Figure 3 - C. The results showed the cytotoxic activity of the [RuCl(bcn)(bipy)(dppe)]PF_6 complex in S180 cells, possibly by its interaction with the DNA molecule, leading to cleavage by the apoptosis process.

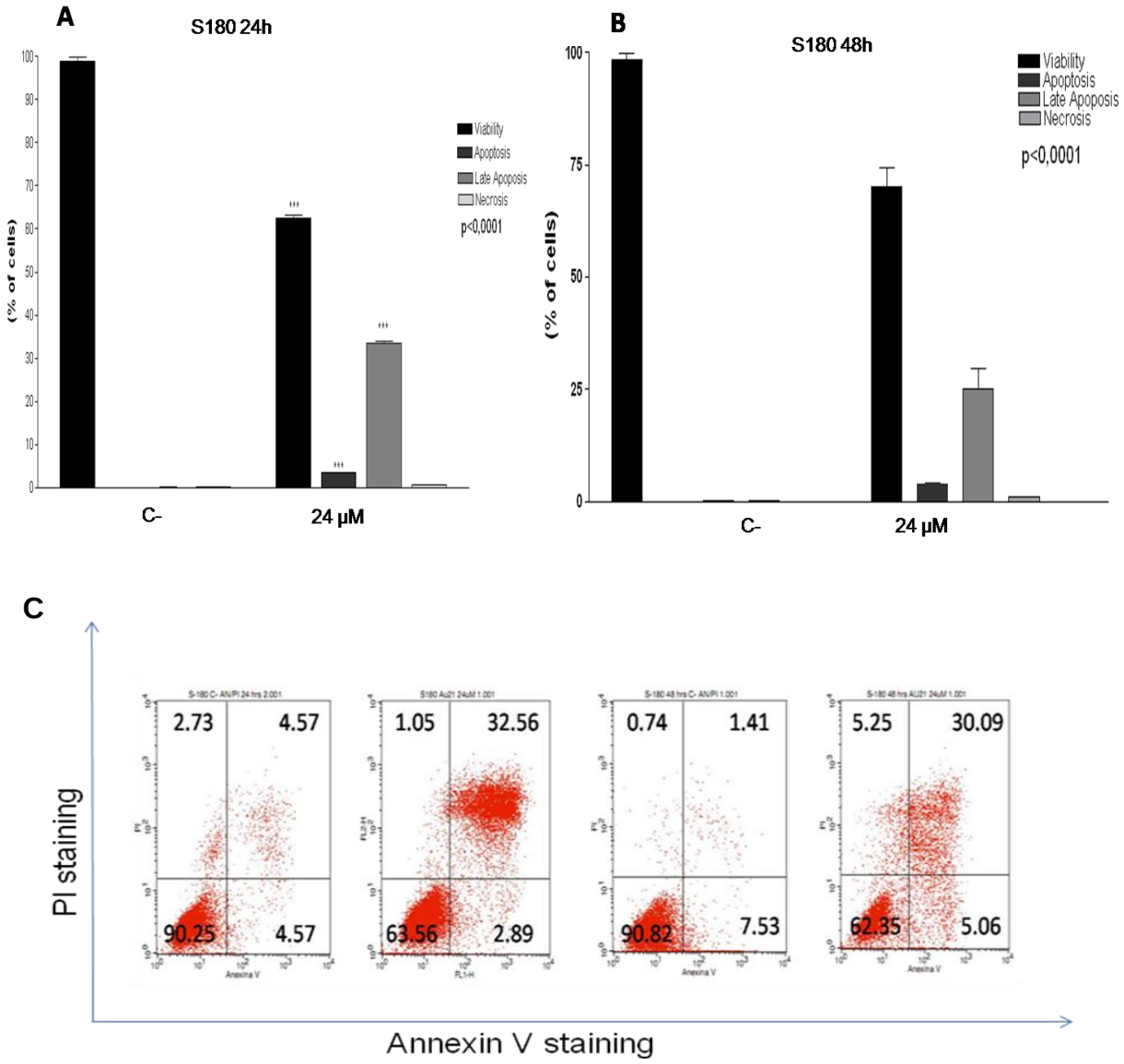

Figure 3 – Effects of $[RuCl(bcn)(bipy)(dppe)]PF_6$ on S180 cells. A and B - The harvested cells were stained and washed with phosphate-buffered saline, and apoptosis was assayed by using an annexin V-fluorescein isothiocyanate/PI assay kit in a double-labeling system for 24 and 48 h. C - The effect of $[RuCl(bcn)(bipy)(dppe)]PF_6$-induced apoptosis on S180 cells. The harvested apoptotic cells (annexin V+/PI+) were analyzed by flow cytometry, and the dot plot displays the annexin V fluorescence (x-axis, logarithmic scale) versus PI fluorescence (y-axis, logarithmic scale). Data show the means±SD of three experiments. Significant differences from the untreated control are indicated by ***p<0.001.

Mitochondrial potential – JC - 1

The mitochondria control the life and death of cells, thus deciding the destiny of a cell because they control the apoptosis process [26]. The different functions of the mitochondria are connected to the mitochondrial membrane potential, which is a

vital component of respiration [27]. Alterations in the mitochondrial membrane potential trigger apoptotic signs that are crucial to the activation of the inner and outer apoptotic paths [28]. The lowering in the mitochondrial membrane potential and the release of apoptotic factors are key elements that trigger the apoptotic process [28]. Studies show that many Ru(II) complexes can lead to a lowering in the mitochondrial membrane potential [29-31]. A JC-1 test was used to find if [RuCl(bcn)(bipy)(dppe)]PF_6 leads to a lower mitochondrial membrane potential. JC-1 is a fluorescent dye, and it was used as an indicator of $\Delta\Psi m$ alterations. JC-1 (lipophilic cationic dyestuff) easily crosses the plasmatic membrane of the cells and agglomerates in active mitochondria [32]. When there is a low $\Delta\Psi m$, the JC-1 begins to act as a monomer that emits green fluorescence. However, when there is a high $\Delta\Psi m$, the J-dye is fixed to the cells. Thus, these dye aggregates induce a change in green fluorescence emission to red fluorescence emission. This finding can be observed in the negative control of Figure 4 with a higher emission of red fluorescence (83%) in relation to the green fluorescence (17%), indicating the presence of mitochondrial activity. After treating cell line S180 with the [RuCl(bcn)(bipy)(dppe)]PF_6 complex for 24 h at a concentration of 24 µM, there was a low of 60% in the emission of red fluorescence in the negative control, and in the cells that were exposed to the [RuCl(bcn)(bipy)(dppe)]PF_6 complex, the green fluorescence emission was 40% ($p<0.0001$). These alterations from red to green fluorescence following exposure to the [RuCl(bcn)(bipy)(dppe)]PF_6 complex demonstrate a decrease in the mitochondrial membrane potential ($\Delta\Psi m$), indicating that the [RuCl(bcn)(bipy)(dppe)]PF_6 complex induces apoptosis in cell line S180 through a mitochondrial pathway (Figure 4).

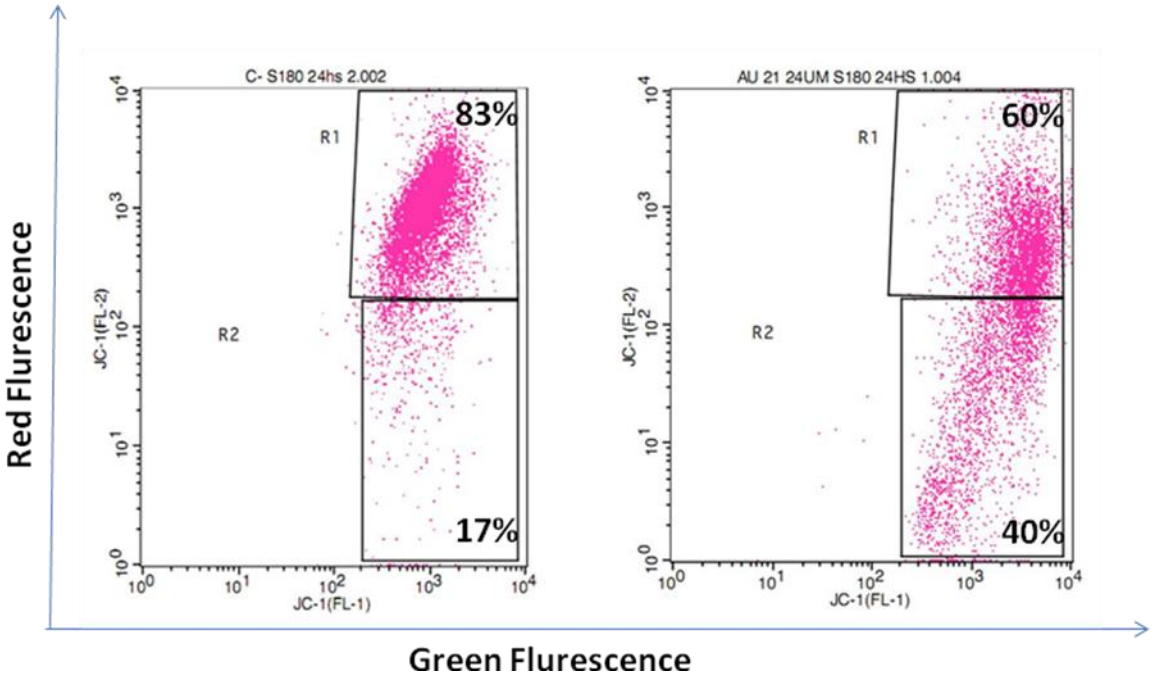

Figure 4- Effects of [RuCl(bcn)(bipy)(dppe)]PF_6 in S180 cells; the ΔΨm was determined by using JC-1 (5,5c,6,6c-tetrachloro-1,1c,3,3c-tetraethylbenzimidazolylcarbocyanine iodide). A - Flow cytometric analysis of cells stained with cell-permeable JC-1 dye revealed that [RuCl(bcn)(bipy)(dppe)]PF_6 depolarized the mitochondrial membrane as indicated by decreases in the FL2-H fluorescence, as analyzed by JC-1 flow cytometry. The number in each dot plot represents the percentage of cells that lost ΔΨm. Each column represents the means ± SD (*bars*) of two experiments. *** $p < 0.0001$ compared with the control.

Bcl-2 Analysis by flow cytometry

After 24 h of exposure, a Bcl-2 antigen marked with FITC was used as an indicator for the increase or decrease of Bcl-2 protein expression in cell line S180. The Bcl-2 protein expression was altered after being exposed to the [RuCl(bcn)(bipy)(dppe)]PF_6 (24 and 48 µM) complex for 24 h. In Figure 5, peak M2 indicates cells that have active Bcl-2, and M1 is the peak relative to the amount of cells that do not have active Bcl-2 protein. The negative control exhibited 5% of the Bcl-2 protein after 24 h in the S180 culture, after the same exposure time with the [RuCl(bcn)(bipy)(dppe)]PF_6 complex at 24 µM, a 2.5-time decrease that was observed for Bcl-2 protein expression when compared with the negative control and a decrease of 28.5 times when compared with the positive control. When the S180 cells were exposed to 48 µM of the [RuCl(bcn)(bipy)(dppe)]PF_6 complex, there was a decrease of 5 times in the Bcl-2 protein when compared with the negative control and a decrease of 57 times when compared with the positive control ($p<0.0001$). These

results demonstrated that the [RuCl(bcn)(bipy)(dppe)]PF_6 complex provoked a decrease in the presence of the Bcl-2 protein (figure 5).

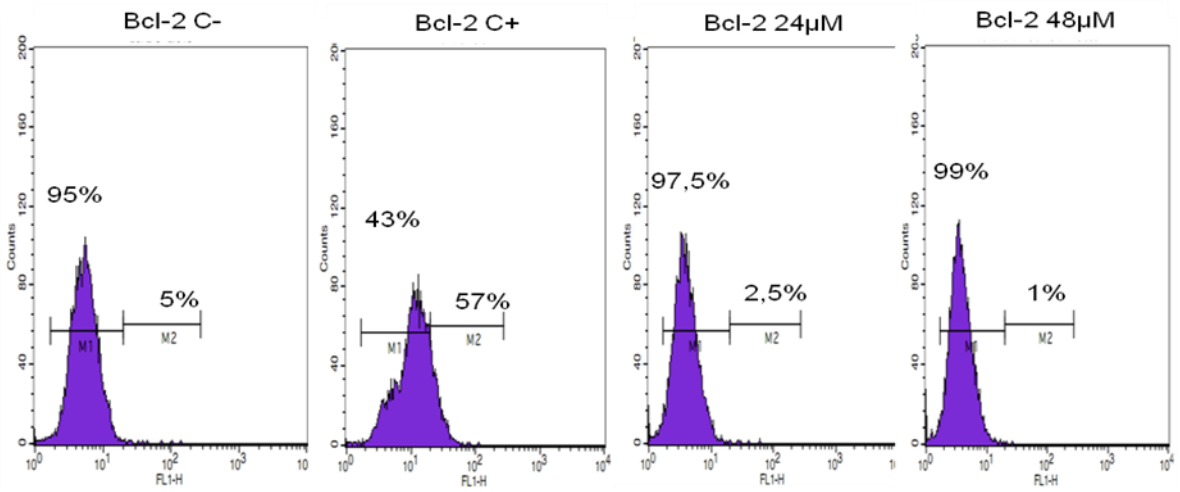

Figure 5 – Effects of [RuCl(bcn)(bipy)(dppe)]PF_6 on the Bcl-2 protein of S180 cells after 24 h of exposure in concentration of 24 and 48 µM. Data show the means±SD of two experiments. Significant differences from the untreated control are indicated by **p<0.01 and***p<0.001.

Colorimetric caspase test

The effects of [RuCl(bcn)(bipy)(dppe)]PF_6 (24 µM) on caspase-3, 8 and 9 activities were investigated in S180 cells after 24 h of treatment (Figure 6). As indicated by these results, the caspase 8 and 9 activities were not changed by [RuCl(bcn)(bipy)(dppe)]PF_6 treated cells when compared with untreated control cells. However, the assessment of caspase-3 activity showed a significant enhancement in relation to the control after incubating the cells with [RuCl(bcn)(bipy)(dppe)]PF_6 for 24 h with an increase of 5 fold relative to the negative control. The maximum enzymatic activity was observed at 24 h for caspase-3 at 450%. Thus, the [RuCl(bcn)(bipy)(dppe)]PF_6 complex induced caspase-3 activation, which confirms the triggering of the apoptotic process. The caspases play an important role in the signaling system and the apoptotic process. Caspases can control the apoptotic process intensity or inhibition [33]. A large activation of caspase-3 was observed in the present study as in many *in vitro* studies, showing that the Ru (II) complexes can activate the apoptotic pathway [34, 35].

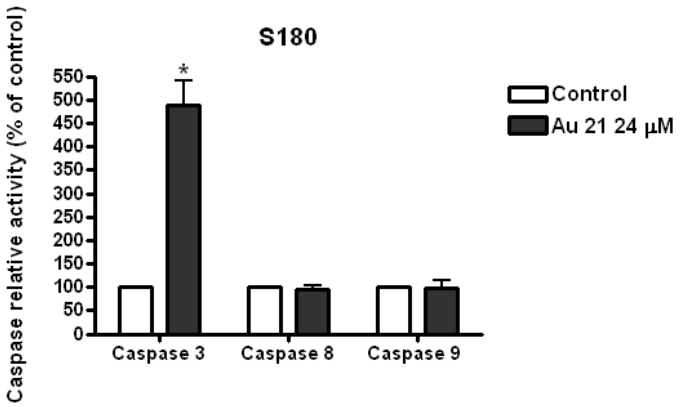

Figure 6 - Activation of caspase-3, -8 and -9 in S180 cells treated with 24 µM of [RuCl(bcn)(bipy)(dppe)]PF_6 for 24 h. Caspase activity was calculated as the fold induction of basal caspase-3, -8 and -9 activities in non-treated S180 samples. Each column represents the means±SD (*bars*) of two experiments. * $p< 0.05$ compared with the control.

Real-time Quantitative PCR

For a better understanding of the apoptosis induction mechanism provoked by the [RuCl(bcn)(bipy)(dppe)]PF_6 complex, the altered expression levels of the genes that were involved in the apoptotic process were investigated. The effects of [RuCl(bcn)(bipy)(dppe)]PF_6 on the messenger RNA (mRNA) expression of Bax, p53, caspase-3, caspase-8 and caspase-9 were analyzed by real-time quantitative PCR. The mRNA expression of Bax with 3 h of exposure to [RuCl(bcn)(bipy)(dppe)]PF_6 was not significant when compared with the control, but it exhibited a slight increase. However, there was a significant increase (3.14-fold) after 6 h of exposure to [RuCl(bcn)(bipy)(dppe)]PF_6 (Figure 7).

Pro-apoptotic Bax/Bak are essential regulators of the mitochondrial or intrinsic pathway of apoptosis [36, 37]. In this intrinsic pathway, an increased level of Bax and/or a decreased level of Bcl-2 may permeabilize the mitochondria following DNA damage [37, 38]. Based on these factors, it can be inferred that the apoptosis induced by the Ru complex caused a lower Bcl-2 expression as observed in the flow cytometry test that led to the translocation of Bax in the mitochondrial membrane within a 6 hour period of exposure.

The p53 expression was increased by 22-fold when treated with 24 µM of the compound after 3 hours of exposure, falling to less than 1-fold after 6 and 12 hours of exposure. There was no gene expression when the cells were treated with 48 µM with 3 hours of exposure, but after 6 hours there was a7-fold increase in gene

expression compared with the negative control. After 12 hours of exposure, there was no gene expression when compared with the negative control. Approximately 50% of human cancer exhibits alterations in the p53 gene, which is a tumoral suppressor; this gene is responsible for cell growth, for cell sensibility to irradiation, and for multiple chemotherapeutics [39-41]. A functional p53 can negatively regulate Bcl-2, protecting the cells from apoptosis and allowing the cells to survive through a variety of fatal cellular events [42]. The results obtained in this study show that the Ru complex increased the expression of p53 after 3 hours of exposure. This finding indicated a probable alteration in the DNA molecule that led to the translocation of the p53 in the cytoplasm to the S180 cell nucleus, thereby inducing the apoptosis process.

The p53 is a key suppressor of tumor regulators in the apoptosis process and has pro-apoptotic activity. Under stressful conditions, p53 is stabilized and acts as a transcription factor that can increase the expression of target pro-apoptotic genes such as Puma, Noxa, Bax and Bid [43]. Cytoplasmic p53 interacts with the members of the Bcl-2 and Bcl-xL family, which leads to the activation and translocation of Bax and Bid in the external mitochondrial membrane. There was also an observable increase in the Bax expression. In addition, the p53 is also translocated to the mitochondria, activating apoptosis by the mitochondria [43-45]. The apoptosis induced by the Ru complex was observed through the increased Bax expression, p53 and caspase 8.

The mRNA expression of caspase 8 was 2-fold higher (compared with the negative control) for 3 h after exposure to the [RuCl(bcn)(bipy)(dppe)]PF6 compound. Caspase-8 expression was not significant after 6 and 12 h of compound exposure. Caspase-9 was not significant at any exposure time. This increased expression was retained after 6 hours of exposure to the compound. The mRNA expression of caspase-3 was not significant after 6 and 12 h of exposure.

Many chemotherapeutics have been shown to induce the apoptosis process in tumor cells [46-48]. These results suggest that [RuCl(bcn)(bipy)(dppe)]PF_6 may be capable of inducing the expression of genes involved in the apoptosis process; this particular conclusion was observed because the compound induces the synthesis of the p53 gene, which acts in a pro-apoptotic manner [49]. These results are similar to those of other areno-organometallic cycloruthenated compounds found in the literature [50]. The evidence suggests that chemotherapeutics induce cell death by

apoptosis after treating with these chemotherapeutics, thus showing that this is an important mechanism of cytotoxic action by these complexes [51]. This characteristic can be observed primarily with the [RuCl(bcn)(bipy)(dppe)]PF_6 complex, which significantly increased the expression of pro-apoptotic genes such as Bax.

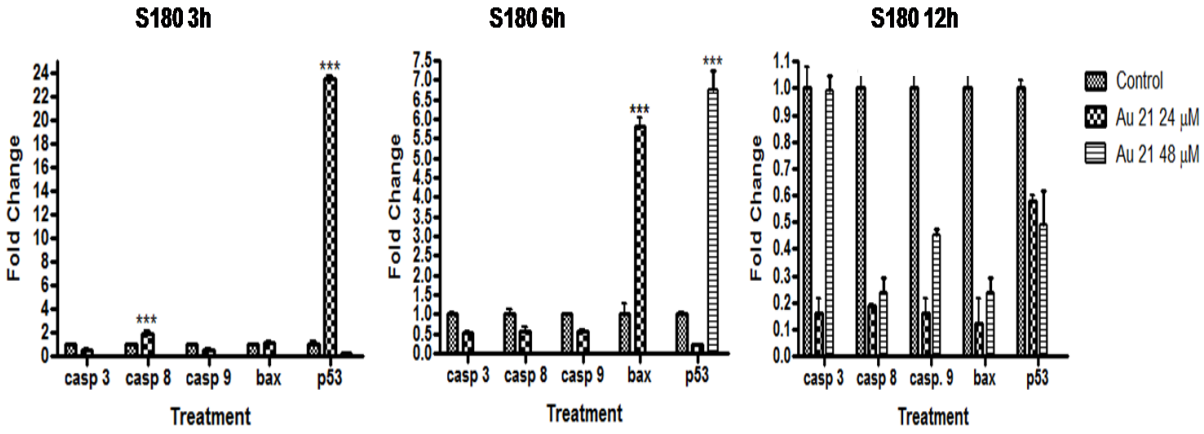

Figure 7 – Effects of [RuCl(bcn)(bipy)(dppe)]PF_6 on the mRNA expression of caspases 3, 8 and 9; Bax and p53 were evaluated by real-time quantitative PCR. Data show the means±SD of experiments performed in triplicate. Significant differences from the untreated control are indicated by ***p<0.001.

Conclusions

The Ru (II) complexes exerted antiproliferative effects over the tested S180 tumor cells. The complexes seem to be effective at inhibiting cell growth, inducing alterations in the G0/G1 and S phases in addition to inducing the apoptosis that was observed in both the annexin and JC-1 trials. Our data suggest that the Ru (II) complexes tested in this work most likely trigger the apoptosis process through an intrinsic pathway, showing that these complexes interfere in DNA replication most likely by interacting with the DNA. Furthermore, the results demonstrated the gene expression involved in the apoptosis process. These results suggest that the Ru complexes tested here are future chemotherapeutic candidates for cancer treatment.

Highlights

- Ru (II) compound [RuCl(bcn)(bipy)(dppe)]PF_6 increases the expression of caspase-3 5-fold, leading to cell death.

- The JC-1 test demonstrated that [RuCl(bcn)(bipy)(dppe)]PF_6 triggers apoptosis, most likely through the mitochondrial pathway.
- The increased expression of caspase 8, p53 and Bax provoked by the Ru (II) [RuCl(bcn)(bipy)(dppe)]PF_6 complex demonstrates the possible activation of extrinsic and intrinsic apoptosis pathways.

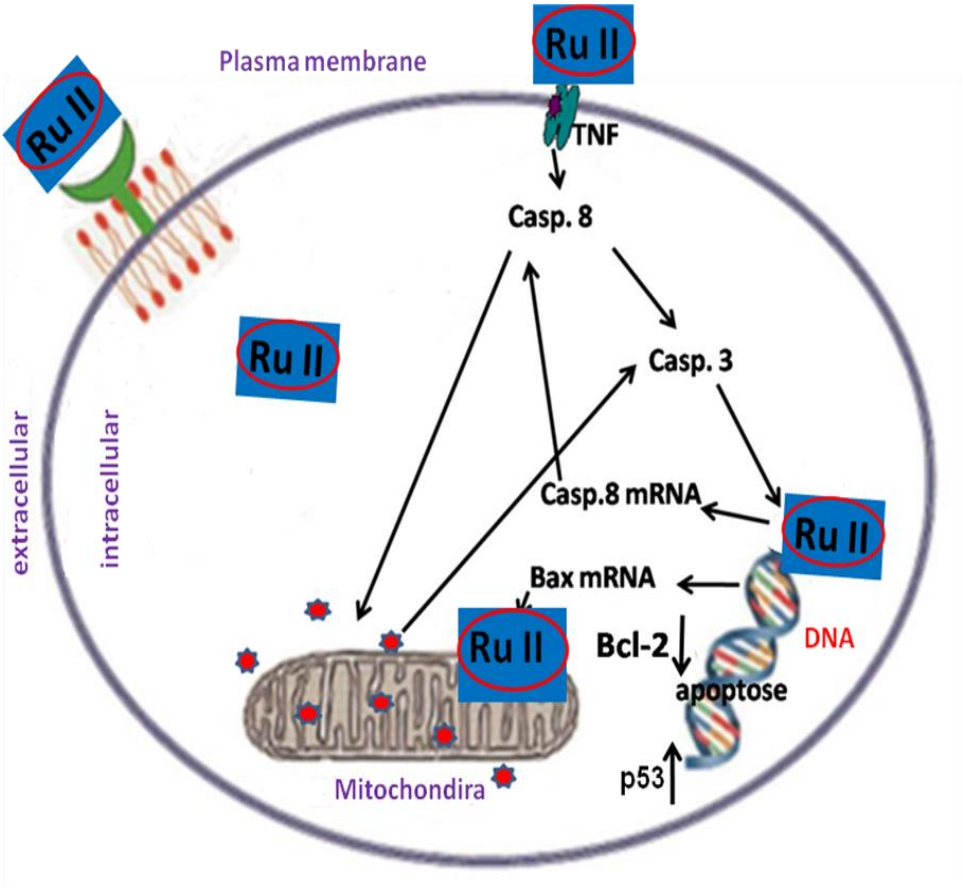

Scheme 1 - A schematic illustration of Ru II activating the intrinsic and extrinsic passage of the carcinogen cell. This scheme illustrates the increased level of caspase 8 expression (originator) in addition to the increased level of protein caspase 3 (effector) triggered by the intrinsic passage and most likely also by extrinsic passage. With Ru II exposure, an alteration in the mitochondrial membrane was observed in response to the large increase in Bax expression, which led the mitochondria to liberate apoptotic factors and activate caspase 3, which amplified the cell death signal.

References

[1] Rosenberg B, Van Camp L, Trosko JE, and Mansour VH. (1969) Platinum compounds: a new class of potent antitumour agents. Nature 222: 385–386.

[2] Reedijk J. (1996) Improved understanding in platinum antitumour chemistry Chem. Commun. 801-806.

[3] Devi CS, Kumar DA, Singh SS, Gabra N, Deepika N, et al. (2013) Synthesis, interaction with DNA, cytotoxicity, cell cycle arrest and apoptotic inducing properties of Ruthenium(II) molecular “light switch” complexes. European Journal of Medicinal Chemistry, 64, 410-421.

[4] Guo ZJ, Sadler PJ. (2000) Medicinal Inorganic Chemistry.Adv. Inorg. Chem. 49 183-306.

[5] Roberts JD, Peroutka J, Beggiolin G, Manzotti C, et al. (1999) Comparison of cytotoxicity and cellular accumulation of polynuclear platinum complexes in L1210 murine leukemia cell lines. J. Inorg. Biochem. 77, 47-50.

[6] Wesselinova D, Kaloyanov N, Dimitrov G. (2009) Cytotoxicity and effects of 1,10-phenanthroline and 5-amino-1,10-phenanthroline. Eur. J. Med. Chem. 44, 5099-5102.

[7] Wu Q, Fan C, Chen T, Liu C, Mei W, et al. (2013) Microwave-assisted synthesis oarene ruthenium(II) complexes that induce S-phase arrest in cancer cells by DNA damage-mediated p53 phosphorylation. European Journal of Medicinal Chemistry 63 57-63.

[8] Scolaro C, Chaplin AB, Hartinger CG, Bergamo A, Cocchietto M, et al. (2007) Tuning the hydrophobicity of ruthenium(II)-arene (RAPTA) drugs to modify uptake, biomolecular interactions and efficacy. Dalton Trans. 5065-5072.

[9] K.K. Lo, T.K. Lee. (2004) Luminescent ruthenium(II) polypyridine biotin complexes: synthesis, characterization, phopophysical and electrochemical properties, and avidin-binding studies. Inorg. Chem. 43 5275-5282.

[10] Ang WH, Dyson PJ. (2006) Classical and non-classical ruthenium-based anticancer drugs: Towards targeted chemotherapy. Eur. J. Inorg. Chem. 2006:4003–4018.

[11] D. Frasca, J. Ciampa, J. Emerson, R.S. Umans, M. Clarke, J. (1996) Effects of hypoxla and Transferrin on toxicity and DNA binding of Ruthenium Antitumor Agents in HELA cells. Metal-Based Drugs 3197-209.

[12] Timerbaev AR, Hartinger CG, Aleksenko SS, Keppler BK. (2006) Interactions of antitumor metallodrugs with serum proteins: Advances in characterization using modern analytical methodology. Chem Rev 106:2224-2248.

[13] Clarke, MJ. (2003) Ruthenium metallopharmaceuticals. Coord. Chem. Rev 236, 209-233.

[14] Allardyce CS, Dyson PJ. (2001) Ruthenium in Medicine: current clinical uses and future prospects. Platinum Metals Rev 45, 62-69.

[15] Gagliardi R, Sava G, Pacor S, Mestroni G, Alessio E. (1994) Antimetastatic action and toxicity on healthy tissues of Na[trans-RuCl4(DMSO)Im] in the mouse. Clin. Exp. Metastasis 1293-100.

[16] I. Bratsos, S. Jedner, T. Gianferrara, E. Alessio. (2007) Increased understanding of platinum anticancer chemistry. Metals Med. 61 11.

[17] Sava G, Clerici K, Capozzi I, M. Cocchietto, Gaglirdi R, et al, (1999). Response of MCa mammary-carcinoma to cisplatin and to Na[trans-RuCl4(dmso)Im] – selective-inibition of spontaneous lung metastases by the ruthenium complex. Anti-Cancer Drugs 10 129-138.

[18] Venugopal R, Mariappan M, Eringathodi S, Mallayan P, Vaiyapuri SP, et al. (2008) Selective Cu^{2+} binding, redox silencing, and cytoprotective effects of the small heat shock proteins αA- and αB-crystallin. Dalton Trans. 2157-2170.

[19] Eliana MAV, Benedicto AVL, Ferreira AG, Nascimento F B, Deflon VM et al, (2009) Driving forces in substitution reactions of octahedral complexes: The influence Ofthecompetitiveeffect. Polyhedron, 28 3473-3478.

[20] Mosmann T. J. Immunol. (1983) Rapid colorimetric assay for cellular growth nasurvival: application proliferation on cytotoxicity assays. J. Immunol. Methods. 16, 55-63.

[21] Das S, Sinha S, Britto R, Somasundaramb K, Samuelson AG. (2010) Cytotoxicity of half sandwich ruthenium(II) complexes with strong hydrogen bond acceptor ligands and their mechanism of action. Journal of Inorganic Biochemistry 104 93-104.

[22] Osti RZ, Serrano FA, Paschoalin T, Massaoka MHS, Travassos LR, et al. (2012) The *in vitro* and *in vivo* antitumour activities of nitrosyl ruthenium amine complexes. Aust. J. Chem., v.65, p.1333-1341.

[23] Zhang P, Chen J, Liang Y. (2010) DNA binding, cytotoxicity, and apoptotic-inducing activity of ruthenium(II) polypyridyl complex. Acta Biochim Biophys Sin, 42: 440-449.

[24] Koopman G, Reutelingsperger CPM, Kuitjen GAM, Keehnen RMJ, Pals ST. (1994) Annexin V for flow cytometric detection of phosphatidylserine expression on B cells undergoing apoptosis Blood 84 1415-1420.

[25] Lecoeur H. (2002) Nuclear Apoptosis Detection by Flow Cytometry: Influence of Endogenous Endonucleases. Experimental Cell Research 277 1–14.

[26] Pradelli LA, Bénéteau M, Ricci JE. (2010). Mitochondrial control of caspase-dependent and -independent cell death, Cell Mol. Life Sci. 67 1589-1597.

[27] Chen TF, Wong YS, Zheng WJ, Liu J, Wong YS. (2010) Rutenium polypyridyl complexes that induce mitochondria-mediated apoptosis in cancer cells. Inorg Chem 49, 6366-6368.

[28] Gurp MV, Festjens N, Loo GV, Saelens X, Vandenabeele P. (2003) Mitochondrial intermembrane proteins in cell death, Biochem. Biophys. Res. Commun. 304 487 - 497.

[29] Yang X, Chen LM, Liu YN, Yang YG, Chen TF, et al. (2012) Ruthenium methylimidazole complexes induced apoptosis in lung cancer A549 cells through intrinsic mitochondrial pathway Biochimie 94 345-353.

[30] Chen TF, Liu YN, Zheng WJ, Liu J, Wong YS. (2010) Ruthenium polypyridyl complexes that induce mitochondria- mediated apoptosis in cancer cells. Inorg Chem 49, 6366–6368.

[31] Pierroz V, Joshi T, Leonidova A, Mari C, Schur J, Ot.t I, et al. (2012) Molecular and cellular characterization of the biological effects of ruthenium (II) complexes incorporating 2-pyridyl-2-pyrimidine-4-carboxylic acid. J. Am. Chem. Soc. 134, 20376.

[32] Malugin A, Kopec ˇková P, Kopec ˇek J. (2006) HPMA copolymer-bound doxorubicin induces apoptosis in ovarian carcinoma cells by the disruption of mitochondrial function.Mol. Pharm. 3 351.

[33] Kuan-Beng Ng, Bustamam A, Sukari M A, Abdelwahab S I, Mohan S, et al. (2013) Induction of selective cytotoxicity and apoptosis in human T4-lymphoblastoid cell line (CEMss) by boesenbergin a isolated from *boesenbergia rotunda* rhizomes involves mitochondrial pathway, activation of caspase 3 and G2/M phase cell cycle arrest. BMC Complementary and Alternative Medicine, 13:41.

[34] Garrido C, Galluzi L, Brunet M, Puig PE, Didelot C, Kroemer G. (2006) Mechanisms of cytochrome c release from mitochondria. Cell Death Differ 13:1423–1433.

[35] Montaner B, Perez-Tomas R. (2002) Prodigiosin induces caspase-9 and caspase-8 activation and cytochrome c release in Jurkat T cells. Ann N Y Acad Sci 973:246-249.

[36] Ranger AM, Malynn BA, Korsmeyer SJ. (2001) Mouse models of cell death. Nat Genet 28:113-8.

[37] Rajesh PR, Rajeshwar PS. (2009) Apoptosis: molecular mechanisms and pathogenicity. Excli Journal 8:155-181 ISSN 1611-2156 .

[38] Crompton M. (2000) Bax, Bid and the permeabilization of the mitochondrial outer memb
rane in apoptosis. Curr Opin. Cell Biol 12:414-9.

[39] Hollstein M, Sidransky D, Vogelstein B, Harris CC. (1991) p53 mutations in human Cancers Science. 253: 49-53 [PMID: 1905840].

[40] Lee JM, Bernstein A. (1995) Apoptosis, cancer and the p53 tumour suppressor gene. Cancer Metastasis Rev. 14: 149-161 [PMID: 7554031].

[41] Liebermann DA, Hoffman B, Steinman RA. (1995) Molecular con-trols of growth arrest and apoptosis: p53-dependent and independent pathways. Oncogene, 11: 199-210 [PMID:7624128].

[42] Chiarugi V, Magnelli L, Cinelli M, Basi G. (1994) Apoptosis and the cell cycle. Cell Mol Biol Res 40: 603-612 [PMID: 7787878].

[43] Vousden KH, Lu X. (2002) Live or let die: the cell's response to p53. Nat Rev Cancer 2: 594-604 [PMID: 12154352].

[44] Chipuk JE, Green DR. (2006) Dissecting p53-dependent apoptosis. Cell Death Differ 13: 994-1002 [PMID: 16543937].

[45] Vaseva AV, Moll UM. (2009) The mitochondrial p53 pathway. Bio-chim Biophys Acta, 1787: 414-420 [PMID: 19007744]

[46] Webster KR. (2000) Therapeutic potential of targeting the cell cycle. Chem. Res. Toxicol. 13 940-943.

.

[47] Sherr CJ. (2000) The Pezcoller lecture: cancer cell cycles revisited. Cancer Res. 60 3689–3695.

[48] Johnstone RW, Ruefli AA, Lowe SW. (2002) Apoptosis: a link between cancer genetics and chemotherapy. Cell 108 153–164.

[49] Thiel G, Cibelli G. (2002) Regulation of life and death by the zinc finger transcription factor Egr-1, J. Cell. Physiol. 193 287–292.

[50] Gaiddon C, Jeannequin P, Bischoff P, Sirlin C, Loeffler JP. (2005) Ruthenium (II)-derived organometallic compounds induce cytostatic and cytotoxic effects on mammalian cancer cell lines through p53-dependent and p53-independent mechanism. J. Pharmacol. Exp. Ther. 315 1403-1411.

[51] Lowe SW, Lin AW. (2000) Apoptosis in cancer. Carcinogenesis 21 485–495.

[52] Silveira-Lacerda E P, Vilanova-Costa CAST, Pereira FC, Hamaguchi A, Pavanin LA, et al. (2009) The Ruthenium Complex cis-(Dichloro) Tetraammineruthenium(III) Chloride Presents Immune Stimulatory Activity on Human Peripheral Blood Mononuclear Cells. Biol Trace Elem Res. DOI 10.1007/s12011-009-8440-8.

[53] Lima AP, Pereira FC, Vilanova-Costa CAST, Soares JR, Pereira LCG, et al. (2010) Induction of Cell Cycle Arrest and Apoptosis by Ruthenium Complex cis-(Dichloro)tetraamineruthenium(III) Chloride in Human Lung Carcinoma Cells A549. Biol Trace Elem Res. DOI 10.1007/s12011-011-9275-7. 2011.

[54] Silveira-Lacerda E P, Vilanova-Costa CAST, Pereira FC, Hamaguchi A, Pavanin LA, et al. (2009) The Ruthenium Complex cis-(Dichloro)tetraammineruthenium(III)

Chloride Presents Selective Cytotoxicity Against Murine B Cell Lymphoma (A-20), Murine Ascitic Sarcoma 180 (S-180), Human Breast Adenocarcinoma (SK-BR-3), and Human T Cell Leukemia (Jurkat) Tumor Cell Lines. Biol Trace Elem Res. DOI 10.1007/s12011-009-8440-8. 2009.

[55] Castedo M, (2002) Quantitation of mitochondrial alterations associated with apoptosis. J.Immunol. Methods 265: 39-47.

6. CONCLUSÕES

A partir dos resultados obtidos neste trabalho, foi possível concluir que:

Artigo 1

- O complexo de rutênio Ditionato de *cis*-Tetraamino(oxalato)rutênio(III) induziu citotoxicidade na linhagem tumoral K562 como evidenciado pelo ensaio de exclusão azul tripano e ensaio MTT com IC_{50} 18.28 µM.;
- O complexo Ditionato de *cis*-Tetraamino(oxalato)rutênio(III) induziu morte celular sugestiva por apoptose nas células K562;
- O complexo Ditionato de *cis*-Tetraamino(oxalato)rutênio(III) alterou a distribuição cinética do ciclo celular de células K562, aumentando o percentual de células em apoptose e reduziu as fases G1, S e G2;
- O complexo Ditionato de *cis*-Tetraamino(oxalato)rutênio(III) induziu dano no DNA da células de K562.

Artigo 2

- O complexo de rutênio (II) induziu citotoxicidade sobre a linhagem tumoral S180 apresentando valor de IC_{50} de 17,02±8,21µM e menor atividade citotóxica sobre linhagem normal de linfócitos, apresentando valor de IC_{50} de 53,02 µM, valor este superior ao verificados para a linhagem tumoral;
- O complexo Ru (II) alterou a cinética do ciclo celular da linhagem tumoral S180 visto que aumentou a porcentagem de células na fase G0/G1 com consequente diminuição da fase S, indicando que este complexo pode ser classificado como um agente ciclo celular específico;
- O complexo Ru (II) induziu morte celular via apoptose como evidenciado pelo aumentou de células Anexina V positiva;
- A apoptose induzida pelo complexo Ru (II) em células S180 envolveu o aumento da atividade de Casp3 e 8 demonstrando assim a participação de ambas as vias intrínseca e extrínsica no mecanismo de indução de apoptose induzida pelo complexo Ru (II);
- O complexo de Ru (II) provocou a diminuição da proteína Bcl-2 intracelular;
- Os mecanismos envolvidos no processo de apoptose após tratamento com

Ru (II) foram também demonstrados pela despolarização do potencial de membrana mitocondrial, aumento da expressão dos genes pró-apotóticos *Bax* e *Casp3*, alterando também a expressão de *Tp53*.

7. CONSIDERAÇÕES FINAIS

Pesquisas para o desenvolvimento de novos fármacos contra o câncer têm levado a grandes e extensas investigações com complexos de rutênio. Os complexos de rutênio tornaram-se atraentes principalmente porque eles apresentam três propriedades importantes e adequadas para aplicações bilogicas: 1 – esses metais tem a cinética de troca de ligantes semelhantes aos complexos de platina II, 2 – tem difirentes estados de oxidação, 3 – são acessíveis sob condições fisiológicas e são semelhantes ao ferro podendo ser transportados para dentro da célula pela albumina e transferrina o que reduz a sua toxicidade.

Embora ainda o mecanismo de ação dos compelxos de rutênio não esteja completamente compreendido estudos têm idenficado vantagens na utilização de complexos de metais a base de rutênio. O fato de se poder trabalhar com ligantes diferentes ao metal de transição possibilita muitas características e aplicações biológicas diferentes aos complexos de rutênio.

Diante dessas possibilidades e para o desenvolvimento deste trabalho decidimos investigarmos a atividade dos complexos de Ru (II) e Ru (III) frente a células tumorais. Por meio de ensaios testamos a atividade dos dois complexos e verificamos que ambos induziram citotoxicidade nas linhagens testadas. O complexo de Ru (III) frente à linhagem tumoral K562 demosntrou induzir citotoxicidade sendo tempo dose dependente. O complexo de rutênio (III) também induziu alteração no ciclo celular e desencadeou o processo de apoptose. O processo de apoptose também foi observado pela degradação do DNA em eletroforese de gel de agarose. Observamos ainda que o rutênio (III) causaou danos na molécula de DNA, mostrando-se tão ativo quanto à cisplatina, provavelmente pela ligação do complexo a fita de DNA.

Os estudos sobre os mecanismos de ação dos complexos de rutênio realizados por vários grupos de pesquisa têm evidenciado que a atividade citotóxica de complexos de rutênio sobre células tumorais não é dependente somente do estado de oxidação, mas depende intensamente da estrutura química do composto, atribuindo uma melhor interação com a molécula de DNA. Os ligantes fosfínico presentes no complexo de rutênio (II) desempenham uma função importante na atividade deste composto frente à linhagem tumoral analisada. A estrutura química presente neste complexo de rutênio (II) sugere que o mesmo permite a entrada na

célula de forma estável; apresenta ainda alta lipofilicidade, o que pode facilitar a passagem da droga pela membrana celular de natureza lipoproteica; apresenta também estabilidade termodinâmica e cinética que impedem reações indesejadas. O complexo de rutênio II ainda é bastante estável devido ao ligante nitrila que pode establilizar metais em vários estados de oxidação.

Em relação ao complexo rutênio (III) devido à presença de ligantes cloro em sua estrutura, sugere-se que o mesmo, sofra alterações através do processo de hidrólise, onde os ligantes cloro, por serem bastante lábeis são substituídos por moléculas de água, semelhante ao mecanismo que ocorre com a cisplatina.

Neste estudo, os testes realizados nos leva a inferir o mecanismo de morte celular causado pelos complexos de rutênio aqui testados. Estudos mostram a interação dos complexos de rutênio com biomoléculas, como o DNA, transferrina e albumina os quais são de grande importância para a investigação do mecanismo de ação destes complexos. Sendo que alguns resultados na literatura têm demonstrado a capacidade de complexos de rutênio de interagirem com essas biomoléculas.

A partir dos resultados observados neste trabalho e das teorias do mecanismo de ativação de complexos de rutênio (III), entende-se que o complexo de rutênio (III) sofra ativação por redução na célula formando Ru (II), o qual é a forma ativa do complexo que irá se ligar ao DNA. A ligação à molécula de DNA leva a ativação de uma cascata de sinalização como externalização fosfatidilserina, ativação de proteases (caspase-3), e indução de morte celular via apoptose, e necrose possivelmente por fragmentação do DNA.

Em relação ao complexo rutênio (II) o qual é a forma ativa do complexo, entende-se que este liga-se ao DNA sem sofrer alterações químicas, levando assim a alteração do potencial de membrana mitocondrial, externalização de fosfafidilserina, liberação e ativação de moléculas apoptogências como Bax, caspases 3 e 8 induzindo de morte da células por via apoptotica.

Com os resultados obtidos neste estudo com os complexos de Ru (II e III) sugere-se uma hipótese para o possível mecanismo de ação de ambos os complexos. A hipótese para o complexo de rutênio (III) esta esquimatizado na figura 12, já a hipótese para o complexo de rutênio (II) segue conforme desmosntrado no esquema 1 do artigo 2.

8. CONTRIBUIÇÕES EM OUTROS PROJETOS

- Contribuição no trabalho de Doutorado do aluno Alcio do curso de pós-graduação em Ciências da Saúde da Faculdade de Medicina da Universidade Federal de Goiás com a realização do teste Anexina V/PI utilizando citometria de fluxo. Trabalho a ser submetido.
- Contribuição no trabalho de Doutorado dos alunos Benito Juarez Nunes Alves de Oliveira e Luiz Augusto de Souza do curso de pós-graduação em Veterianaria da faculdade de Veterinaria da Universidade Federal de Goiás com a realização do teste Anexina V/PI utilizando citometria de fluxo. Trabalhos a serem submetidos.
- Contribuição no trabalho de Doutorado da aluna Aliny Pereira de Lima do curso de pós-graduação em Biologia Celular e Molecular da faculdade de Biologia da Univesidade Federal de Goiás com a realização do teste de AnexinaV/PI, Ciclo celular e teste JC-1. Um trabalho publicado e o restante em vias de submissão.
- Contribuição no trabalho de Mestrado da aluna Paula Roberta Nunes do curso de pós-graduação em Farmácia da Faculdade de Farmacia da Universidade Federal de Goias com a realização dos testes de Anexina V/PI e ciclo celular. Trabalho publicado.
- Contribuição no trabalho de Mestrado da aluna Hellen Karine Paes Porto do curso de pos-graduação em Farmacia da Faculdade de Farmacia da Universidade Federal de Goias com a realização dos testes de Anexina V/PI e ciclo celular. Trabalho em vias de submissão.
- Contribuição no trabalho de Graduação e Mestrado da aluna Wanessa Carvalho Pires do curso de Bioloiga da Universidade Federal de Goiás com a realização dos testes de Anexina V/PI e ciclo celular. Trabalho em vias de conclusão.

9. REFERÊNCIAS BIBLIOGRÁFICAS

1. AIRD, R.E; CUMMINQS, A.A; RITCHIE, M.M; MORRIS, R.E.; CHEN, H; SADLER, P.J.; JODREL, D.I. (2002). In vitro and in vivo activity and cross resistance profiles of novel Ruthenium (II) organometallic arene complexes in human ovarian cancer. British Journal of Cancer 86, 1652.

2. ALAMA, A.; TASSO, B; NOVELLI, F.; SPARATORE, F. (2009). Organometallic compound in oncology: implications of novel organotins as antitumor agents. Drug Discovery Today. v. 14. p. 500-509.

3. ALEKTIAR KM, BRENNAN MF, SINGER S. (2002). Influence of site on the therapeutic ratio of adjuvant radiotherapy in soft-tissue sarcoma of the extremity. Int J Radiat Oncol Biol Phys. 63(1):202-208.

4. ALLARDICE, C.S.; DYSON, P.J. (2001). Ruthenium in Medicine: current clinical uses and future prospects. Platinum Metals Review 45 (2), 62-69.

5. ALMEIDA, V. L *et al*. (2005). Câncer e Agentes Antineoplásicos Ciclo-Celular Específicos e Ciclo-Celular não Específicos que Interagem com o DNA: Uma Introdução. Quim. Nova. v. 28, n. 1, p. 118-129.

6. ANDERSSON, B.S.; MROUE, M.; BRITTEN, R.A.; MURRAY, D. (1994). The role of DNA damage in the resistance of human chronic myeloid leukemia cells to cyclophosphamide analogues. *Cancer Research*. 15;54(20),5394-400.

7. ANTONARAKIS, E.S E EMADI, A. (2010). Rutheniuem-based chemotherapeutics: are they ready for prime time? Cancer Chemother Pharmacol. v.66, p.1-9.

8. BARTEK, J ELUKAS, J. (2007). DNA damage checkpoints: from initiation to recovery or adaptation. Current Opinion in Cell Biology, v. 19, p.238-245.

9. BERGAMO, A. & SAVA, G. (2011). Ruthenium anticancer compounds: myths and realities of the emerging metal-basead drugs. Dalton Trans., 40, 7817.

10. BERGAMO, A. et al. (2008). Modulation of the metastatic progression of breast cancer with an organometallic ruthenium compound. Int J of Oncol. V.33, p.1281-1289.

11. BONVALOT S; KHANFIR K, ALZIEU L, TERRIER P, LE PECHOUX C; VANEL D, et al. (2006). Does adjuvant radiation therapy increase loco-regional control after optimal resection of soft-tissue sarcoma of the extremities? Eur J Cancer.;39 (13):1872-880.

12. BRENES, O. et al. (2007). Characterization of cell death events induced by anti-neoplastic drugs cisplatin, paclitaxel and 5-fluorouracil on human hepatoma cell lines: Possible mechanisms of cell resistance. Biomedicine & Pharmacotherapy. v. 61. p. 347-355.

13. BROWN, J. M E ATTARDI, .D. (2005). The role of apoptosis in câncer development and treatment response. Nature Reviews. v.5, p.231-237.

14. CALAMAI, P.; CAROTTI, S.; GUERRI, A.; MAZZEI, T.; MESSORI, L.; MININ, E.; ORIOLI, P. E SPERONI, G.-P. (1998) Cytotoxic effects of gold (III) complexes on establish human tumor cell lines sensitive and resistant to cisplatin. Anti-Cancer Drug Desing 13, 67-80.

15. CASTEDO, M. et al. (2004). Cell death by mitotic catástrofe: a molecular definition. Oncogene. v.23, p. 2825-837.

16. CAVALCANTI JR, G.B.; KLUMB, C.E.; MAIA, R.C. (2002) p53 e as hemopatias malignas. Revista Brasileira de Cancerologia 48 (supl. 3), 419-427.

17. CHEN, Y. et al. (2013). Synthesis, characterization, and anticancer activity of ruthenium(II)-β-carboline complex. European journal of medicinal chemistry, v. 70, p. 120-129, Dec.

18. CLARKE, M. J. (2003). Ruthenium metallopharmaceuticals Coord. Chem. Rev. v. 236. p. 209-233.

19. COLLINS, A.R.; DOBSON, V.L; DUINSKÁ, M; KENNEDY, G; TTINA, R. (1997) The comet assay: what can it really tell us? Mutation Research 375, 183-193.

20. COOPER, G.M. E HAUSMAN. (2007). A Célula, uma abordagem molecular. 3° ed. Porto Alegre: Artmed. de Baixo Grau. Soft Tissue Sarcomas: Treatment Results in Low-grade Tumors Serviço de Tecido Conjuntivo do Hospital Araújo Jorge da Associação de Combate ao Câncer em Goiás (HAJ-ACCG), Goiânia (GO), Brasil.

21. DANTAS, E.L.R.; SÁ F.H.L.; CARVALHO, S.M.F.; ARRUDA, A.P., RIBEIRO, E.M. (2009). Genética do Câncer Hereditario. Revista Brasileira de Cancerologia; 55(3): 263-269.

22. DEBNATH, J.; BAEHRECKE, E. H.; KROEMER, G. Does autophagy contribute to cell death? (2005). Autophagy, v. 1, n. 2, p. 66-74, July.

23. DELCROS, J.G; MEHLEN, P. (2013). Dependence receptors: life or death choices. Bull Cancer, v. 100, p.1261-1274.

24. DEMETRI, G.D. et al. (2010). Soft Tissue Sarcoma. J Natl Compr Canc Netw. v. 8, p.630-674.

25. DIFFLEY, J.F.X.; EVAN, G. (1999). Oncogenes and cell proliferation. Cell cycle, genome integrity and cancer - a millennial view. Current Opinion in Genetics & Development 10, 13-16.

26. DOBBIN, J.A.; GADELHA, M. I.P. (2002). Mesilato de imatinibe para tratamento da leucemia mielóide crônica. Rev Bras Cancerol.v.;48. p.429-38.

27. DOUCAS H, BERRY DP. (2006). Basic principles of the molecular biology of cancer I. Sugery; 24(2): 43-7.

28. DU et al. (2011). Synthesis, DNA-binding and topoisomerase inhibitory activity of ruthenium(II) polypyridyl complexes. European Journal of Medicinal Chemistry. v.46 p.1056-1065.

29. DYSON, P.J.; SAVA, G. (2006). Metal-based antitumor drugs in the post genomic era. Dalton Transactions. p.1929-1933.

30. ELMORE, S. (2007). Apoptosis: A review of Programmed Cell Death. Toxicology Pathology, v. 35, n. 4, p. 495-516, June.

31. FLINT, O.P. (1998) Predicting *in vivo* toxicity. Toxicology *in vitro* 12, 591 595.

32. FONTES, A. P. S.; CÉSAR, E. T. (2005). A química inorgânica na terapia do câncer. Cadernos Temáticos de Química Nova na Escola. n. 6. p. 13-18.

33. FORMIGLI L, PAPUCCI L, TANI A, SCHIAVONE N, TEMPESTINI A, ORLANDINI GE, CAPACCIOLI S, ORLANDINI SZ. (2000). Aponecrosis: morphological and biochemical exploration of a syncretic process of cell death sharing apoptosis and necrosis. J Cell Physiol;182:41–9. [PubMed: 10567915].

34. FRESHNEY, I. Culture of Animal Cells: A Manual of Basic Technique, 4th Edition, 2000. R. ISBN: 0471348899. Publisher: Wiley-Liss.

35. FULDA, S. (2013). Alternative Cell Death Pathways and Cell Metabolism. International Journal of Cell Biology. v, p.1-4.

36. FULDA, S. & DEBATIN, K.M. Extrinsic versus intrinsic apoptosis pathways in anticâncer chemotherapy. Oncogene. v.25, p.4798-4811, 2006.

37. GABRIELLI, B.; BROOKS, K.; PAVEY, S. Defective cell cycle checkpoints as targets for anti-cancer therapies. Pharmacology. v.3. p.1-9, 2012.

38. GAETANO J. FORTE; AMY HANLEY, KAREN HAGERTY, MD, ANUPAMA KURUP, MD, MICHAEL N. NEUSS, MD AND THERESE M. MULVEY, MD. American Society of Clinical Oncology Nacional Census of Oncology Parctives: Preliminary Report. Copyright © 2013 by American Society of Clinical Oncology. Acessado em 12/02/2013.

39. GALLORI et al. DNA as a Possible Target for Antitumor Ruthenium (III) Complexes. Archiv of Bichem and Biophsics. v.376, p.156-162, 2000.

40. GALLUZZI, L. et al. Cell death modalities: classification and pathophysiological implications. Cell Death and Differentiation. v.14, p.1237-1266, 2007.

41. GALLUZZI, L. et al. Chapter one – Programmed Necrosis: From Molecules to Health and Disease. International Review of Cell and Molecular Biology. v.289, p.1-35, 2011.

42. GALLUZZI, L. et al. Molecular definitions of cell death subroutines: recommendations of Ihe Nomenclature Commitee on Cell Death 2012. Cell and Differentiation. v.10. p.107-120, 2012.

43. GAO et al. Targeting topoisomerase II with the chiral DNA-intercalating ruthenium(II) polypyridyl complexes. J Biol Inorg Chem. v.12, p.1015-1027, 2007.

44. GHOBRIAL, I. M.; WITZIG, T.E.; ADJEI, A.A. Targeting Apoptosis Pathways in Cancer Therapy. CA Cancer J Clin. v.55, p.178-194. 2005.

45. GLEICH, L.L.; SALAMONE, F.N. Molecular genetics of head and neck cancer. *Cancer Control* 9(5): 396-378, 2002 .

46. GOODMAN, A & GILMAN, A. The Pharmacological basis of Therapeutics, Joel G. Hardman, Lee E. Limbird (Editor), Alfred Goodman Gilman (Editor), 2002.

47. HAHN W.C.; WEINVERG, R.A. Modelling the molecular circuitry. Nat. Rev. Cancer. May; 2(5):331-41, 2002.

48. HAIL JR., N. et al. Apoptosis effector mechanisms: A requiem performed in different keys. Apoptosis, v. 11, n. 6, p. 889-904, June 2006.

49. HAJRA, K. M.; LIU, J. R. Apoptosome dysfunction in human cancer. Apoptosis, v. 9, n. 6, p. 691-704, Nov. 2004.

50. HAMÚ, C.S., OLIVEIRA, M.V.P. ANTONIO MÁRCIO T. C. SILVA, A.M.T.C. SILVA, C.C. CRUZ, A.D. Polimorfismo do gene tp53 no códon 72 em pacientes com suspeita de LMC, Rev. bras. hematol. hemoter. 29(4): 346-350; 2007.

51. HANAHAN, D.; WEINBERG, R.A. Hallmarks of cancer: the next generation. Cell. v. 144, p. 646 – 674, 2011.

52. HARTINGER, C.G. et al. From bench to beside – preclinical and early clinical development of the anticancer agent indazolium trans- [tetrachlorobis (1 H-indazazole)ruthenate (III)] KP1019 or FFC14A). Journal of Inorganic Biochemistry.v.100. p. 891-904. 2006.

53. HENDERSON ER, PEPPER AM, MARULANDA G, BINITIE OT, CHEONG D, LETSON GD. Outcome of lower-limb preservation with an expandable endoprosthesis after tumor ressection in children. Journal of bone and joint surgery 2012 Mar 21;94(6):537-47. doi: 10.2106/JBJS.I.01575.

54. HENGARTNER, M.O. The Biochemistry of apoptosis. Nature. v.407, p.770-776, 2000.

55. HOLLSTEIN, M.; SIDRANSKY, D.; VOGELSTEIN, B.; HARRIS, C.C. (1991) p53 Mutations in Human Cancers. Science 253(5015): 49-53.

56. HUXHAM, L.A.; CHEU, E.L.S.; PATRICK, B.O. E JAMES, B.R. (2003) The synthese, structural characterization, and in vitro anti-cancer activity of chloro(p-cymene) complexes of Ruthenium(II) containing a disulfoxide ligand. Inorganica Chimica Acta 352, 238-246.

57. INSTITUTO NACIONAL DO CÂNCER. Estimativa 2012: Incidência de Câncer no Brasil. Disponível em URL: http://www.inca.gov.br/estimativa/2014 Acesso em: 03/01/2014.

58. INSTITUTO NACIONAL DO CÂNCER. Estimativa 2014: Incidência de Câncer no Brasil. Disponível em URL:http://www2.inca.gov.br/wps/wcm/connect/tiposdecancer/site/home/leucemia/definicao. Acesso em: 28/02/2014.

59. INSTITUTO NACIONAL DO CÂNCER. Estimativa 2014: Incidência de Câncer no Brasil. Disponível em URL: http://www.inca.gov.br/estimativa/2014. Acesso em: 27/02/2014.

60. JAATTELA, I.S e MATHIASEN, M. Triggering caspase-independent cell death to combat câncer. Trends in Molecular Medicine. v.8, p.212-220, 2002.

61. JIRSOVA, K.; MANDYS, V.; GISPEN, W.H.; BAR, P.R. Cisplatin-Induced Apoptosis in Cultures of Human Schwann Cell. Neuroscience Letters. v 392. p. 2-26. 2006.

62. KAPITZA, S. et al. The heterocyclic ruthenium(III) complex KP1019 (FFC14A) causes DNA damage and oxidative stress in colorectal tumor cells. Cancer Letters. v. 226. p.115-121. 2005.

63. KARTALOU, M.; ESSIGMANN, J. M. Mechanisms of Resistance to Cisplatin. Mutation Research. v. 478. p. 23-43. 2001.

64. KELEKAR, A. Autophagy. Annals of the New York Academy of Sciences. v.1066, p.259-271. 2006.

65. KERR JF, WYLLIE AH, CURRIE AR. Apoptosis: a basic biological phenomenon with wide-ranging implications in tissue kinetics. Br J Cancer 1972;26:239–57. [PubMed: 4561027].

66. KERR JF. A histochemical study of hypertrophy and ischaemic injury of rat liver with special reference to changes in lysosomes. J Pathol Bacteriol 1965; 90: 419–435.

67. KERR JF. History of the events leading to the formulation of the apoptosis concept. Toxicology 2002;181– 182:471–4.

68. KIM, R et al. Current status of the molecular mechanisms of anticancer drug-induced apoptosis. Cancer Chemother Pharmacol. v.50, p. 343-352. 2002.

69. KOSTOVA, I. (2006) Ruthenium complexes as anticancer agents. Current Medicinal Chemistry 13(9),1085-107.

70. KROEMER, G. et al. Classification of cell death: recommendations of lhe Nomenclature Committee on Cell Death 2009. Cell Death and Differentiation. v.16, p.3-11, 2009.

71. KÜNG, A.; PIEPER, T. KEPPLER, B.K. (2001) Investigations into the interaction between tumor-inhibiting Ruthenium(III) complexes and nucleotides by capillary electrophoresis. Journal of Chomatography B 759, 81-89.

72. KUROSAKA, K., TAKAHASHI, M., WATANABE, N., AND KOBAYASHI, Y. (2003). Silent cleanup of very early apoptotic cells by macrophages.J Immunol171, 4672–9.

73. LATORRE MRDO, FRANCO EL. Epidemiologia dos sarcomas.In: Lopes A (ed). Sarcomas de partes moles. Rio de Janeiro: Medsi; 1999:3-18.

74. LEVINA, A. MITRA, A e LAY P.A. Recents developments in ruthenium anticâncer drugs. Metallomics. v.1, p.458-470, 2009.

75. LI et al. Ruthenium complexes containing bis-benzimidazole derivates as a new class of apoptosis inducers. Dalton Transaction. v.41, p.1139-1141. 2012.

76. LI, J e YUAN, J. Caspases in apoptosis and beyond. Oncogene. v.27, .p. 6194-6206, 2008.

77. LIMA, A.P. et al. The compound *cis*-(dichloro)tetramminеruthenium(III) chloride induces caspase-mediated apoptosis in K562 cells; Toxicology in vitro. 24 (6) 1562-8. 2010a.

78. LIMA, A.P. et al. The ruthenium complex *cis*-(dichloro)tetramminеruthenium(III) chloride induces apoptosis and damages DNA in murine sarcoma 180 cells; J. Biosci. 35.2010b.

79. LIU et al. DNA binding and photocleavage proeperties and apoptosis-inducing activities of a ruthenium porpyrin complex and its heterometallic. Chemico Biological Interactions. v.183. p.349-356, 2010.

80. LOCKSHIN RA, WILLIAMS CM. Programmed cell death – I. Cytology of degeneration in the intersegmental muscles of the pernyi silkmoth. J Insect Physiol 1965; 11: 123–133).

81. LOCKSHIN RA, WILLIAMS CM. Programmed cell death – II. Endocrine potentiation of the breakdown of the intersegmental muscles of silkmoths. J Insect Physiol 1964; 10:643–649.

82. LODISH, H.; BERK, A.; ZIPURSKY, S.L.; MATSUDAIRA, P.; BALTIMORE, D. E DARNELL, J. Molecular Cell Biology, New York, W.H. Freeman and company, 4ed., 1084p., 2000.

83. LOKICH, J.; ANDERSON, N. (1998) Carboplatin versus cisplatin in solid tumors: an analysis of the literature. Annals of Oncology 9, 13-21.

84. MAJNO, G., AND JORIS, I. (1995). Apoptosis, oncosis, and necrosis. An overview of cell death.Am J Pathol146, 3–15.

85. MANOEL, W.J.; SARMENTO, B.J.Q.; JÚNIOR, L.P.S.; ABREU, D.C.B.; NETO, I.P.A.; FERREIRA, E.C. (2008). Sarcomas de Partes Moles: Resultados do Tratamento dos Tumores de Baixo Grau. Revista Brasileira de Cancerologia; 54(1): 17-24.

86. MARTIN, S. J. et al. Early redistribution of plasma membrane phosphatidylserine is a general feature of apoptosis regardless of the initiating stimulus: inhibition by overexpression of Bcl-2 and Abl. J. Exp. Med.v.182, p.1545-1556,1995.

87. MATHER, J. (1998) Introduction to Cell and Tissue Culture. New York and London, Plenum Press.

88. MAURILLO, L.; POETA, G.D.; VENDITTI, A. (2001) Quantitative analysis of Fas and bcl-2 expression in hematopoietic precursors. Haematologica 86, 237-243.

89. MEDEMA R. H., MACUREK L. Checkpoint control and cancer. Oncogene. v.31, p.2601-2613, 2012.

90. MENEZES, C.S.R.; COSTA, L.C.G.P.; ÁVILA, V.M.R.; FERREIRA, M.C.; UEIRA, C.V.; PAVANIN, L. A.; HOMSI-BRANDEBURGO, M. I.; HAMAGUCHI, A.; SILVEIRA-LACERDA, E.P. (2007) Interaction between plasmid DNA and the *cis*-dichloroTetraammineRuthenium(III) chloride, . Chemico-Biological Interactions 167, 116-124.

91. MIZUTANI, H.; TADA-OIKAWA, S.; HIRAKU, Y.; KOJIMA, M.; KAWANISHI, S. Mechanisms of Apoptosis Induced by doxorubicin through the generation of hydrogen peroxide. Life Scienses. v. 76. p.1439-1453. 2005.

92. MANOEL, W.J.; SARMENTO. B.J.Q.; JÚNIOR, L.P.S.; ABREU, D.C.B.; NETO, I.P.A.; FERREIRA, E.C. (2008). Revista Brasileira de Cancerologia; 54(1): 17-24.

93. MORAES, A.M.; AUGUSTO, E.F.P.; CASTILHO, L.R. Tecnologia do cultivo de células animais: de biofármacos a terapia gênica – São Paulo; Roca 2007.

94. MORBIDELLI, L. et al. Antiangiogenic properties of selected ruthenium(III) complexes that are nitric oxide scavengers. British Journal of Cancer. v. 88. p. 1484-1491. 2003.

95. MORENO et al. DNA interaction and cytotoxicity studies of new ruthenium (II) cyclopentadienyl derivate complexes containing heteroaromatic ligands. J Inorg Biochem. v.105, p.241-249, 2011.

96. MOTOYAMA, N.; NAKA, K. DNA damage tumor suppressor genes and genomic instability. Current Opinion in Genetics & Development. v.14, p.11-16. 2004.

97. NAGAI, M.A. (1999). Genetic alterations in head and neck squamous cell carcinomas. Brazilian Journal of Medical and Biological Research 32(7), 897-904.

98. NIKOLETOPOULOU, et al., Crosstalk between apoptosis, necrosis and autophagy. Biochimica et Biophysica Acta. v.1822, p.3448-3459, 2013.

99. OJOPI, E.P.B.; DIAS NETO, E. (2002) Genes e Câncer – alguns eventos moleculares envolvidos na formação de um tumor. Biotecnologia Ciência e Desenvolvimento 27, 28-38.

100. OSTI RZ, SERRANO FA, PASCHOALIN T, MASSAOKA MHS, TRAVASSOS LR, et al. (2012) The *in vitro* and *in vivo* antitumour activities of nitrosyl ruthenium amine complexes. Aust. J. Chem., v.65, p.1333-1341.

101. PACOR, S. et al. Intratumoral NAMI-A Treatment Triggers Metastasis Reduction, Which Correlates to CD44 Regulation and Tumor Infiltrating Lymphocyte Recruitment. J of Pharmacology and Experimental Therapeutics. v.310, n.2, p.737-744, 2004.

102. PARMIGIANI, R.B.; CAMARGO, A.A. In: Ferreira, C.G e Rocha, J.C. Oncologia Molecular. Ed. Atheneu. 469p. 2004.

103. PAWELETZ, N. (2001). Walther Flemming: pioneer of mitosis research.Nat Rev Mol Cell Biol2, 72–5.

104. PETRILLI, A.S., CAMARGO, B., FILHO, V.O., BRUNIERA, P., BRUNETTO A.L., JESUS-GARCIA, R., CAMARGO,O.P., PENA, W. et al., (2006). Results of the Brazilian Osteosarcoma Treatment Group Studies III and IV: Prognostic Factors and Impact on Survival. *Journal of Clinical Oncology*, Vol 24, No 7 (March 1): pp. 1161-1168.

105. PINTO, L.F.R. e FELZENSZWALB, I. Genética do Câncer. In: RIBEIRO, L.R., SALVADORI, D.M.F.; MARQUES, E.K.Mutagênese Ambiental. 1° ed. Canoas: Ulbra. 2003. p. 247-279.

106. PIZARRO, A. M. e SADLER, P. J. Unsual DNA modes for metal anticancer complexes. Biochimie. p. 1-14. 2009. doi: 10.1016.

107. PLUIM, D. et al. Cytotoxicity of the organic ruthenium anticancer drug NAMI-A is correlated with DNA binding in four different human tumor cell line. Cancer Chemother Pharmacol. v. 54. p. 71-78. 2004.

108. RAMENGHI, U.; BONISSONI, S.; MIGLIARETTI, G. (2000) Deficiency of the Fas apoptosis pathway without Fas gene mutations is a familial trait predisposing to development of autoimmune diseases and cancer. Blood 95, 3176-3182.

109. SABALE, P.M.; PATEL, J.; PATEL, Y. Metal Complexes: Current trends and future potential. IJPCBS. v.2, p.251-265, 2012.

110. SAVA, G. et al. Dual Action of NAMI-A in Inhibition of Solid Tumor Metastasis: Selective Targeting of Metastatic Cells and Binding to Collagen. Clinical Cancer Research. v. 9. p. 1898-1905. May, 2003.

111. SAVA, G.; ALESSIO, E.; BERGAMO, E.; MESTRONI, G. (1999) Topics in Biological Inorganic Chemistry 1, 143-170.

112. SAVA, G.; BERGAMO, A.; ZORZET, A. (2002) Influence of chemical stability on the activity of the antimetastasis Ruthenium compound NAMI-A, European Journal of Cancer 38, 427-435.

113. SAVA, G.; PACOR, S.; MESSTRONI, G.; ALESSIO, E. (1992) Na[trans-RuCl4(DMSO)Im], a metal complex of Ruthenium with antimetastatic properties. Clinical & Experimental Metastasis 10(4), 273-80.

114. SAWYERS, C. L. Chronic myeloid leukemia. N Engl J Med. v.340. p. 1330-40, 1999.

115. SCHWARTZ, G. K e SHAH, M.A. Targeting the Cell Cycle: A New Approach to Cancer Therapy. J Clin Oncol. v.23, n. 36, p. 9408-9421, 2005.

116. SCHWEICHEL JU, MERKER HJ. The morphology of various types of cell death in prenatal tissues. Teratology 1973; 7: 253–266).

117. SHAFFER, A.L.ROSENWALD, A., STAUDT, L.M. Lymphoid malignancies: the dark side of B-cell differentiation, Nat. Rev. Immunol. 2 (12) (2002) 920–932.

118. SHARMA, A.; TALUKDER, G. (1987) Effects of metals on chromosome of higher organisms. Environmental Mutagenesis 9, 191-226.

119. SHI, Y. Mechanism of Caspase Activation and Inhibition during Apoptosis. Molecular Cell. v.9. p.459-470, 2002.

120. SIGAL, A; ROTTER, V. (2000). Oncogenic mutations of the p53 tumor supressor: the demons of the guardian of the genome. Cancer Research 60, 6788-6793.

121. SILVA, J.; ERDTMANN, B.; HENRIQUE, J. A. P. Genética toxicológica. Editora Alcance, 2003.

122. SILVEIRA-LACERDA, E. P. Avaliação da Atividade Antitumoral do cis-[RuCl2(NH3)4]Cl sobre linhagens tumorais humanas e de camundongos. 2003. 67 f. Tese de Doutorado – Universidade Federal Uberlândia, Uberlândia.

123. SILVEIRA-LACERDA, E. P. et al. The Ruthenium Complex cis-(Dichloro)tetraammineruthenium(III) Chloride Presents Selective Cytotoxicity Against Murine B Cell Lymphoma (A-20), Murine Ascitic Sarcoma 180 (S-180), Human Breast Adenocarcinoma (SK-BR-3), and Human T Cell Leukemia (Jurkat) Tumor Cell Lines. Biol Trace Elem Res. 2009 doi: 10.1007/s12011-009-8498-3.

124. SINGER S, DEMETRI GD, BALDINI EH. Management of softtissue sarcomas: An overview and update. Lancet Oncol. 2000;1:75-85.

125. SONIS, ST. Mucositis as a biological process: a new hypothesis for the development of chemotherapy-induced stomatotoxicity. Oral Oncol., Kidlington, 34: 39-43. 1998.

126. SPERANDIO S, DE BELLE I, BREDESEN DE. An alternative, non- apoptotic form of programmed cell death. Proc Natl Acad Sci USA 2000;97:14376–81. [PubMed: 11121041].

127. SPIRA, A.I. e DAVID S. ETTINGER, D.S. The Use of Chemotherapy in Soft-Tissue Sarcomas. The Oncologist. v.7, p.348-359, 2002.

128. STEWART, Z.A.; WESTFALL, M.D., PIETENPOL, J.A. Cell-cycle dysregulation and anticancer therapy. Trends in Pharmacological Sciences. v.24, n.3, March 2003.

129. SUSS-FINK, G. Arene ruthenium complexes as anticancer agents. Dalton Transactions. v.39, p.1673-1688, 2010.

130. TAJARA, E. H. Ciclo Celular. In: FERREIRA, C.G. ; ROCHA, J.C. Oncologia Molecular. 1 ed. São Paulo: Atheneu. 2004. p. 65-76.

131. The World Health Organisation (2008). 2008-2013 action plan for the global strategy for the prevention and control of noncommunicable diseases: prevent and control cardiovascular diseases, cancers, chronic respiratory diseases and diabetes. The World Health Organisation: Geneva. Acessado feveriro de 2013.

132. The World Health Organisation. Media centre. Cancer. Disponível em URL: http://www.who.int/mediacentre/factsheets/fs297/en/. Acesso em 27/02/2014.

133. TICE, R.R.; AGURELL, E.; ANDERSON, D.; BURLINSON, B.; HARTMANN, A.; KOBAYASHI, H.; MIYAMAE, Y.; ROJAS, E.; RYU, J. C.; SASAKI, F. (2008) Single cell gel/comet assay: guidelines for in vitro and in vivo genetic toxicology testing. Radiation Research 169, 110-121.

134. TOLEDO, S.R.C. Sarcomas Ósseos e de Partes Moles. In: Ferreira, C.G. e Rocha, J.C. Oncologia Molecular .1. ed. São Paulo: Atheneu, 2004. p.263- 284.

135. Trump, B. F., Berezesky, I. K., Chang, S. H., and Phelps, P. C. (1997). The pathways of cell death: oncosis, apoptosis, and necrosis.Toxicol Pathol 25, 82–8.

136. TRZECIAK, A.R., KOWALIK, J., MAŁECKA-PANAS, E., DRZEWOSKI, J., WOJEWODZKA, M., IWANENKO, T., BŁASIAK, J. 2000. Genotoxicity of chromium in human gastric mucosa cells and peripheral blood lymphocytes evaluated by the single cell gel electrophoresis (comet assay). Medical Science Monitor 6, 24-29.

137. VILLEDIEU, M. et al. Absence of Bcl-xL down-regulation in response to cisplatin is associated with chemoresistence in ovarian carcinoma cells. Gynecologic Oncology. 105, p. 31-44, 2007.

138. WYLLIE, A.H.; KERR, J.F.R.; CURRIE, A.R. (1980) Cell death: the significance of apoptosis. International Review of Cytology 68, 251-306.

139. ZHANG, P.; CHEN, J.; LIANG, Y. DNA binding, cytotoxicity, and apoptotic-inducing activity of ruthenium (II) polypyridyl complex. Acta Biochim Biophis Scin. v.42, p.440-449, 2010.

140. ZLOTECKI RA, KATZ TS, MORRIS CG, LIND DS, HOCHWALD SN. Adjuvant radiation therapy for resectable retroperitoneal soft tissue sarcoma: the University of Florida experience. Am J Clin Oncol. 2005;28(3):310-16.

10. Anexos

Anexo 1

European Journal of Medicinal Chemistry 55 (2012) 67–73

Contents lists available at SciVerse ScienceDirect

European Journal of Medicinal Chemistry

journal homepage: http://www.elsevier.com/locate/ejmech

Original article

Atypical fluoroquinolone gold(III) chelates as potential anticancer agents: Relevance of DNA and protein interactions for their mechanism of action

Ligiane R. Gouvea [a], Luciene S. Garcia [b], Daniela R. Lachter [b], Paula Roberta Nunes [c], Flávia de Castro Pereira [c], Elisângela P. Silveira-Lacerda [c], Sônia R.W. Louro [d], Paulo Jorge S. Barbeira [a], Letícia R. Teixeira [a,*]

[a] Departamento de Química, Universidade Federal de Minas Gerais, Av. Antonio Carlos 6627, 31270-901 Belo Horizonte (MG), Brazil
[b] Departamento de Química, Pontifícia Universidade Católica do Rio de Janeiro, 22653-900 Rio de Janeiro (RJ), Brazil
[c] Departamento de Biologia Geral, Universidade Federal de Goiás, 74001-970 Goiânia (GO), Brazil
[d] Departamento de Física, Pontifícia Universidade Católica do Rio de Janeiro, 22653-900 Rio de Janeiro (RJ), Brazil

ARTICLE INFO

Article history:
Received 7 February 2012
Received in revised form
28 June 2012
Accepted 2 July 2012
Available online 14 July 2012

Keywords:
Fluoroquinolones
Gold(III) complexes
Cytotoxic activity
Interaction with calf-thymus DNA
Interaction with bovine serum albumin

ABSTRACT

Quinolones are known for their antimicrobial and antitumor activities. Gold(III) compounds constitute an emerging class of biologically active substances, of special interest as potential anticancer agents. In this work three gold(III) complexes of the fluoroquinolones antimicrobial agents norfloxacin (NOR), levofloxacin (LEVO) and sparfloxacin (SPAR) were prepared and characterized with physicochemical and spectroscopic techniques. In these complexes, NOR, LEVO and SPAR act as bidentate neutral ligands bound to gold(III) through the nitrogen atoms of the piperazine ring, which is an unusual mode of coordination for this class of compounds. Two chloride ions occupy the remaining coordination sites.

The cytotoxic activity of the fluoroquinolones and their gold(III) complexes was tested against the A20 (murine lymphoma), B16-F10 (murine melanoma) and K562 (human myeloid leukemia) tumor cell lines as well as the L919 (murine lung fibroblasts) and MCR-5 (human lung fibroblasts) normal cells lines. All complexes were more active than their corresponding free ligands. Complex $[AuCl_2(LEVO)]Cl$ was selected for DNA fragmentation and cell cycle analysis.

Spectroscopic titration with calf-thymus DNA (CT DNA) showed that the complexes can bind weakly to CT DNA, probably by an external contact (electrostatic or groove binding). The complexes exhibit good binding propensity to bovine serum albumin (BSA) having relatively high binding constant values.

1. Introduction

Quinolones are known for their antimicrobial and antitumor activities through DNA intercalation and alteration of the normal functions of bacterial gyrase, and were found to be a topoisomerase II inhibitor in humans [1].

Thadepalli and collaborators (2005) evaluated the *in vivo* activity of trovafloxacin and ciprofloxacin against murine leukemic cells in neutropenic mice with lung infection due to *Klebsiella pneumoniae*. The results showed that both quinolones were effective in clearing lung infection. However, just trovafloxacin was effective in preventing metastasis of leukemia cells to the lungs and other tissue and in prolonging the survival of mice [2].

Voreloxin is a quinolone derivative that has not antibacterial activity, but shows potent cytotoxicity towards eukaryotic cancer cell lines. This compound intercalates DNA and inhibits topoisomerase II and it is currently being evaluated in a Phase 2 clinical trial for resistant ovarian cancer [3].

Numerous studies regarding the interaction between quinolones and metal ions were reported in the literature [4–7]. However, few studies regarding metal complexes of quinolones as antitumor agents can be found.

Generally, the coordination of the fluoroquinolones with metallic ions occurs through the carboxylate and the carbonyl oxygen atoms. It's much less common for the coordination to happen by way of the piperazine nitrogen atoms. The literature contains only one work, with few examples, such as platinum(II) complexes with ciprofloxacin, levofloxacin, ofloxacin, sparfloxacin and gatifloxacin. The resulting complexes present the fluoroquinolone coordinated through the nitrogen atoms of the piperazine ring [4].

Gold(III) compounds constitute an emerging class of biologically active substances, of special interest as potential anticancer agents. During the past decade a number of structurally diverse gold(III)

* Corresponding author. Tel.: +55 31 3409 5764; fax: +55 31 3409 5700.
E-mail address: lregina@qui.ufmg.br (L.R. Teixeira).

0223-5234/$ – see front matter © 2012 Elsevier Masson SAS. All rights reserved.
http://dx.doi.org/10.1016/j.ejmech.2012.07.004

Anexo 2

Biol Trace Elem Res
DOI 10.1007/s12011-011-9275-7

Induction of Cell Cycle Arrest and Apoptosis by Ruthenium Complex *cis*-(Dichloro)tetramineruthenium(III) Chloride in Human Lung Carcinoma Cells A549

Aliny Pereira de Lima · Flávia de Castro Pereira · Cesar Augusto Sam Tiago Vilanova-Costa · Jordana Ribeiro Soares · Lucas Carlos Gomes Pereira · Hellen Karine Paes Porto · Luiz Alfredo Pavanin · Wagner Batista dos Santos · Elisângela de Paula Silveira-Lacerda

Received: 20 January 2010 / Accepted: 13 November 2011

Abstract Lung cancer is one of the leading causes of death in the world, and non-small cell lung carcinoma (NSCLC) accounts for approximately 75–85% of all lung cancers. In the present work, we studied the cytotoxic activity, cell cycle arrest and induction apoptosis of the compound *cis*-(dichloro) tetramineruthenium(III) chloride {*cis*-$[RuCl_2(NH_3)_4]Cl$} in human lung carcinoma tumor cell line A549. The results of MTT and trypan blue assays showed that *cis*-$[RuCl_2(NH_3)_4]$ Cl causes reduction in the viability of A549 cells when treating with 95 and 383 μM of the compound for 48 and 72 h. Lower concentrations of the compound (19, 3.8 and 0.38 μM), however, only slightly affected cell viability. The IC_{50} value for the compound was about 383 μM. Survival analysis of the A549 cells after treatment with ruthenium(III) compound using long term clonogenic assay showed that it reduced colony formation ability at concentrations of 0.38 and 3.8 μM, and at concentrations of 95 and 383 μM no colonies were observed. Cell cycle analysis showed that compound ruthenium led to an accumulation of A549 cells in S phase and increased in the sub-G1 peak. In addition, *cis*-(dichloro) tetramineruthenium(III) chloride treatment induced apoptosis, as observed by the increased numbers of annexin V-positive cells and increased messenger RNA expression of caspase-3.

Keywords A549 · *cis*-(Dichloro)tetramineruthenium(III) chloride · Cytotoxicity · Lung cancer

Introduction

Lung cancer is one of the leading causes of death in the world, and non-small cell lung carcinoma (NSCLC)

A. P. de Lima · F. C. Pereira · C. A. S. T. Vilanova-Costa · J. R. Soares · L. C. G. Pereira · H. K. P. Porto · E. P. Silveira-Lacerda (✉)
Laboratório de Genética Molecular e Citogenética, Instituto de Ciências Biológicas- ICB I - Sala 200 - UFG, Campus Samambaia (Campus II), Universidade Federal de Goiás—UFG, Goiânia, Goiás, Brazil
e-mail: silveiralacerda@gmail.com

A. P. de Lima
e-mail: alinypereirallima@gmail.com

F. C. Pereira
e-mail: pereirafc@gmail.com

C. A. S. T. Vilanova-Costa
e-mail: vilanovacosta@gmail.com

J. R. Soares

L. C. G. Pereira
e-mail: lucascarlos_bio@hotmail.com

H. K. P. Porto
e-mail: paesporto@gmail.com

L. A. Pavanin
Instituto de Química, Universidade Federal de Uberlândia—UFU., Uberlândia, Minas Gerais, Brazil
e-mail: pavanin@ufu.br

W. B. dos Santos
Instituto de Química, Universidade Federal de Mato Grosso—UFMT., Barra do Garças, Mato Grosso, Brazil

Anexo 3

ARTICLE IN PRESS
JIB-09693; No of Pages 11
Journal of Inorganic Biochemistry xxx (2015) xxx–xxx
Contents lists available at ScienceDirect
Journal of Inorganic Biochemistry
journal homepage: www.elsevier.com/locate/jinorgbio

Cis-[RuCl(BzCN)(N–N)(P–P)]PF_6 complexes: Synthesis and in vitro antitumor activity (BzCN = benzonitrile; N–N = 2,2′-bipyridine; 1,10-phenanthroline; P–P = 1,4-bis(diphenylphosphino) butane, 1,2-bis(diphenylphosphino)ethane, or 1,1′-(diphenylphosphino)ferrocene)

Flávia de C. Pereira [a], Benedicto A.V. Lima [b], Aliny P. de Lima [a], Wanessa C. Pires [a], Thallita Monteiro [a], Lorena F. Magalhães [a], Wanderson Costa [a], Angélica E. Graminha [b], Alzir A. Batista [b,*], Javier Ellena [c], Elisângela de P. Siveira-Lacerda [a,*]

[a] Laboratory of Molecular Genetics and Cytogenetics, Institute of Biological Sciences, Federal University of Goiás – UFG, Goiânia, GO CEP 74001-970, Brazil
[b] Department of Chemistry, Federal University of São Carlos, São Carlos, SP CEP 13.565-905, Brazil
[c] São Carlos Institute of Physics, University of São Paulo, São Carlos, SP CEP 13560-970, Brazil

ARTICLE INFO

Article history:
Received 21 November 2014
Received in revised form 18 March 2015
Accepted 20 March 2015
Available online xxxx

Keywords:
Ruthenium complexes
Sarcoma 180
Apoptosis induction
Expression of pro-apoptotic genes
Chemotherapeutic agent

ABSTRACT

The motivation to use ruthenium complexes in cancer treatment has led our research group to synthesize complexes with this metal and test them against several types of tumor cells, yielding promising results. In this paper the results of biological tests, assessed by the MTT (3-(4,5-dimethylthiazol-2-yl)-2,5-diphenyltetrazolium bromide) assay, were carried out on the complexes *cis*-[RuCl(BzCN)(bipy)(dppe)]PF_6 (**1**), *cis*-[RuCl(BzCN)(bipy)(dppb)]PF_6 (**2**), *cis*-[RuCl(BzCN)(bipy)(dppf)]PF_6 (**3**) and *cis*-[RuCl(BzCN)(phen)(dppb)]PF_6 (**4**) which are described [BzCN = benzonitrile; bipy = 2,2′-bipyridine; phen = 1,10-phenanthroline; dppe = 1,2-bis(diphenylphosphino) ethane; dppb = 1,4-bis-(diphenylphosphino)butane; dppf = 1,1′-bis(diphenylphosphino)ferrocene]. The present study is focused on the cytotoxic activity of complexes (**1**)–(**4**) against four tumor cell lines and on the apoptosis and changes in the cell cycle and gene expression observed in the sarcoma 180 (S180) tumor cell line treated with complex (**1**). The results demonstrated that this complex inhibits S180 cell growth, with an IC_{50} of 17.02 ± 8.21 μM, while exhibiting lower cytotoxicity (IC_{50} = 53.73 ± 5.71 μM) towards lymphocytes (normal cells). Flow cytometry revealed that the complex inhibits the growth of tumor cells by inducing apoptosis as evidenced by an increase in the proportion of cells positive for annexin V staining and G0/G1 phase cell-cycle arrest. Further investigation showed that complex (**1**) induces a drop in the mitochondrial membrane potential and provokes a decrease in Bcl-2 protein expression and increase in caspase 3 activation, while the increased activation of caspase 8 caused a decrease in the gene expression in caspases 3 and 9. Increases in Tp53 and Bax expressions were also observed.

1. Introduction

Chemotherapy based on transition metal compounds became a promising research area after the discovery of cisplatin by Barnett Rosenberg [1]. Cisplatin is a chemotherapeutic drug used to treat carcinomas of the ovary, testis, bladder, head and neck [2]. However, because of the high toxicity, tumor resistance and other side effects of cisplatin and its derivatives, a search for more effective and less toxic antitumor metallodrugs began. In this context, ruthenium complexes are considered very promising, primarily because of their relatively low toxicity and high antitumor activity [3,4]. Ruthenium has the ability to mimic iron in its binding and transferring properties, and this is the most likely reason for its low toxicity. Such low toxicity allows the drug to be administered to the patient at a higher dose for a longer period, leading to more efficient antineoplastic chemotherapy.

NAMI, ImH[*trans*-$RuCl_4$(DMSO)(Im)] (Im = imidazole) and InH [*trans*-$RuCl_4(In)_2$] (In = indazole) have successfully completed phase II clinical trials for the treatment of metastatic tumors and colon cancers, respectively, but both have limitations as antitumor drugs [5]. Few studies have been performed on the anticancer activity of ruthenium (II) polypyridyl complexes [6–12]. Therefore, the potential use of ruthenium complexes for cancer treatment has motivated our research group to synthesize new ruthenium complexes of this class and to test them against a range of tumor cells, yielding promising results [13–19]. In this paper, we describe the results of biological studies of the complexes *cis*-[RuCl(BzCN)(bipy)(dppe)]PF_6 (**1**), *cis*-[RuCl(BzCN)(bipy)(dppb)]PF_6 (**2**), *cis*-[RuCl(BzCN)(bipy)(dppf)] PF_6 (**3**) and *cis*-[RuCl(BzCN)(phen)(dppb)]PF_6 (**4**) [BzCN = benzonitrile; bipy = 2,2′-bipyridine;

* Corresponding authors.
E-mail addresses: daab@ufscar.br (A.A. Batista), silveiralacerda@gmail.com (E.P. Siveira-Lacerda).

http://dx.doi.org/10.1016/j.jinorgbio.2015.03.011
0162-0134/

Please cite this article as: F.C. Pereira, et al., *Cis*-[RuCl(BzCN)(N–N)(P–P)]PF_6 complexes: Synthesis and in vitro antitumor activity..., J. Inorg. Biochem. (2015), http://dx.doi.org/10.1016/j.jinorgbio.2015.03.011

phen = 1,10-phenanthroline; dppe = 1,2-bis(diphenylphosphino)ethane, dppb = 1,4-bis-(diphenylphosphino)butane; dppf = 1,1′-bis(diphenylphosphino)ferrocene]. Diphosphines were chosen as ligands due to their ability to stabilize Ru(II) complexes, as well as their π acceptor properties, and the diimines can assist complex intercalation with DNA. The benzonitrile ligand was introduced into the complexes to make them anionic, and thus more soluble in the cell culture medium.

Thus, considering that complex (**1**) presented better selectivity indexes, among all four complexes, against all the tumor cells studied here, it was selected for other additional biological experiments.

2. Material and methods

2.1. Chemicals

The reactions were carried out under an atmosphere of purified argon using the standard Schlenk technique. Reagent grade solvents were appropriately distilled and dried before use. All chemicals used in this study were purchased from Aldrich. The starting complexes, *cis*-[$RuCl_2$(dppb)(bipy)], *cis*-[$RuCl_2$(dppf)(bipy)], *cis*-[$RuCl_2$(dppb)(phen)] and *cis*-[RuCl(BzCN)(bipy)(dppe)]PF_6, were prepared using the methods described in the literature [19]. The syntheses of the complexes *cis*-[RuCl(BzCN)(bipy)(dppb)]PF_6, *cis*-[RuCl(BzCN)(bipy)(dppf)]PF_6 and *cis*-[RuCl(BzCN)(phen)(dppb)]PF_6 were published elsewhere [20,21].

2.2. Synthesis

The syntheses of complexes *cis*-[RuCl(BzCN)(P–P)(N–N)]PF_6 (N–N = bipy or phen, P–P = dppb or dppf, and BzCN) were performed as described in reference [21], by allowing the corresponding *cis*-[$RuCl_2$(P–P)(N–N)] precursor, dissolved in CH_2Cl_2, to react with a threefold excess of BzCN, using KPF_6, in methanol, under an argon atmosphere. Typically, *cis*-[RuCl(BzCN)(dppe)(bipy)]PF_6, was synthesized from *cis*-[$RuCl_2$(bipy)(dppe)]PF_6 (0.10 mmol), which was dissolved in 40 mL CH_2Cl_2, with an excess of benzonitrile (21 μL, 0.20 mmol). KPF_6 (27.70 mg, 0.15 mmol) was dissolved in ca. 5 mL methanol, and added to the ruthenium solution and then stirred for 24 h under an argon atmosphere. The volume of the solution was reduced to approximately 2 mL and diethyl ether (15 mL) was added to precipitate the product, which was filtered off and washed with water (2 × 10 mL) and diethyl ether (2 × 5 mL). The yield was 90%. Crystals suitable for determining the X-ray structure of the species *cis*-[RuCl(BzCN)(bipy)(dppe)]PF_6 were produced from the CH_2Cl_2/Et_2O solution, by slow evaporation. Microanalysis of *cis*-[RuCl(BzCN)(bipy)(dppe)]$PF_6 \cdot 2H_2O$: Found/calc. (%): C, 52.98/52.96; H, 4.53/4.23; N, 4.19/4.30; ^{1}H NMR data [400 MHz, $(CD_3)_2CO$]: δ 9.40 ppm (1 H, m; bipy); 8.63 ppm (1 H, d, J = 8.4 Hz; bipy); 8.49 ppm (2 H, t, J = 9.2 Hz; Ph); 8.36–8.28 ppm (2 H, m; bipy); 8.25–8.18 ppm (2 H, m; Ph); 7.86 ppm (1 H, t, J = 6.4 Hz; bipy); 7.81–7.71 ppm (1 H, bipy; 3 H, Ph, m); 7.65 ppm (1 Hp, t, J = 7.3 Hz; BzCN); 7.50–7.37 ppm (8 H, m, Ph); 7.31 ppm (2 Ho, dd, J = 8.0 and 2.4 Hz, BzCN); 7.20 ppm (1 H, m, bipy); 7.12 ppm (1 H, m, bipy); 6.97 ppm (2 Hm, dt, J = 7.8, 1.6 Hz BzCN); 6.82–6.75 ppm (2 H, t, J = 8.8; Ph); 6.68–6.62 ppm (1 H, m; Ph); and 2.95–2.79 ppm (br m, 4 H, CH_2CH_2).

The synthesis of *cis*-[RuCl(BzCN)(dppb)(bipy)]PF_6 was performed in the same way as the complex with the dppe ligand. In this case, the yield was 92%. Microanalysis of *cis*-[RuCl(BzCN)(bipy)(dppb)]$PF_6 \cdot H_2O$: Found/calc. (%): C, 54.39/54.86; H, 4.73/4.40; N, 4.45/4.26; RMN ^{1}H (400 MHz, $(CD_3)_2CO$): δ 9.05 ppm (1 H, m; bipy); 8.87 ppm (1 H, d, J = 6.0 Hz; bipy); 8.40 ppm (2 H, t, J = 8.4 Hz; Ph); 8.31 ppm (1 H, d, J = 8.0 Hz; bipy); 8.12 ppm (2 H, m; Ph); 8.00–7.85 ppm (2 H, bipy; 3 H, Ph, m); 7.73 ppm (1 H, t, J = 6.0 Hz, bipy); 7.54 ppm (1 Hp, t, J = 7.4 Hz, BzCN); 7.40–7.31 ppm (5 H, m, Ph); 7.20 ppm (2 Ho, dd, J = 7.9 Hz, BzCN); 7.08 ppm (1 H, t, J = 7.2 Hz, bipy); 7.00 ppm (1 H, t, J = 7.2 Hz, bipy); 6.77 ppm (2 Hm, dt, J = 7.6, 1.5 Hz BzCN); 6.32 ppm (2 H, t, J = 8.8; Ph); 2.40–2.00 ppm (br, m, 4 H, $CH_2(CH_2)_2CH_2$); and 1.43–1.54 ppm (br m, 4 H, $CH_2(CH_2)_2CH_2$).

2.3. Apparatus

C, H and N contents were recorded in a Fisons EA1108 Instrument CHNS/O elemental analyzer at the Microanalytical Laboratory at the Federal University of São Carlos (São Carlos, Brazil). The IR spectra of the complexes were recorded in a FTIR Bomem-Michelson 102 spectrometer in the 4000–200 cm^{-1} region, using solid samples pressed in CsI pellets. The electronic spectra were recorded in a Hewlett-Packard diode array model 8452A spectrophotometer. $^{31}P\{^1H\}$ NMR experiments were performed using a BRUKER 9.4 T spectrometer (400 MHz for hydrogen frequency), in CH_2Cl_2, using a capillary containing D_2O. The circular dichroism (CD) spectra were recorded using a JASCO 720 spectropolarimeter.

2.4. X-ray crystallography

The crystals of the isolated complexes were grown by slow evaporation of dichloromethane/diethyl ether solutions. One of these crystals was mounted in an Enraf-Nonius Kappa-CCD diffractometer with graphite monochromated Mo Kα (λ = 0.71073 Å) radiation. The final unit cell parameters were based on all reflections. Data were collected with the COLLECT program [22]. The integration and scaling of the reflections were performed using the HKL Denzo-Scalepack computer package [23]. Gaussian absorption corrections were carried out [24]. The structures were solved by direct methods with SHELXS-97 [25]. The models were refined by full-matrix least squares on F^2 by means of SHELXL-97 [25]. All hydrogen atoms were stereochemically positioned and refined with the riding model. The ORTEP molecular structure shown in Fig. 1 was prepared with ORTEP-3 for Windows [26]. The data were collected and some experimental details are summarized in Table 1.

2.5. Cell culture

S180 (mouse sarcoma), DU145 (prostate cancer), K562 (chronic myeloid leukemia) and A549 (lung cancer) cells were obtained from the Rio de Janeiro Cell Bank (RJ, Brazil). The cells were cultured in RPMI 1640 or DMEM medium (pH 7.2–7.4), supplemented with 100 μm L^{-1} penicillin G, 100 μg mL^{-1} streptomycin, 2 mM L-glutamine, 1.5 g L^{-1} sodium bicarbonate, 10 mM HEPES [4-(2-hydroxyethyl)1-piperazineethanesulfonic acid] and 10% fetal bovine serum (FBS) (all reagents were obtained from Gibco, Grand Island, NY) at 37 °C under a 5% CO_2, humidified atmosphere. Human peripheral blood mononuclear cells (PBMCs) were collected from healthy volunteers aged 20–30 years with no history of smoking, drinking or chronic drug use. The PBMCs were isolated by density gradient centrifugation of heparinized blood on Lymphoprep (Nycomed, Oslo, Norway), washed three times with Hank's balanced salt solution (Sigma Chemical, St. Louis, MO, USA), counted, suspended in RPMI 1640 medium (Gibco, Invitrogen, Carlsbad, CA, USA), supplemented with 10% fetal bovine serum (Gibco), and incubated (37 °C, 5% CO_2) for 24 h before the drug treatment [27].

The protocol (043/2007) for these experiments was approved by the Ethics Committee of the Federal University of Goiás and, prior to joining the study, all blood donors signed an informed consent form.

2.6. Cytotoxicity assays

The effects of the complexes on the viability of S180, DU145, K562, A549 and lymphocyte cells were studied using the MTT [3-(4,5-dimethylthiazol-2-yl)-2,5-diphenyltetrazolium bromide] assay as described previously [28]. In brief, 1.0 × 10^5 S180, DU145, K562, A549 or lymphocyte cells were plated in 96-well tissue culture plates and treated with

Please cite this article as: F.C. Pereira, et al., *Cis*-[RuCl(BzCN)(N–N)(P–P)]PF_6 complexes: Synthesis and in vitro antitumor activity..., J. Inorg. Biochem. (2015), http://dx.doi.org/10.1016/j.jinorgbio.2015.03.011

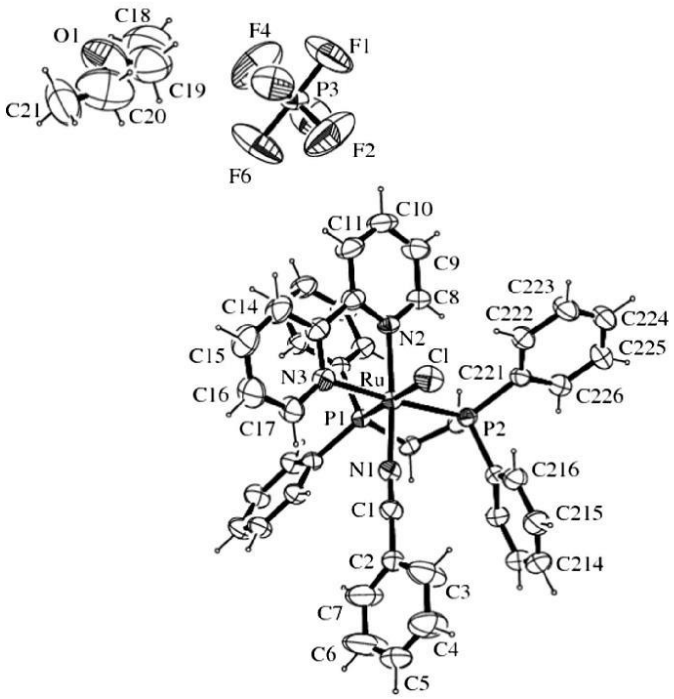

Fig. 1. ORTEP structure of *cis*-[RuCl(BzCN)(bipy)(dppe)]PF_6·0.75$C_4H_{10}O$, showing the atom labels and 50% probability ellipsoids: Ru–P1 = 2.2775(9) Å; Ru–P2 = 2.3096(10) Å; Ru–N3 = 2.128(3) Å; Ru–N2 = 2.079(3) Å; Ru–Cl = 2.4336(10) Å; Ru–N1 = 2.022(3) Å; N1–C1 = 1.140(5) Å; O(1)–C(19) = 1.239(17) Å; O(1)–C(20) = 1.360(15) Å; P–Ru–P = 84.84(3)°; and Cl–Ru–N≡C = 86.40(9)°.

various concentrations of the ruthenium (II) complex (0.2, 2, 20, 50, 100 and 200 μM) for 48 h. After treatment, 10 μL of MTT (5 mg mL^{-1}) was added to each well, and the plates were incubated at 37 °C for another 3 h. The formed purple formazan crystals were dissolved in 50 μL of SDS, and the absorbance was determined at 565 nm with a Stat Fax 2100 microplate reader (Awareness Technology, Palm City, FL, USA). The cell viability was calculated as follows: Viability (%) = (absorbance of the treated wells) / (absorbance of the control wells) × 100. Each concentration was tested in triplicate. The IC_{50} (the compound concentration that produces a 50% reduction in cell viability) was extracted from the dose–response curves by GraphPad Prism 4.02 for Windows (GraphPad Software, San Diego, CA, USA). After screening the ruthenium complexes, the best compound was taken as the one that exhibited the lowest IC_{50} for the tumor strains, relative to that of the healthy cells (PBMCs), and other tests on the cell death mechanism were applied to this complex. The cytotoxicity was assessed in terms of the selectivity index (SI) for each ruthenium(II) complex and cisplatin, with the following formula: SI = IC_{50} [non-tumor cells] (PBMCs)/IC_{50} [tumor cells]; the compound was considered significant at SI ≥ 2.0 [29].

Table 1
Crystallographic data for complex *cis*-[RuCl(BzCN)(bipy)(dppe)]PF_6.

Empirical formula	$[RuC_{43}H_{37}N_3P_2Cl]PF_6$·0.75($C_4H_{10}O$)
Formula weight	994.78
Temperature/wavelength	293(2) K/0.71073 Å
Crystal system	Monoclinic
Space group	$P2_1/c$
Unit cell dimensions	a = 16.4610(2) Å b = 17.2827(2) Å, β = 98.408(1)° c = 16.5738(2) Å
Volume/Z	4664.41(10) $Å^3$/4
Density (calculated)	1.417 mg/m^3
Absorption coefficient	0.557 mm^{-1}
F(000)	2030
Crystal size	0.26 × 0.38 × 0.15 mm^3
Theta range for data collection	3.02 to 25.68°
Index ranges	$-20 \le h \le 20, -20 \le k \le 21, -19 \le l \le 20$
Reflections collected	32,036
Independent reflections	8831 [R(int) = 0.0534]
Completeness to theta = 25.35°	99.6%
Max. and min. transmission	0.939 and 0.819
Data/restraints/parameters	8831/1/559
Goodness-of-fit on F^2	1.038
End R indices [I > 2σ(I)]	R1 = 0.0493, wR2 = 0.1391
R indices (all data)	R1 = 0.0671, wR2 = 0.1511
Largest diff. peak and hole	0.639 and −0.563 e·$Å^{-3}$

In this work the *cis*-[$RuCl_2$(P–P)(N–N)] precursors were not used because their solubility in the cell culture medium is much less than that of the complexes with the general formula [RuCl(BzCN)(N–N)(P–P)]PF_6, in the same medium.

2.7. Analyzing the cell cycle by flow cytometry

The possible effect of a ruthenium complex on cell-cycle progression was investigated after treating the S180 cells for 24 and 48 h with 24 μM *cis*-[RuCl(BzCN)(bipy)(dppe)]PF_6 (**1**). In brief, 5.0 × 10^5 cells were harvested by centrifugation, washed with PBS, fixed with 70% (v/v) cold aqueous ethanol and stored overnight at −20 °C. The fixed cells were

Please cite this article as: F.C. Pereira, et al., *Cis*-[RuCl(BzCN)(N–N)(P–P)]PF_6 complexes: Synthesis and in vitro antitumor activity..., J. Inorg. Biochem. (2015), http://dx.doi.org/10.1016/j.jinorgbio.2015.03.011

washed with PBS and incubated with propidium iodide (PI; Sigma-Aldrich, St. Louis, MO, USA) containing 0.05% RNase. The samples were incubated at 4 °C in the dark and analyzed by flow cytometry (FACSCalibur, BD Biosciences, San José, CA, USA). The percentage of cells in phases sub-G1, G0/G1, S, and G2/M was analyzed using the ModFit LT software (Verity Software House, Topsham, ME, USA) [30].

2.8. Detection of apoptosis with annexin V binding assay

Apoptosis-mediated cell death and necrosis were distinguished by means of double-labeling assays. After treating the cells with complex (**1**), S180 cells were examined using a FITC (fluorescein isothiocyanate)-labeled annexin V/propidium iodide (PI) apoptosis detection kit (BD Biosciences), following the manufacturer's instructions. In brief, the S180 cells were first treated with 24 μM *cis*-[RuCl(BzCN)(bipy)(dppe)]PF_6 for 24 and 48 h. A total of 5.0×10^5 cells were then harvested by centrifugation and washed with PBS. The cells were than suspended in a 400 μL binding buffer and 5 μL of annexin V-FITC and 3 μL of PI solutions were added. Flow cytometry was performed immediately after supravital staining. Data were acquired directly from the flow cytometer (FACSCalibur, BD Biosciences, Franklin Lakes, NJ), and analyzed online using the Cell Quest software. The positive criteria for cells in the early stages of apoptosis were Annexin V-positive and PI-negative, whereas cells in the late apoptosis were both Annexin V-positive and PI-positive [31]. Cells positive for Annexin V were stained fluorescent green and those positive for PI, red.

2.9. Detecting the mitochondrial membrane potential ($\Delta\Psi m$)

The dual emission dye, called JC 1, was used to measure $\Delta\Psi m$ by previously described methods [32]. In brief, 3.0×10^5 S180 cells treated as above with 24 μM of complex (**1**) were incubated for 15 min with 2.5 mg mL^{-1} JC 1 (dissolved in DMSO) at 37 °C, with 5% CO_2, in the dark. After centrifugation for 5 min at 200 ×*g*, the cells were washed twice with PBS at 4 °C, suspended in 5 mL of PBS and analyzed in a FACSCalibur flow cytometer. JC 1 is a lipophilic ionic fluorescence dye, capable of selectively entering the mitochondria, which change color from red (FL-2) to greenish (FL-1) when the $\Delta\Psi m$ declines. The data were analyzed using Cell Quest, and the value output represents the proportion of cells with depolarized mitochondria.

2.10. Assaying caspase-3, 8 and 9 activities

Caspase 3, 8, and 9 activities were measured using an ApoTarget Caspase-3, 8, and 9 Protease Assay kit (Invitrogen), following the manufacturer's recommendations. After treating the S180 cells with 24 μM *cis*-[RuCl(BzCN)(bipy)(dppe)]PF_6 for 24 h, they were lysed with a chilled cell lysis buffer. The protein concentration was then measured using a BSA Protein Assay Kit (BioRad). An aliquot of the protein extract (75 μg) was mixed with 50 μL of 2× reaction buffer supplemented with 10 mM DTT (dithiothreitol) and the substrates DEVD-pNA (caspase-3), IETD-pNA (caspase-8) or LEHD-pNA (caspase-9). The mixtures were then incubated for 2 h at 37 °C. The formation of p-nitroanilide in the samples was subsequently measured in an ELISA (enzyme-linked immunosorbent assay) microplate reader set at 405 nm. The increases in caspase-3, caspase-8, and caspase-9 activities were determined by comparing the results with the control.

2.11. Analyzing Bcl-2 protein expression by flow cytometry

After treating the S180 cells with 24 and 48 μM of complex (**1**) for 24 h, the cells were transferred to a flow cytometry tube, and centrifuged at 1800 rpm for 3 min. The supernatant was discarded, and the cells were washed with 1× PBS (phosphate buffered saline) and centrifuged again. After the supernatant was discarded again, the cells were suspended in 500 μL of the lysis buffer for 10 min at room temperature (20 °C to 30 °C). The cells were centrifuged once more and the supernatant was removed. 500 μL of permeabilization solution was then added for 10 min, and the cells were centrifuged again and the supernatant discarded. The cells were then washed with a BSA (bovine serum albumin) buffer [1× PBS, 0.5% FBS (fetal bovine serum) and 0.1% sodium azide] and centrifuged and the supernatant was discarded. 20 μL of the Bcl-2 reagent was added and the tube was mixed and incubated for 30 min at room temperature (20 °C to 30 °C). Finally, the cells were centrifuged, the supernatant was discarded, and the cells were washed again with BSA, centrifuged and resuspended in 500 μL BSA and analyzed immediately.

2.12. Total RNA extraction and cDNA synthesis

The S180 cells were treated with 24 μM of *cis*-[RuCl(BzCN)(bipy)(dppe)]PF_6 for 3, 6 and 12 h. The total RNA was extracted with trizol reagent (Sigma-Aldrich, USA), following the manufacturer's protocol (Sigma or Applied Biosystems, USA). 2.0 μg of this RNA was then used to produce complementary DNA (cDNA), with random primers (Applied Biosystems, USA) in a 20 μL reaction mixture, as recommended by the manufacturer. The cDNA was analyzed in real-time quantitative PCR to estimate the expression of genes involved in apoptosis.

2.13. Real-time quantitative PCR

Real-time PCR was performed in a Line Gene K (Bioer Technology) instrument. Real-time PCR reactions were performed in a 20 μL reaction mixture, including 2 μL of cDNA, 10 μL of SYBR Green PCR Master Mix (LGC Biotechnology, UK), and 2.0 μL of 400 nM forward and reverse primers for sequences of genes Bax, caspases (3, 8 and 9) and Tp53. The PCR program was initiated at 95 °C for 15 min, followed by 40 cycles of 95 °C for 15 s, 55 °C for 15 s and 72 °C for 30 s. The data were analyzed by the comparative threshold cycle (CT) method and normalized to the β-actin reference gene expression in each sample. The primer sequences are shown in Table 2.

2.14. Statistical analysis

The results were analyzed using one-way ANOVA (analysis of variance) followed by the Tukey's test or Dunnett's test package for multiple comparisons with a control. All statistical analysis was performed using the statistical GraphPad Prism package. A probability of 0.05 or less was deemed statistically significant. The following notation was used throughout the analysis: $^*p < 0.05$ and $^{**}p < 0.01$, relative to the control.

3. Results and discussion

Complexes (**1**)–(**4**) were synthesized as described in the Material and methods section, according to Scheme 1. In our previous work, it was shown that initially the entering ligand (BzCN) is *trans* to a

Table 2
Primer sequences used for the RT-PCR assay.

Gene	Primer sequences
β-Actin	F5′CACACCCGCCACCAGTTC3′ R5′ATTCCCACCATCACACCCTG3′ (161 bp)
Bax	F5′GCTACAGGGTTTCATCCAGC3′ R5′GGAGACACTCGCTCAGCTTC3′ (113 bp)
Caspase 3	F5′GGAGCTTGGAACGCTAAGAA3′ R5′GTCCACTGACTTGCTCCCAT3′ (112 bp)
Caspase 8	F5′AGGTACTCGGCCACAGGTTA3′ R5′TGGGATGTAGTCCAAGCACA3′ (137 bp)
Caspase 9	F5′TAGCTGGAACACTGGGCATTGAGT3′ R5′AACATACCCATCGGTGCATTTGGC3′ (146 pb)
Tp53	F5′TGGAAGACTCCAGTGGGAAC3′ R5′TCTTCTGTACGGCGGTCTCT3′ (87 pb)

Please cite this article as: F.C. Pereira, et al., *Cis*-[RuCl(BzCN)(N–N)(P–P)]PF_6 complexes: Synthesis and in vitro antitumor activity..., J. Inorg. Biochem. (2015), http://dx.doi.org/10.1016/j.jinorgbio.2015.03.011

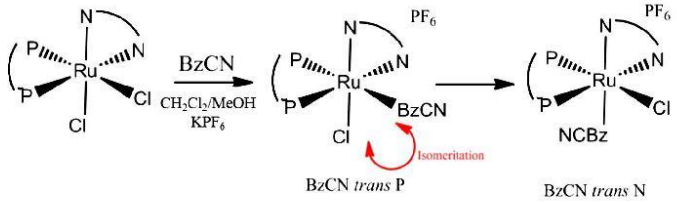

Scheme 1. Route for the synthesis of complexes (**1**)–(**4**) (P–P = diphosphines; N–N = diimines).

phosphorus atom, which isomerizes to the final position, *trans* to a nitrogen [21].

The $^{31}P\{^1H\}$ NMR spectrum of the *cis*-[RuCl(BzCN)(bipy)(dppe)]PF_6 complex, in CH_2Cl_2 solution, exhibits two doublets [66.2 and 58.4 ppm; $^2J_{P-P}$ (Hz) = 17.8 Hz], showing that the two phosphorus atoms in the dppe ligand are magnetically different, as expected from the X-ray structure. The stability of the complexes, dissolved in trizma hydrochloride solution (Sigma-Aldrich, USA), and 3% of DMSO, was tested using the $^{31}P\{^1H\}$ NMR technique, and they are shown to be stable for at least 48 h.

The X-ray structure of *cis*-[RuCl(BzCN)(bipy)(dppe)]PF_6 (**1**) is illustrated in Fig. 1. The bond lengths and angles of this species are similar to those reported for similar complexes, *cis*-[RuCl(BzCN)(bipy)(dppf)]PF_6 (**3**) and *cis*-[RuCl(BzCN)(phen)(dppb)]PF_6 (**4**), previously published by us [21].

In all four complexes under study, the benzonitrile ligand is *trans* to one nitrogen (N2), of the diimine. The bond lengths of Ru–N for the nitrogen *trans* to the phosphorus atom (P2) are longer than the distance between Ru and the nitrogen *trans* to the cyano group, as a consequence of the strong *trans* effect of the phosphorus atoms. For the *cis*-[RuCl(BzCN)(bipy)(dppe)]PF_6 complex, the Ru–N3 and Ru–N2 distances are 2.128(3) Å and 2.079(3) Å, respectively (see Fig. 1).

3.1. Cytotoxicity assay

The cytotoxicity of the four complexes, for four different tumor cell lines, S180 (mouse sarcoma S180), DU145 (prostate cancer), K562 (chronic myeloid leukemia) and A549 (lung), and for PBMCs (human peripheral blood mononuclear cells) from healthy adults, was assayed by observing cell survival after 48 h of exposure to the desired concentration range (0.2–200 μM) of MTT [20]. The resulting IC_{50} and SI values are listed in Table 3.

These compounds have a variety of phosphine ligands coordinated to the ruthenium atom, and the results indicated a significant difference in their activity. As can be seen in Table 3, the complexes, in general, showed good cytotoxicity for all four tumor cell lines tested. The selectivity indexes (SIs) indicate selectivity of the observed cytotoxicity against tumor lines and thus suggest in vivo preclinical and clinical testing of complexes. The cytotoxicity of the complexes studied here, against DU 145 tumor cells, are better than that presented by Ru(II)/diphosphine/diimine complexes with the general formula [Ru(AA-H)(bipy)(dppb)]PF_6 (AA = amino acids), probably due to their higher solubility in water [32,33]. In particular, complex (**1**) has a good selectivity index of 3, for S180 cells. The better activity of complex (**1**), when compared with the others can be due the presence of 1,2-bis(diphenylphosphine)ethane, a small species, in its structure. Thus, the complex *cis*-[RuCl(BzCN)(bipy)(dppe)]PF_6 was assessed for its possible mechanism of cell death in S180 tumor cells.

3.2. Analyzing the cell cycle by flow cytometry

The cell cycle phase distribution of S180 cells after treatment with a near-IC_{50} concentration of *cis*-[RuCl(BzCN)(bipy)(dppe)]PF_6 (24 μM) was examined by flow cytometry. The effect of this ruthenium complex on the S180 cell cycle was evident in the status of cells revealed by flow cytometry. In Fig. 2, histograms indicate the DNA quantity distribution. After 24 h of exposing S180 cells to (24 μM) *cis*-[RuCl(BzCN)(bipy)(dppe)]PF_6, there was an increase in the G0/G1 phase from 22% to 50% relative to the negative control ($p < 0.001$) and there was a 25% decrease in the S phase (Fig. 2A). The cell cycle distribution at 48 h showed a time-dependent 12% increase in the sub-G1 peak ($p < 0.01$). There was also an increase of 35% in the G2/M phase (Fig. 2B). This indicated that the antiproliferative mechanism induced by *cis*-[RuCl(BzCN)(bipy)(dppe)]PF_6 in S180 cells was G0/G1 and G2/M phase arrest and induction of apoptosis as observed in sub-G1 (Fig. 2C and D).

3.3. Detection of apoptosis using the annexin V binding assay

Apoptosis is a tightly regulated physiological process that is characterized by a series of biochemical events and ultra-structural alterations (e.g., the activation of caspases, phosphatidylserine (PS) externalization, membrane blebbing, cell shrinkage, nuclear fragmentation, chromatin condensation and chromosomal DNA fragmentation) [33]. In apoptotic cells, the membrane phospholipid (PS) is translocated from the inner face of the plasma membrane to the cell surface, where it can be detected by its avid binding to the cell protein annexin V, which is labeled with a fluorophore [34]. The annexin V assay is able to distinguish apoptotic cells from viable or necrotic cells on the basis of the resulting fluorescence of the PS-presenting cells. A simultaneous dead cell stain uses the fluorochrome propidium iodide, which can only penetrate dead cells that have lost or are losing membrane integrity. PI intercalates into DNA to produce a highly fluorescent adduct, which is indicative of late apoptosis or necrosis [35].

Table 3
The inhibitory concentration [IC_{50} (μM)] and selectivity indexes (SIs) of Ru(II) complexes against tumor cell lines and normal PBMCs. Data show means ± SD of three independent experiments.

Complex	IC_{50} (μM)					SIs			
	S180	DU145	K562	A549	PBMCs	S180	DU145	K562	A549
(**1**)	17.0 ± 8.2	7.2 ± 1.2	11.6 ± 5.7	20.0 ± 0.0	53.7 ± 5.7	3	8	5	3
(**2**)	13.8 ± 4.2	1.8 ± 1.0	9.8 ± 0.0	20.4 ± 0.7	10.5 ± 0.0	1	6	1	0.5
(**3**)	14.9 ± 3.1	10.0 ± 8.8	10.2 ± 1.1	38.3 ± 0.8	51.1 ± 0.0	3	5	5	1
(**4**)	8.9 ± 3.9	4.2 ± 0.3	4.4 ± 0.9	20.9 ± 0.1	17.2 ± 0.0	2	4	4	1

Please cite this article as: F.C. Pereira, et al., *Cis*-[RuCl(BzCN)(N–N)(P–P)]PF_6 complexes: Synthesis and in vitro antitumor activity..., J. Inorg. Biochem. (2015), http://dx.doi.org/10.1016/j.jinorgbio.2015.03.011

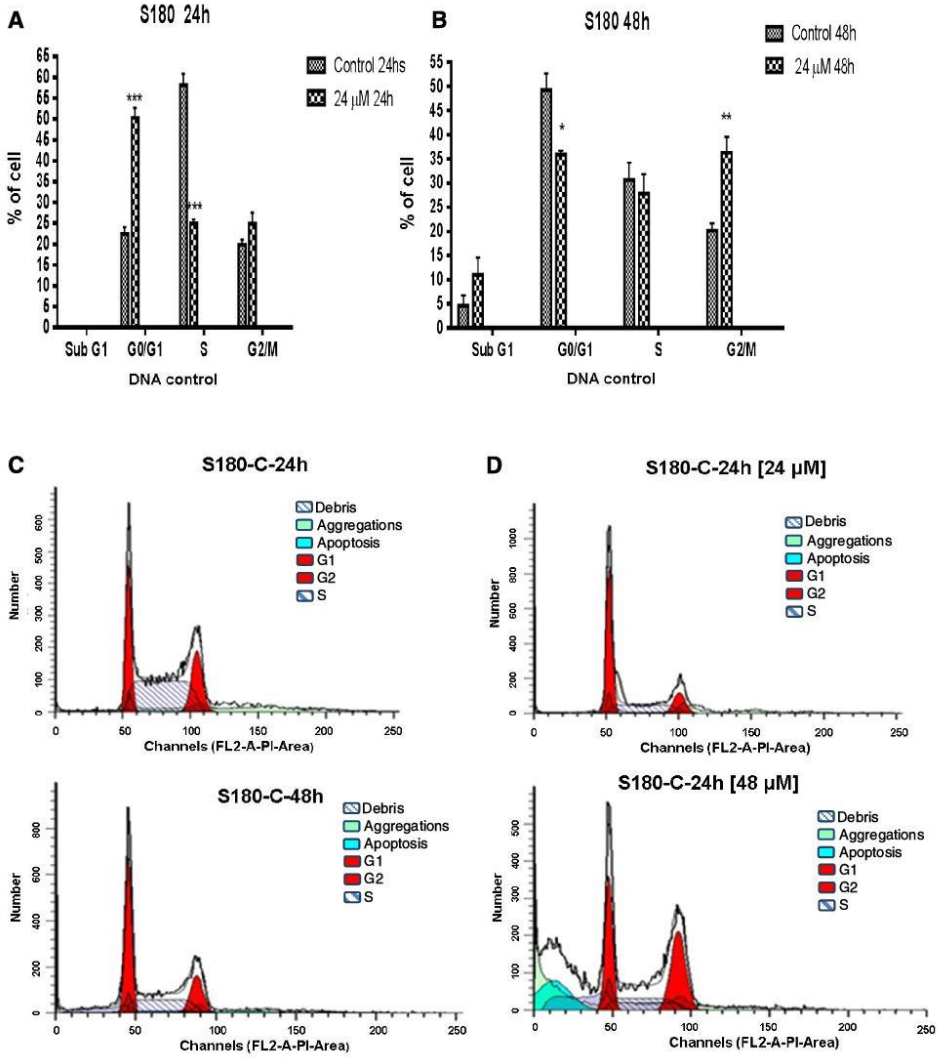

Fig. 2. (A, B) Cell-cycle status of the S180 cells after treatment with (24 μM) *cis*-[RuCl(BzCN)(bipy)(dppe)]PF_6 complex for 24 and 48 h. (C, D) Profile of PI fluorescence (x-axis) versus counts (y-axis) of cells in various phases (G0/G1, S, and G2/M). Data were analyzed with ModFit software (Becton Dickinson, San José, CA, USA). Data are the means ± SD of three experiments. Significant differences from the untreated control are indicated by p: *$p < 0.05$, **$p < 0.01$ and ***$p < 0.001$.

One of the main objective of this study was to determine whether *cis*-[RuCl(BzCN)(bipy)(dppe)]PF_6 induces apoptosis or necrosis in S180 cells, using annexin V-FITC/propidium iodine staining. As shown in Fig. 3A and B, after treating S180 cells with 24 μM of *cis*-[RuCl(BzCN)(bipy)(dppe)]PF_6 for 24 and 48 h, the cells in initial apoptosis (annexin V+ and PI−) represented 2.89% (24 h) and 5.06% (48 h) of the total number, and those in late apoptosis (annexin V+ and PI+) represented 32.56% (24 h) and 30.09% (48 h) ($p < 0.001$) of the total cells, respectively. The distribution of cells is shown in the dot plot in Fig. 3C. The results that showed the cytotoxic activity of *cis*-[RuCl(BzCN)(bipy)(dppe)]PF_6 in S180 cells may involve interaction with the DNA molecule, possibly leading to its cleavage during the apoptosis process.

3.4. Mitochondrial potential (JC 1)

Mitochondria control the energy supply of cells and decide the destiny (life or death) of them, since they control the apoptosis process [36]. The vital function of mitochondria is connected to the mitochondrial membrane potential ($\Delta\Psi m$), which is an essential component of

Please cite this article as: F.C. Pereira, et al., *Cis*-[RuCl(BzCN)(N–N)(P–P)]PF_6 complexes: Synthesis and in vitro antitumor activity..., J. Inorg. Biochem. (2015), http://dx.doi.org/10.1016/j.jinorgbio.2015.03.011

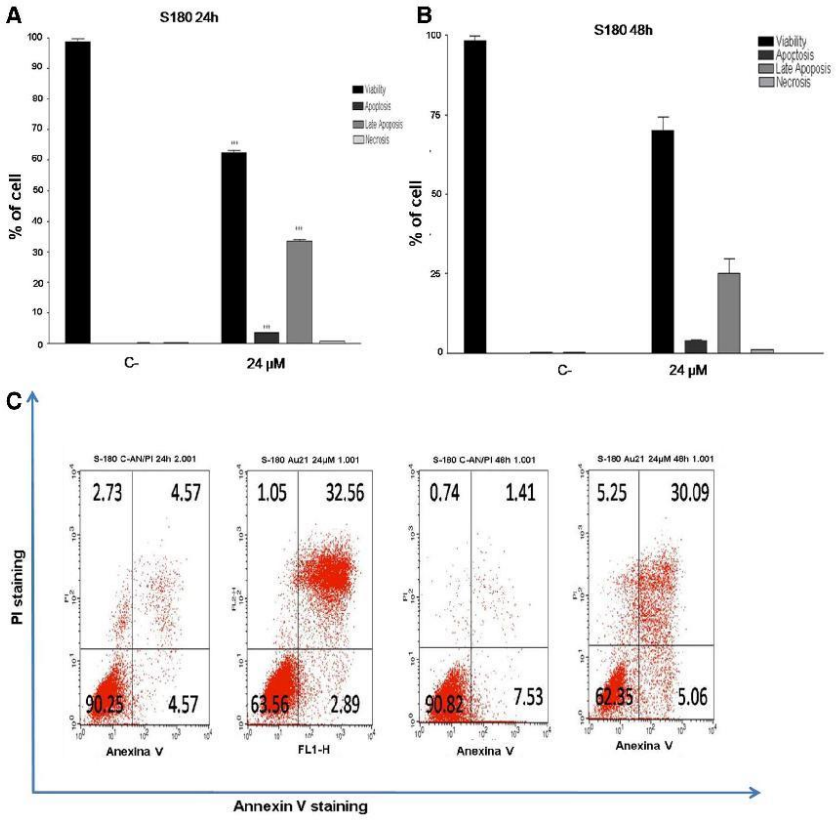

Fig. 3. Effects of *cis*-[RuCl(BzCN)(bipy)(dppe)]PF_6 on S180 cells. (A and B) The harvested cells were stained and washed with phosphate-buffered saline, and apoptosis was assayed with an annexin V-fluorescein isothiocyanate/PI assay kit in a double-labeling system for 24 and 48 h. (C) The effect of [RuCl(BzCN)(bipy)(dppe)]PF_6-induced apoptosis on S180 cells. The harvested apoptotic cells (annexin V+/PI+) were analyzed by flow cytometry, and the dot plot displays the annexin V fluorescence (x-axis, logarithmic scale) versus PI fluorescence (y-axis, logarithmic scale). Data are means ± SD of three experiments. Significant differences from the untreated control are indicated by ***$p < 0.001$.

respiration [37]. Alterations in the ΔΨm trigger apoptotic signals, which are crucial to the activation of the apoptotic paths [38]. Thus, the lowering of ΔΨm and the release of apoptotic factors are key elements that trigger the apoptotic process [38]. Studies show that several Ru(II) complexes can lead to a lowering of ΔΨm [39–41].

The JC 1 test was used to find out if *cis*-[RuCl(BzCN)(bipy)(dppe)]PF_6 leads to a low ΔΨm. JC 1 is a fluorescent dye that was used as an indicator of ΔΨm. JC 1 is a lipophilic cation and easily crosses the plasma membrane of the cells and aggregates in active mitochondria [42].

When there is a low ΔΨm, JC 1 begins to act as a monomer that emits green fluorescence. However, when ΔΨm is high, the dye is fixed to the cells and these aggregates induce a change from green to red fluorescence emission. This can be observed in the negative control in Fig. 4, with a higher emission of red (83%) than green fluorescence (17%), indicating the presence of normal mitochondrial activity.

After treating cell line S180 with 24 µM *cis*-[RuCl(BzCN)(bipy)(dppe)]PF_6, for 24 h, the emission of red fluorescence fell to 60% in the cells exposed to this complex, while the green fluorescence emission rose to 40% ($p < 0.0001$). This change from red to green fluorescence following exposure to the complex demonstrates a fall in the mitochondrial membrane potential (ΔΨm), indicating that *cis*-[RuCl(BzCN)(bipy)(dppe)]PF_6 induces apoptosis in cell line S180 through a mitochondrial pathway (Fig. 4).

3.5. Bcl-2 analysis by flow cytometry

After 24 h of exposure to complex (**1**), a Bcl-2 antibody marked with FITC was used as an indicator for the increase or decrease of Bcl-2 protein expression in the S180 cells. The Bcl-2 protein expression was altered after cells were exposed to 24 and 48 µM of *cis*-[RuCl(BzCN)(bipy)(dppe)]PF_6 for 24 h. In Fig. 5, peak M2 indicates the number of cells that showed active Bcl-2, while M1 is proportional to the number of cells that did not. The negative control exhibited active Bcl-2 (peak M2) in 5% of the cells of the S180 culture after 24 h. The Bcl-2 protein expression, after exposure to 24 µM *cis*-[RuCl(BzCN)(bipy)(dppe)]PF_6 for 24 h, was 2.5 times lower than the negative control and 28.5 times lower than the positive control (Bcl-2 C+). When the S180 cells were exposed to 48 µM *cis*-[RuCl(BzCN)(bipy)(dppe)]PF_6 for 24 h, there was a decrease of 5 times in the Bcl-2 active protein, compared to the negative control, and a decrease of 57 times, compared to the positive control ($p < 0.0001$) (Fig. 5).

Please cite this article as: F.C. Pereira, et al., *Cis*-[RuCl(BzCN)(N–N)(P–P)]PF_6 complexes: Synthesis and in vitro antitumor activity..., J. Inorg. Biochem. (2015), http://dx.doi.org/10.1016/j.jinorgbio.2015.03.011

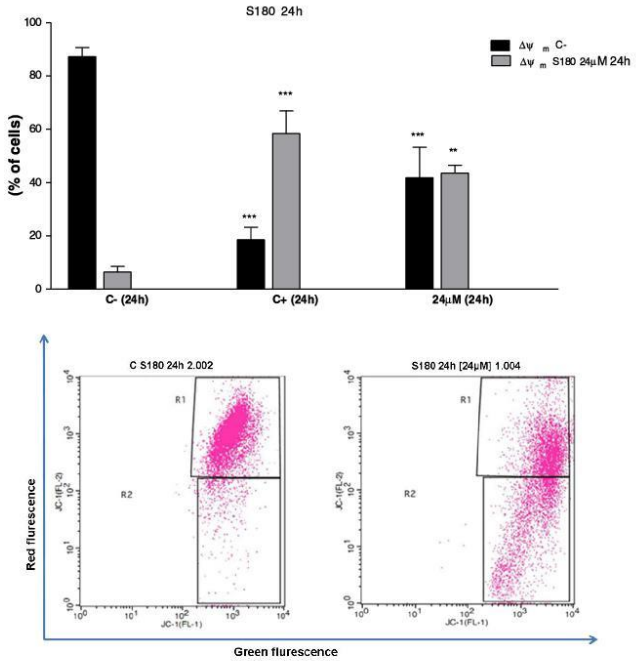

Fig. 4. Effects of *cis*-[RuCl(BzCN)(bipy)(dppe)]PF_6 on S180 cells; the ΔΨm was determined by means of the dye JC 1 (5,5c,6,6c-tetrachloro-1,1c,3,3c-tetraethylbenzimidazolylcarbocyanine iodide). Flow cytometric analysis of cells stained with membrane-permeable JC 1 dye revealed that [RuCl(BzCN)(bipy)(dppe)]PF_6 depolarized the mitochondrial membrane, as indicated by drop in FL2-H fluorescence, as analyzed by JC 1 flow cytometry. The number in each dot plot represents the percentage of cells that lost ΔΨm. Each experiment represents the means ± SD of two experiments. ***$p < 0.001$ compared with the control. (For interpretation of the references to color in this figure, the reader is referred to the web version of this article.)

3.6. Colorimetric caspase test

The effects of 24 μM *cis*-[RuCl(BzCN)(bipy)(dppe)]PF_6 on caspase-3, 8 and 9 activities were investigated in S180 cells, after 24 h of treatment (Fig. 6). As indicated by these results, the caspase 8 and caspase 9 activities did not change significantly from those in the untreated control cells. However, caspase-3 activity showed a significant enhancement, after the cells were incubated with the complex for 24 h, with a fivefold increase relative to the negative control.

The maximum enzyme induction (450% of basal level) was observed at 24 h in caspase-3. Thus, the complex *cis*-[RuCl(BzCN)(bipy)(dppe)]PF_6 activated caspase-3, which confirms triggering of the apoptotic process. Caspases can regulate activation or inhibition of the apoptotic process [43] and play an important role in the signaling system and in the apoptotic process itself. A large activation of caspase-3 was observed in the present study, as in many in vitro studies, showing that the Ru(II) complexes can activate the apoptotic pathway [44,45].

3.7. Real-time quantitative PCR

To understand more about the apoptosis induction mechanism provoked by complex (**1**), the expression levels of genes involved in the apoptotic process were investigated. The effects of the complex on the messenger RNA (mRNA) expression of Bax, Tp53, caspase-3, caspase-8 and caspase-9 were analyzed by real-time quantitative PCR. The mRNA expression of Bax after 3 h of exposure to the complex was not significantly different from the control, but it showed a slight increase. However, there was a significant increase (3.14 times) after 6 h of exposure to *cis*-[RuCl(BzCN)(bipy)(dppe)]PF_6 (Fig. 7). The Bax expression increased in 6 h time, at a concentration of 24 μM, but it did not increase in any concentration in 12 h time. The Tp53 expression increased in 3 h time, at a concentration of 24 μM, but showed a decrease in 6 h time, at the same concentration. The Tp53 expression increased in 6 h time only at the concentration of 48 μM.

Pro-apoptotic Bax/Bak genes are essential regulators of the mitochondrial or intrinsic apoptosis pathway [46,47]. In this intrinsic pathway, an increased level of Bax and/or a decreased level of Bcl-2 may permeabilize the mitochondria following DNA damage [47,48]. Induction of apoptosis by complex (**1**) caused a lower Bcl-2 expression, as observed in the flow cytometry experiment, leading to the translocation of Bax to the mitochondrial membrane within a 6 hour period of exposure.

The Tp53 expression increased by 22-fold when treated with 24 μM of compound (**1**), after 3 h of exposure, falling to less than 1-fold after 6 and 12 h of exposure. There was no gene expression when the cells were treated with 48 μM for 3 h of exposure, but after 6 h of exposure there was a 7-fold increase in the gene expression, compared to the negative control. After 12 h of exposure there was no gene expression, compared to the negative control. Approximately 50% of human cancers exhibit alterations in the Tp53 gene, which is a tumor suppressor. This gene is responsible for cell growth, for cell sensitivity to irradiation and for multiple chemotherapeutics [49–51]. A functional Tp53 gene can down-regulate Bcl-2, protecting the cells from apoptosis and allowing the cells to survive through a variety of fatal cell events [52]. The results obtained in this study show that complex (**1**) increased the expression of Tp53 after 3 h of exposure. This finding indicates a

Please cite this article as: F.C. Pereira, et al., *Cis*-[RuCl(BzCN)(N–N)(P–P)]PF_6 complexes: Synthesis and in vitro antitumor activity..., J. Inorg. Biochem. (2015), http://dx.doi.org/10.1016/j.jinorgbio.2015.03.011

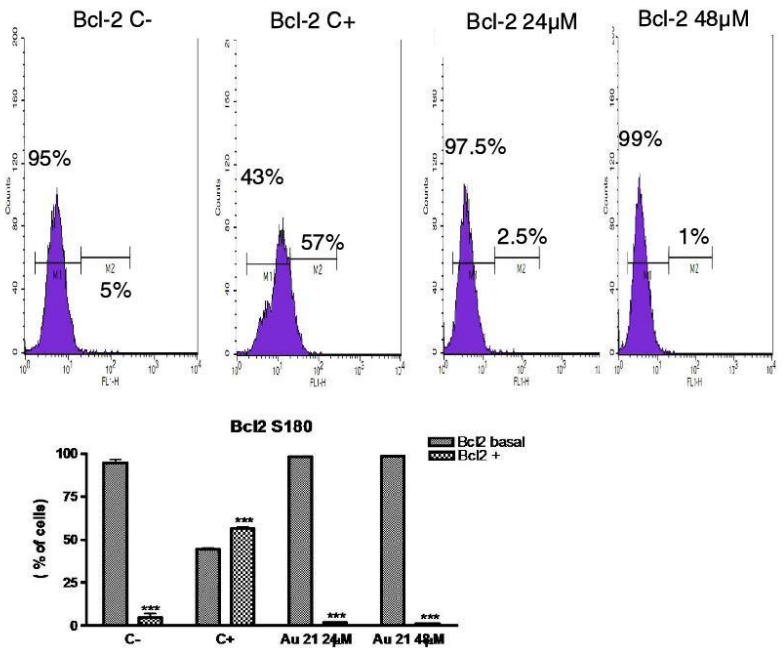

Fig. 5. Effects of 24 and 48 μM *cis*-[RuCl(BzCN)(bipy)(dppe)]PF_6 on the expression of Bcl-2 protein in S180 cells after 24 h of exposure. Data are for mean ± SD of experiments performed in triplicate. Significant differences from the untreated control are indicated by ***$p < 0.001$.

probable alteration in the DNA molecule that led to the translocation of Tp53 from the cytoplasm to the S180 cell nucleus, thereby inducing apoptosis.

Tp53 is a key suppressor of tumor regulators in the apoptosis process and has pro-apoptotic activity. Under stressful conditions, Tp53 is stabilized and acts as a transcription factor that can increase the expression of target pro-apoptotic genes such as Puma, Noxa, Bax and Bid [53]. Cytoplasmic Tp53 interacts with the members of the Bcl-2 and Bcl-xL families, which leads to the activation and translocation of Bax and Bid into the external mitochondrial membrane. Thus, in this study there was also an observable increase in the Bax expression with the Tp53 exposure with complex (**1**). In addition, Tp53 was also translocated to the mitochondria, activating the apoptosis by the mitochondria [53–55]. The apoptosis induced by complex (**1**) was observed in the increased expression of Bax, Tp53 and caspase 8.

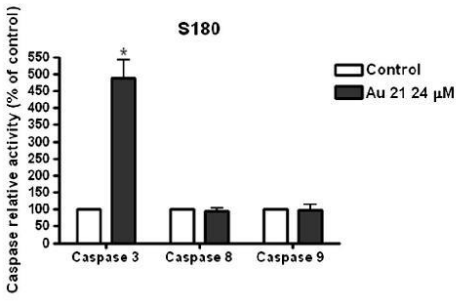

Fig. 6. Activation of caspase-3, -8 and -9 in S180 cells treated with 24 μM of *cis*-[RuCl(BzCN)(bipy)(dppe)]PF_6 for 24 h. Caspase activity was calculated as the percent in basal caspase-3, -8 and -9 activities in untreated S180 samples. Each column represents the means ± SD (error bar) of two experiments. *$p < 0.05$ compared to the control.

The expression of caspase 8 mRNA was twice as high as in the negative control 3 h after exposure to complex (**1**). Caspase-8 expression was not significant at 6 or 12 h after exposure, and caspase-9 was not significant at any time after exposure. This increased expression was retained after 6 h of exposure to the compound. The mRNA expression of caspase-3 was not significant after 6 or 12 h of exposure.

Many chemotherapeutic agents have shown to induce apoptosis in tumor cells [56,57]. The present results suggest that *cis*-[RuCl(BzCN)(bipy)(dppe)]PF_6 may be capable of inducing or repressing the expression of genes involved in the apoptosis process. In particular, it was observed that the complex induced the synthesis of the Tp53 protein, which acts in a pro-apoptotic manner [58]. These results are similar to those areno-organometallic ruthenium compounds, found in the literature [59]. The evidence suggests that cell death occurs by apoptosis after treatment with these chemotherapeutics, thus showing that this is an important mechanism in the cytotoxic action of these complexes [60]. This mechanism was observed specifically with the complex *cis*-[RuCl(BzCN)(bipy)(dppe)]PF_6, which significantly increased the expression of pro-apoptotic genes such as Bax.

The CD spectral technique is very sensitive for diagnosing changes in the secondary structure of DNA, resulting from small molecule–DNA interactions [61,62]. A typical CD spectrum of CT-DNA shows a maximum at 275 nm due to the base stacking and a minimum at 248 nm attributed to the right-handed helicity, a characteristic of the B conformation. In

Please cite this article as: F.C. Pereira, et al., *Cis*-[RuCl(BzCN)(N–N)(P–P)]PF_6 complexes: Synthesis and in vitro antitumor activity..., J. Inorg. Biochem. (2015), http://dx.doi.org/10.1016/j.jinorgbio.2015.03.011

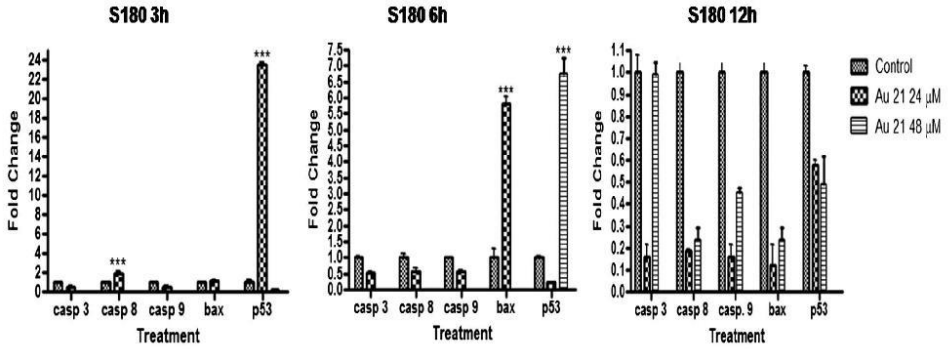

Fig. 7. Effects of *cis*-[RuCl(BzCN)(bipy)(dppe)]PF_6 on the expression of mRNA caspases 3, 8 and 9; Bax and p53 were evaluated by real-time quantitative PCR (3 h, 6 h and 12 h after exposure to the complex, treated with 24 μM and 48 μM). Data are for mean ± SD of experiments performed in triplicate. Significant differences from the untreated control are indicated by ***$p < 0.001$.

order to confirm the interaction of the complexes with the DNA, CD spectra of DNA before and after adding the ruthenium complexes were recorded. Thus, as can be seen in Fig. 8, the conformation of DNA changes gradually by increasing the concentration of ruthenium complex (**1**). The same behavior was observed for the other three complexes, suggesting that all four complexes act by the same mechanism in cell death.

4. Conclusions

The *cis*-[RuCl(BzCN)(bipy)(dppe)]PF_6, *cis*-[RuCl(BzCN)(bipy)(dppb)]PF_6, *cis*-[RuCl(BzCN)(bipy)(dppf)]PF_6 and *cis*-[RuCl(BzCN)(phen)(dppb)]PF_6 complexes exerted an antiproliferative influence over the tested tumor cells [S180 (mouse sarcoma S180), DU145 (prostate cancer), K562 (chronic myeloid leukemia) and A549 (lung cancer)], yielding promising results. The complexes seem to be effective at inhibiting tumor cell growth, inducing alterations in the G0/G1 and S phases of the cell cycle and inducing apoptosis, which was observed in JC 1 trials. Our data suggest that the complexes used in this work probably trigger the apoptosis process through an intrinsic pathway, showing that they interfere in DNA replication, most likely by interacting directly with the DNA molecule. Furthermore, the results demonstrated the gene expression involved in the apoptosis process. These results suggest that the ruthenium complexes tested here are promising chemotherapeutic candidates for cancer treatment.

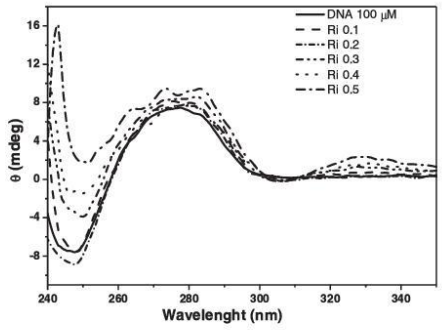

Fig. 8. Effect of ruthenium complex (**1**) on CD spectra of DNA before and after incubation at 37 °C, during 48 h: 1.0×10^{-3} mol L^{-1} of (**1**) in trizma hydrochloride solution, with 3% DMSO.

Acknowledgments

The authors gratefully acknowledge the financial support from the Brazilian Federal organ Research and Projects Financing (FINEP) (Grant No. 01.06.0941.00/CT-Saúde to Elisângela de Paula Silveira-Lacerda) and the São Paulo Research Foundation (FAPESP Grant 2012/06013-4, Alzir A. Batista). The Coordinating Committee for the Advancement of Higher Education Staff in Brazil (CAPES) provided a fellowship to Flavia de Castro Pereira, and the Brazilian National Council of Technological and Scientific Development (CNPq) gave a fellowship to Aliny Pereira de Lima.

References

[1] B. Rosenberg, L.V. Camp, J.E. Trosko, V.H. Mansour, Nature 222 (1969) 385–386.
[2] J. Reedijk, Chem. Commun. (1996) 801–806.
[3] Z.J. Guo, P.J. Sadler, Adv. Inorg. Chem. 49 (1999) 183–306.
[4] C.S. Devi, D.A. Kumar, S.S. Singh, N. Gabra, N. Deepika, Y. Praveen Kumar, S. Satyanarayana, Eur. J. Med. Chem. 64 (2013) 410–421.
[5] A. Bergamo, C. Gaiddon, J.H.M. Schellens, J.H. Beijnen, G. Sava, J. Inorg. Biochem. 106 (2012) 90–99.
[6] Q. Yu, L. Yanan, W. Chuan, S. Dongdong, Y. Xingcheng, L. Yanyu, L. Jie, PLoS One 7 (12) (2012) e50902.
[7] A. Bencini, V. Lippolis, Coord. Chem. Rev. 254 (17–18) (2010) 2096–2180.
[8] R. Hage, R. Print, J.G. Hassnoot, J. Reedijk, J. Chem. Soc. Dalton Trans. (1987) 1389–1396.
[9] G. Orellana, C. Ibarra, J. Santoro, Inorg. Chem. 27 (1988) 1025–1030.
[10] C. Hiort, P. Lincoln, B. Norden, J. Am. Chem. Soc. 115 (1993) 3448–3454.
[11] I. Haq, P. Lincoln, D. Suh, B. Norden, B.Z. Chowdhry, J.B. Chair, J. Am. Chem. Soc. 117 (1995) 4788–4796.
[12] P. Lincoln, A. Broo, B. Norden, J. Am. Chem. Soc. 118 (1996) 2644–2653.
[13] E.R. dos Santos, M.A. Mondeli, L.V. Pozzi, R.S. Corrêa, H.S. Salistre-de-Araújo, F.R. Pavan, C.Q.F. Leite, J. Ellena, V.R.S. Malta, S.P. Machado, A.A. Batista, Polyhedron 51 (2013) 292–297.
[14] F.R. Pavan, G.V. Poelhsitz, M.I.F. Barbosa, S.R.A. Leite, A.A. Batista, J. Ellena, L.S. Sato, S.G. Franzblau, V. Moreno, D. Gambino, C.Q.F. Leite, Eur. J. Med. Chem. 46 (2011) 5099–5107.
[15] C.C. Golfeto, G.V. Poelhsitz, F.B. do Nascimento, A.A. Batista, H.S. Selistre-de- Araújo, M. Lanznaster, M.H. Torre, Met. Ions Biol. Med. 10 (2008) 104–109.
[16] A.E. Graminha, C. Rodrigues, A.A. Batista, L.R. Teixeira, E.S. Fagundes, H. Beraldo, Spectrochim. Acta A 69 (2008) 1073–1076.
[17] F.B. do Nascimento, G.V. Poelhsitz, F.R. Pavan, D.N. Sato, C.Q.F. Leite, H.S. Selistre-de-Araújo, J. Ellena, E.E. Castellano, V.M. Deflon, A.A. Batista, J. Inorg. Biochem. 102 (2008) 1783–1789.
[18] F.R. Pavan, G.V. Poelhsitz, F.B. do Nascimento, S.R.A. Leite, A.A. Batista, V.M. Deflon, D.N. Sato, S.G. Franzblau, C.Q.F. Leite, Eur. J. Med. Chem. 45 (2010) 598–601.
[19] C.C. Golfeto, G.V. Poelhsitz, H.S. Selistre-de-Araújo, M.P. de Araujo, J. Ellena, E.E. Castellano, L.G.L. Lopes, I.S. Moreira, A.A. Batista, J. Inorg. Biochem. 104 (2010) 489–495.
[20] S.L. Queiroz, A.A. Batista, G. Oliva, M.T.P. Gambardella, R.H.A. Santos, K.S. MacFarlane, S.J. Rettig, B.R. James, Inorg. Chim. Acta 267 (1998) 209–221.

Please cite this article as: F.C. Pereira, et al., *Cis*-[RuCl(BzCN)(N–N)(P–P)]PF_6 complexes: Synthesis and in vitro antitumor activity..., J. Inorg. Biochem. (2015), http://dx.doi.org/10.1016/j.jinorgbio.2015.03.011

[21] E.M.A. Valle, B.A.V. Lima, A.G. Ferreira, F.B. do Nascimento, V.M. Deflon, I.C.N. Diogenes, U. Abram, J. Ellena, E.E. Castellano, A.A. Batista, Polyhedron 28 (2009) 3473–3478.
[22] Enraf-Nonius COLLECT, Nonius BV, Delft, The Netherlands, 1997–2000.
[23] Z. Otwinowski, W. Minor, HKL Denzo and Scalepack, In Methods in Enzymology, 276, Academic Press, New York, 1997.
[24] R.H. Blessing, Acta Crystallogr. A 51 (1995) 33–38.
[25] G.M. Sheldrick, Program for Crystal Structure Resolution SHELXS-97, University of Göttingen, Göttingen; Germany, 1997.
[26] L.J. Farrugia, J. Appl. Crystallogr. 30 (1997) 565–566.
[27] E.P. Silveira-Lacerda, C.A. Vilanova-Costa, F.C. Pereira, A. Hamaguchi, L.A. Pavanin, L.R. Goulart, M.I. Homsi-Brandenburgo, A.M. Soares, W.B. dos Santos, A. Nomizo, Biol. Trace Elem. Res. 133 (3) (2010) 270–283.
[28] T.J. Mosmann, J. Immunol. Methods 16 (1983) 55–63.
[29] R.Z. Osti, F.A. Serrano, T. Paschoalin, M.H.S. Massaoka, L.R. Travassos, D.R. Truzzi, L.C. Rodrigues, D.W. Franco, Aust. J. Chem. 65 (2012) 1333–1341.
[30] A.P. Lima, F.C. Pereira, C.A. Vilanova-Costa, J.R. Soares, L.C. Pereira, H.K. Porto, L.A. Pavanin, W.B. dos Santos, E.P. Silveira-Lacerda, Biol. Trace Elem. Res. 147 (1–3) (2012) 8–15.
[31] M. Castedo, K. Ferri, T. Roumier, D. Métivier, N. Zamzami, G. Kroemer, J. Immunol. Methods 265 (1–2) (2002) 39–47.
[32] P. Zhang, J. Chen, Y. Liang, Acta Biochim. Biophys. Sin. 42 (2010) 440–449.
[33] G. Koopman, C.P.M. Reutelingsperger, G.A.M. Kuitjen, R.M.J. Keehnen, S.T. Pals, M.H.V. Oers, Blood 84 (1994) 1415–1420.
[34] H. Lecoeur, Exp. Cell Res. 277 (2002) 1–14.
[35] L.A. Pradelli, M. Bénéteau, J.E. Ricci, Cell. Mol. Life Sci. 67 (2010) 1589–1597.
[36] C. Qian, J.K. Wang, C.L. Song, L.L. Wang, L.N. Jin, H. Chao, Metallomics 5 (7) (2013) 844–854.
[37] G.M. Van, N. Festjens, L.G. Van, X. Saelens, P. Vandenabeele, Biochem. Biophys. Res. Commun. 304 (2003) 487–497.
[38] X. Yang, L. Chen, Y. Liu, Y. Yang, T. Chen, W. Zheng, J. Liu, Q.Y. He, Biochimie 94 (2012) 345–353.
[39] T. Chen, Y. Liu, W.J. Zheng, J. Liu, Y.S. Wong, Inorg. Chem. 49 (2010) 6366–6368.
[40] V. Pierroz, T. Joshi, A. Leonídova, C. Mari, J. Schur, I. Ott, L. Spiccia, S. Ferrari, G. Gasser, J. Am. Chem. Soc. 134 (2012) 20376–20387.
[41] A. Malugin, P. Kopecková, J. Kopecek, Mol. Pharm. 3 (2006) 351–361.
[42] Ng Kuan-Beng, A. Bustamam, M.A. Sukari, S.I. Abdelwahab, S. Mohan, M.J.C. Buckle, B. Kamalidehghan, N.M. Nadzri, T. Anasamy, A.H.A. Hadi, H.S. Rahman, BMC Complement. Altern. Med. 13 (41) (2013).
[43] C. Garrido, L. Galluzi, M. Brunet, P.E. Puig, C. Didelot, G. Kroemer, Cell Death Differ. 13 (2006) 1423–1433.
[44] B. Montaner, R. Perez-Tomas, Ann. N. Y. Acad. Sci. 973 (2002) 246–249.
[45] A.M. Ranger, B.A. Malynn, S.J. Korsmeyer, Nat. Genet. 28 (2001) 113–118.
[46] R.P. Rastogi, R.P. Sinha, EXCLI J. 8 (2009) 155–181.
[47] M. Crompton, Curr. Opin. Cell Biol. 12 (2000) 414–419.
[48] M. Hollstein, D. Sidransky, B. Vogelstein, C.C. Harris, Science 253 (1991) 49–53.
[49] J.M. Lee, A. Bernstein, Cancer Metastasis Rev. 14 (2) (1995) 149–161.
[50] D.A. Liebermann, B. Hoffman, R.A. Steinman, Oncogene 11 (1995) 199–210.
[51] V. Chiarugi, L. Magnelli, M. Cinelli, G. Basi, Cell. Mol. Biol. Res. 40 (1994) 603–612.
[52] K.H. Vousden, X. Lu, Nat. Rev. Cancer 8 (2002) 594–604.
[53] J.E. Chipuk, D.R. Green, Cell Death Differ. 13 (2006) 994–1002.
[54] A.V. Vaseva, U.M. Moll, Biochim. Biophys. Acta Bioenerg. 1787 (5) (2009) 414–420.
[55] K.R. Webster, Chem. Res. Toxicol. 13 (2000) 940–943.
[56] C.J. Sherr, Cancer Res. 60 (2000) 3689–3695.
[57] R.W. Johnstone, A.A. Ruefli, S.W. Lowe, Cell 108 (2002) 153–164.
[58] G. Thiel, G. Cibelli, J. Cell. Physiol. 193 (3) (2002) 287–292.
[59] C. Gaiddon, P. Jeannequin, P. Bischoff, M. Pfeffer, C. Sirlin, J.P. Loeffler, J. Pharmacol. Exp. Ther. 315 (2005) 1403–1411.
[60] S.W. Lowe, A.W. Lin, Carcinogenesis 21 (2000) 485–495.
[61] V.I. Ivanov, L.E. Minchenkova, G. Burckhardt, E. Birch-Hirschfeld, H. Fritzsche, C. Zimmer, Biophys. J. 71 (1996) 3344–3349.
[62] B. Nordén, F. Tjerneld, Biopolymers 21 (1982) 1713–1734.

Please cite this article as: F.C. Pereira, et al., *Cis*-[RuCl(BzCN)(N–N)(P–P)]PF_6 complexes: Synthesis and in vitro antitumor activity..., J. Inorg. Biochem. (2015), http://dx.doi.org/10.1016/j.jinorgbio.2015.03.011